ISSN 1831-9424

European Commission

Global Flood Monitoring - Annual Product and Service Quality Assessment Report 2023

Seewald, M., Gruber, C., Innerbichler, F., Pasik, A., Duffy, C., Riffler, M., Reimer, C., Stachl, T., Kidd, R., Mccormick, N., Salamon, P.

2024

Joint Research Centre

EUR 32022

Contact information
Name: Peter Salamon
Address: European Commission, JRC, Office 102/028, Via Enrico Fermi 2749, 21027 Ispra, Italy.
Email: peter.salamon@ec.europa.eu
Tel.: +39-0332-786013

EU Science Hub
https://joint-research-centre.ec.europa.eu

JRC138200

EUR 32022

PDF ISBN 978-92-68-20049-0 ISSN 1831-9424 doi:10.2760/41122 KJ-NA-32-022-EN-N

Luxembourg: Publications Office of the European Union, 2024

How to cite this report: European Commission, Joint Research Centre, Seewald, M., Gruber, C., Innerbichler, F., Pasik, A., Duffy, C., Riffler, M., Reimer, C., Stachl, T., Kidd, R., Mccormick, N. and Salamon, P., *Global Flood Monitoring - Annual Product and Service Quality Assessment Report 2023*, Publications Office of the European Union, Luxembourg, 2024, https://data.europa.eu/doi/10.2760/41122, JRC138200.

Table of Contents

Abstract

This Technical Report presents the results of the annual product and service quality assessment of the Global Flood Monitoring (GFM) product of the Copernicus Emergency Management Service (CEMS), which was performed on a quarterly basis during 2023. This report is the second of its kind: the first (Seewald et al., 2023a) was focused on the GFM product and service quality assessment for 2022.

The main part of the 2023 GFM product and service quality assessment was the thematic accuracy assessment of the GFM output layers Observed Flood Extent and Reference Water Mask, for 12 selected Use Cases of worldwide flood events. Five of the Use Cases were flood events during 2023, which were mapped by the operational, near real-time GFM product, while seven of the Use Cases were flood events during the period 2017-2021, which are included in the GFM re-processed Sentinel-1 archive of worldwide observed flood events and water extent. The 2023 GFM product and service quality assessment also includes a qualitative assessment of the GFM results for the flood disaster following the destruction of the Kakhovka hydroelectric dam in the Kherson region of southern Ukraine, on 6 June 2023.

As required by the Technical Specifications (European Commission, 2020), the GFM product should have a thematic accuracy of at least 70%, computed based on the Critical Success Index (CSI). The main results of the GFM thematic accuracy assessment are summarized below:

- Regarding the Observed Flood Extent, as shown in Table 8, eight of the 12 Use Cases met or exceeded the target accuracy (CSI = 69.9 to 82.1%), and two Use Cases were slightly below the target accuracy (CSI = 61.6% and 64.1%). Two Use Cases (Morocco and Myanmar) had very low CSI values (i.e. 11.0 and 18.1%), for reasons that are explained in the relevant sections (4.2.2 and 4.2.3).

- Regarding the permanent water of the Reference Water Mask, as shown in Table 9, seven of the 12 Use Cases exceeded the target accuracy (CSI = 72.4 to 86.3%), and four Use Cases were slightly below the target accuracy (CSI = 60.0 to 67.5%). One Use Case had a low CSI value (32.8%), for reasons that are explained in the relevant section (4.2.5).

The thematic accuracies of the seasonal (i.e. monthly) water of the Reference Water Mask are not presented, since - as was highlighted in the 2022 GFM annual product and service quality assessment (Seewald et al., 2023a) - this is generally very low, due to major discrepancies between the seasonal water extent in the GFM product and the reference datasets. (The reasons for these discrepancies are outlined in Section 4.1 of this report).

The results of the assessment of (a) the GFM service availability, product timeliness, and user uptake and experience, and (b) the general plausibility of the Exclusion Mask, which was carried out as part of 2023 GFM product and service quality assessment, are also presented in this report. During 2023, the GFM service availability and product timeliness generally met or exceeded the expected targets, while user uptake and experience improved compared to the previous year (2022), due partly to a significant system update at the beginning of 2023.

1. Introduction

Copernicus, the EU's Earth Observation programme, is a flagship component of the EU space programme (established by EU Space Regulation 2021/696), and is coordinated and managed by the European Commission.[1] The Copernicus Emergency Management System (CEMS), one of six services of Copernicus, provides information for emergency response to different types of disasters, including meteorological and geophysical hazards, deliberate and accidental man-made disasters and other humanitarian disasters, as well as prevention, preparedness, response and recovery activities.[2] CEMS consists of the following three components:

- On-demand mapping (i.e. Rapid Mapping, and Risk and Recovery Mapping), from satellite or airborne image data.
- Exposure mapping, via the Global Human Settlement Layer (GHSL).
- Early warning and monitoring, via the following systems:

- *European and Global Flood Awareness Systems (EFAS and GloFAS).*[3]
- *European Forest Fire Information System (EFFIS).*
- *European and Global Drought Observatories (EDO and GDO).*

The Global Flood Monitoring (GFM) product of CEMS complements the existing CEMS components for flood early warnings (i.e. EFAS and GloFAS) and on-demand mapping, by:

- Enabling a continuous global, systematic monitoring of flood events.
- Enhancing the timeliness of flood maps for emergency response, since no user activation request is required, and the process is fully automated.
- Improving the effectiveness of Rapid Mapping activation requests through a better identification of the area of interest, where additional information from contributing missions and / or a higher spatial resolution is required.

The GFM product provides a continuous monitoring of flood events worldwide, by processing and analysing in near real-time all incoming Sentinel-1 Synthetic Aperture Radar (SAR) satellite imagery, utilizing a data cube (or time-series) approach enabling high product timeliness, and implementing an ensemble flood mapping approach that integrates three independent, state-of-the-art SAR-based flood mapping algorithms, to improve robustness and accuracy of the flood and water extent maps, and build a high degree of redundancy into the service (Salamon, et al., 2021), (Matgen, et al., 2020), (Wagner, et al., 2020).

Implementing and operating the GFM product requires a set of procedures to ensure the technical and scientific quality of the GFM output layers of flood information, and of the generating service, in order to deliver the GFM output layers (i.e. Observed Flood Extent, Reference Water Mask, Exclusion Mask, etc.) with the best possible quality.

[1] https://www.copernicus.eu/en
[2] https://emergency.copernicus.eu
[3] https://www.efas.eu/en, https://www.globalfloods.eu/

The GFM product and service quality assessment procedures include both systematic automated and planned offline quality checks, considering all aspects of the production, from data ingestion to data processing, data delivery, and the thematic accuracy of the main GFM output layers. Central to the quality assessment is a set of Key Performance Indicators (KPIs) that are used for the quarterly monitoring and reporting of the following aspects of the GFM service and product delivery performance:

- The thematic accuracy of the Observed Flood Extent and Reference Water Mask.
- The product timeliness with which the GFM output layers are delivered.
- The availability to users of all service components of the GFM product, as well as aspects related to user uptake and usability of the service (i.e. unique visitors, total visitors, total downloads, and service performance experience).
- The general plausibility of the Exclusion Mask, which denotes areas where SAR-based flood and water mapping is not technically feasible.

The main part of the GFM product and service quality assessment is the thematic accuracy assessment of the Observed Flood Extent and Reference Water Mask. This task is performed systematically using appropriate procedures, based on representative Use Cases of worldwide flood events. The analysis protocol is designed to estimate the accuracy objectively, based on independent sample data, and is applied according to the main principles for any validation, as supported by the following standard specifications:

- The INSPIRE directive[4], describing standard Implementing Rules for use in the areas of Metadata, Data Specifications, Network Services, Data and Service Sharing, and Monitoring and Reporting.
- The GEO QA4EO guidelines[5], describing the general principles for the validation and verification of Earth Observation products.
- The framework developed by the CEOS Land Product Validation (LPV) group[6], defining several principles for validation activities in agreement with INSPIRE and QA4EO.

This Technical Report describes the GFM annual product and service quality assessment that was performed on a quarterly basis for 2023. Previously, the GFM annual product and service quality assessment was performed for 2022 (Seewald et al., 2023a). A product and service quality assessment was also performed for the pre-operational version of the GFM product (Seewald et al., 2023b). The remainder of this Technical Report is structured as follows:

- In Chapter 2, a brief technical overview of the GFM product is presented, including a description of the main GFM output layers of global flood-related information, and of the underlying state-of-the-art SAR-based flood mapping algorithms, and highlighting specific aspects designed to enhance the thematic accuracy, for example the combination of the three flood mapping algorithms in an ensemble approach, and application of an Exclusion Mask.

[4] https://inspire.ec.europa.eu/inspire-implementing-rules/51763
[5] https://earth.esa.int/eogateway/activities/gscb-and-ltdp/qa4eo-guidelines
[6] https://lpvs.gsfc.nasa.gov/

- In Chapter 3, the following main components of the methodology used for the GFM product and service quality assessment, are described:

  - The KPIs used for the quarterly monitoring and reporting.
  - The 12 Use Cases of worldwide flood events used for the quality assessment of the Observed Flood Extent, Reference Water Mask and Exclusion Mask.
  - The reference datasets used for the quality assessment of the Observed Flood Extent and Reference Water Mask.
  - The computation of the KPIs for GFM service availability, product timeliness, and user uptake and experience.

- In Chapter 4, the validation results for the Observed Flood Extent and Reference Water Mask, for 12 Use Cases of worldwide flood events, are presented and discussed. Chapter 4 also includes a qualitative analysis of the GFM results for the flooding disaster that followed the destruction of the Kakhovka Dam, southern Ukraine on 6 June 2023.

- In Chapter 5, the results of the assessment of the GFM product timeliness, service availability and user uptake, are presented and discussed.

- In Chapter 6, the results of the general plausibility analysis of the Exclusion Mask for the 12 Use Cases of worldwide flood events, are presented and discussed.

- Finally, in Chapter 7, the main conclusions of the 2023 GFM product and service quality assessment, and the updates that have been made to the GFM product in 2024, as well as planned evolutions, are summarized.

The GFM product has been developed and implemented under a Framework Contract with the European Commission's Joint Research Centre (European Commission, 2020), by an international consortium (the "Expert Flood Monitoring Alliance") consisting of six partners:

- EODC (Earth Observation Data Centre for Water Resources Monitoring GmbH)
- GeoVille (GeoVille Information Systems and Data Processing GmbH)
- TUW (Technische Universität Wien)
- DLR (the German Aerospace Centre / Deutsches Zentrum für Luft- und Raumfahrt e.V.)
- LIST (Luxembourg Institute for Science and Technology)
- CIMA (Centro Internazionale in Monitoraggio Ambientale Research Foundation)

2. Technical overview of the GFM product

The Global Flood Monitoring (GFM) product of CEMS is an automated, global flood monitoring system that provides a continuous (i.e. all-weather, day-and-night), systematic monitoring of all major global flood events, in near real-time (NRT), based on the latest Sentinel-1 Synthetic Aperture Radar (SAR) satellite images. The GFM product is accessed mainly through (a) the GloFAS Map Viewer[7], or (b) a dedicated single-page web application, for defining areas of interest, and downloading GFM output layers[8]. A brief technical overview of the GFM product is provided below. Full technical details on the GFM product are provided on-line in the Product User Manual (PUM) and the Product Definition Document (PDD).[9]

For each newly acquired Sentinel-1 SAR satellite image, the GFM product provides ten output layers of global flood-related information, which are shown in Table 1 below. Central to the GFM product are three state-of-the-art algorithms for the SAR-based detection and delineation of flooded areas, which were developed by members of the GFM consortium (i.e. LIST, DLR, TUW), and which are summarized in Table 2 below.

Table 1: The ten GFM output layers of global flood-related information, generated in near real-time based on Sentinel-1 SAR satellite imagery.

#	*GFM OUTPUT LAYER*	*DESCRIPTION*
1	***Observed Flood Extent:***	Flooded areas mapped by applying the GFM ensemble flood mapping algorithm to the latest Sentinel-1 images of SAR backscatter intensity.
2	***Observed Water Extent:***	Open and calm water mapped as the union of the Observed Flood Extent and the Reference Water Mask.
3	***Reference Water Mask:***	Normal (i.e. permanent and seasonal) water mapped by applying the GFM ensemble water mapping algorithm to an historical, five-year time-series (or data cube) of Sentinel-1 images of SAR backscatter intensity.
4	***Exclusion Mask:***	Areas where SAR-based water mapping is not technically feasible, due to no sensitivity (e.g. urban areas, dense vegetation), low backscatter (e.g. flat impervious areas, sandy surfaces), topographic distortions, radar shadows, or low coverage of Sentinel-1.
5	***Likelihood Values:***	Estimated likelihood of flood classification, for all areas outside the Exclusion Mask.
6	***Advisory Flags:***	Flags indicating potential reduced quality of flood mapping, due to prevailing environmental conditions (e.g. wind, ice, snow, dry soil), or degraded input data quality due to signal interference from other SAR missions.
7	***Sentinel-1 Footprint and Metadata:***	Image boundaries of the Sentinel-1 data used, and in addition information on the "metadata", i.e. the acquisition parameters of the Sentinel-1 data used.
8	***Sentinel-1 Schedule:***	Next scheduled Sentinel-1 data acquisition.
9	***Affected Population:***	Number of people in flooded areas, mapped by a spatial overlay of Observed Flood Extent and gridded population, from the Copernicus GHSL project.
10	***Affected Landcover:***	Land cover / use (e.g. artificial surfaces, agricultural areas) in flooded areas, mapped by a spatial overlay of Observed Flood Extent and the Copernicus GLS land cover.

[7] https://global-flood.emergency.copernicus.eu/glofas-forecasting/
[8] https://portal.gfm.eodc.eu/
[9] https://extwiki.eodc.eu/GFM/

The two main GFM output layers are the **Observed Flood Extent** and the **Reference Water Mask**. The main features of both output layers are briefly described below:

- The Observed Flood Extent indicates flooded areas mapped in near real-time from Sentinel-1 SAR satellite imagery, using an ensemble of three algorithms (developed independently by three leading research teams) that run in parallel and access the same pre-processed Sentinel-1 input data. The resulting three flood maps are then combined into one "consensus map", in which a pixel is accepted as flooded when a majority rule classifies it as such. The final flood map is generated by subtracting the permanent or seasonal water bodies, as delineated by the Reference Water Mask (see below).

- The Reference Water Mask delineates permanent water bodies, mapped based on the median backscatter of a recent five-year time series (or data cube) of Sentinel-1 SAR image data, as well as seasonal water bodies, mapped based on the median backscatter of all Sentinel-1 data from a given month, over the same five-year reference period.

To ensure optimal accuracy of the Observed Flood Extent, and to build a high degree of redundancy into the service, the GFM product deploys its three state-of-the-art flood mapping algorithms in an "**ensemble**" approach, whereby each grid-cell is mapped as flooded if (a) it is classified as flooded by **at least two of the three algorithms**, in the normal case when all three algorithms produce a result, or (b) it is classified as flooded by **two algorithms**, in the exceptional case when only two of the algorithms produce a result.

In order to optimize further the quality of the results of the GFM product, as can be seen in Table 1, an Exclusion Mask is used to exclude those areas where SAR-based water (and flood) detection is technically not feasible. The Exclusion Mask is created by combining global information layers delineating the following ground surface characteristics:

- **No sensitivity areas** (e.g. urban areas, dense vegetation), where Sentinel-1 SAR is not sensitive to flooding (or any other type of change) of the ground surface.
- Water look-alikes (e.g. flat impervious areas, sand surfaces), which are indistinguishable from flooded areas due to a **low backscatter** signature.
- Areas with strong topography (and low probability of flood occurrence), where the Sentinel-1 signals are affected by **topographic distortions**.
- **Radar shadows** cast by mountains, high vegetation canopies or man-made structures.
- Areas with **low coverage** (i.e. low revisit frequency) of Sentinel-1 observations, where there is an inadequate historical time-series of SAR data available.

Finally, as well as the NRT generation of the ten output layers of flood-related information listed in Table 1, the GFM product is also used to generate a processed archive of worldwide observed floods and water bodies, from 1 January 2015 until 2021. As will be seen, the thematic accuracy assessment of the Observed Flood Extent and Reference Water Mask, which is described in this report, includes Use Cases from the GFM processed archive. During 2024, the archive will be re-processed for the years 2015 to 2023, using updated algorithms. An extensive quality assessment of the re-processed products will be performed, and the results included in the next GFM Annual Product and Service Quality Assessment Report.

Table 2: Overview of the GFM product's three state-of-the-art algorithms for Sentinel-1 (S-1) SAR-based flood mapping.

GFM FLOOD MAPPING ALGORITHM	*MAIN TECHNICAL FEATURES*	*SCIENTIFIC REFERENCE*
Algorithm 1 (LIST):	▪ Hierarchical split-based approach enabling re-calibration of parameters in NRT based on the most recent pair of S-1 images. ▪ Uses a highly innovative sequence of hierarchical image splitting, statistical modelling, and region-growing to delineate and classify areas that changed their flooding-related backscatter response between two image acquisitions from the same orbits.	(Chini, et al., 2017)
Algorithm 2 (DLR):	▪ Fuzzy logic-based approach enabling a post-classification and region-growing, taking advantage of topography-derived indices in addition to SAR backscatter.	(Martinis, et al., 2015)
Algorithm 3 (TUW):	▪ A fully automatic, pixel-based flood extent mapping workflow which exploits the per-pixel full S-1 signal history in a time-series (or data cube) of backscatter measurements. ▪ Enables a very fast, scalable production of flood and water extent maps through pre-computed global parameters, at high quality.	(Bauer-Marschallinger, et al., 2022)

On 2 January 2023, version V2.0.0 of the GFM product was released[10]. This version included:

- Modification of the GFM ensemble flood mapping algorithm to use a consensus (versus split-decision) approach, if only two of the three individual algorithms produce a result.
- Updates of the GFM individual flood mapping algorithms, for improved performance of the TUW algorithm, and better handling of the scale factor for the DLR algorithm.
- Updates of the sub-layers of the Exclusion Mask, delineating areas of no-sensitivity, low backscatter, and radar shadows, using the latest methods and auxiliary data, including the latest CEMS Global Human Settlement Layer (GHSL) datasets.
- Update of the Reference Water Mask, by extending the two-year reference period for the Sentinel-1 SAR time-series (or data cube) to 2020-2021.

On 24 January 2024, version V3.0.0 of the GFM product was released[10]. This version included:

- Further refinements of the GFM flood and water mapping algorithms, and updating of the sub-layers of the Exclusion Mask.
- Updating of the Reference Water Mask, by extending the Sentinel-1 SAR time-series (or data cube) from two to five years (i.e. 2018-2022).
- Upgrading of the GFM product delivery times, and the functionality of the GFM product access and dissemination.

At the time of publication, the entire Sentinel-1-based GFM archive of worldwide observed floods and water bodies, is being re-processed using the latest version of the GFM product, to re-generate the entire GFM flood archive for 2015-2023. Further adaptations of the GFM flood and water mapping algorithms, aimed at reducing the effects of flood over- and under-detection (as identified during the thematic quality assessment) are foreseen during 2024.

[10] https://extwiki.eodc.eu/GFM/GFMVersioning

3. Methodology for GFM product and service quality assessment

In accordance with the Technical Specifications for implementing and operating the GFM product (European Commission, 2020), the scientific and technical quality of the near real-time GFM product generation and service and product delivery, is ensured through well-defined procedures for product and service quality assessment.

A key element of the GFM product and service quality assessment is the monitoring and reporting of the **thematic accuracy** of the GFM output layers Observed Flood Extent and Reference Water Mask (delineating permanent and seasonal water bodies), as well as the GFM processed archive of worldwide observed floods and water bodies.

Briefly, the thematic accuracy assessment (or validation) has been performed using a set of independently created flood and water reference datasets, and based on 12 Use Cases of world-wide flood events, which were selected to be representative, in space and time, of the scientific challenges to be addressed by the GFM flood and water mapping algorithms.

The remainder of this Chapter is structured as follows:

- In Section 3.1, the Key Performance Indicators (KPIs) used for the quarterly monitoring of the GFM service and product delivery performance, are described in detail.

- In Section 3.2, the 12 Use Cases of worldwide flood events, used for the thematic accuracy assessment of the Observed Flood Extent and Reference Water Mask, and for analysing the general plausibility of the Exclusion Mask, are described in detail.

- In Section 3.3, the reference datasets for the 12 Use Cases of worldwide flood events, which were used for the purposes of comparison with the Observed Flood Extent and Reference Water, and which were created independently and without any knowledge of the methods used for the GFM data, are described in detail.

- Finally, in Section 3.4, the computation of the KPIs for GFM service availability, product timeliness, and user uptake and experience, is described in detail.

3.1 Key Performance Indicators (KPIs) used for GFM quality assessment

As outlined in the Technical Specifications (European Commission, 2020), the performance of the GFM product is assessed and reported on a quarterly basis, using a minimum set of Key Performance Indicators (KPIs) to monitor **Service Availability** (KPI-1), **Product Timeliness** (KPI-2), **Thematic Accuracy** (KPI-3), **Unique Visitors** (KPI-4), **Total Visitors** (KPI-5), **Total Downloads** (KPI-6), and **Service Performance Experience** (KPI-7). The KPIs are described in Table 3 below. KPI-2 and KPI-3 are further divided into various sub-categories, as described in Sections 3.1.1 and 3.1.2 below. Regarding KPI-4, KPI-5 and KPI-6, while no target values are defined for these KPIs, monitoring them over time provides important feedback, and should ideally indicate an increasing or steady uptake and usage of the GFM product. Further details on how KPI-1, KPI-2, KPI-4, KPI-5, KPI-6, and KPI-7 are calculated, are provided in Section 3.4 below.

In addition to the KPIs listed in Table 3, automated file quality checks are performed to ensure the consistent quality of all GFM output datasets. To this end, each file is compared with the GFM product technical specifications, which cover geometric (spatial) resolution, Coordinate Reference System, coverage (extent of raster file), datatype, raster coding, metadata, data format, and file-naming. Further details are provided in **Annex 1**.

Table 3: Definition of the KPIs used for GFM product and service quality assessment.

KPI	*NAME*	*DESCRIPTION*	*TARGET VALUE*
KPI-1	***Service Availability***	Percentage the service was available to users per quarter of a year.	*>=99 %*
KPI-2	***Product Timeliness***	Percentage of products delivered within 8 hours. (See Section 3.1.1).	*>=95 %*
KPI-3	***Thematic Accuracy***	Critical Success Index (CSI) and other accuracy metrics, computed by comparing the Observed Flood Extent and Reference Water Mask with independent reference datasets. (See Section 3.1.2).	*>=70 % (CSI)*
KPI-4	***Unique Visitors***	Number of unique users visiting via API / WMS-T (front-end application).	-
KPI-5	***Total Visitors***	Total number of user visits via API / WMS-T (front-end application).	-
KPI-6	***Total Downloads***	Number and volume of data downloads via API / WMS-T / web download (front-end application).	-
KPI-7	***Service Performance Experience***	Percentage change (absolute value) of the mean response time for users of the GFM single-page application[8], over a quarter of a year.	*< 20 %*

3.1.1 Sub-categories of KPI-2 (Product Timeliness) used for GFM quality assessment

KPI-2 (Product Timeliness) refers to the total time from actual observation of a Sentinel-1 scene to availability of the near-real-time GFM output layers for access and dissemination to users. As is shown in Table 4, there are three main sub-categories of KPI-2:

- **KPI-2a** represents the end-to-end timeliness of the Sentinel-1 data flow from the satellite sensor to availability to users of the GFM flood products. Sentinel-1 data is available for the GFM product via a dedicated ESA hub (i.e. the Copernicus Data Hub).
- **KPI-2b** represents the timeliness from availability of Sentinel-1 data on the Copernicus Data Hub to availability to users of the GFM flood products.
- **KPI-2c** complements KPI-2a and KPI-2b, by indicating the timeliness from retrieval and download of the Sentinel-1 dataset at EODC to availability to users of the GFM flood products, for further uptake.

Each KPI-2 sub-category represents individual time-stages of the data flow of the Sentinel-1 datasets, as is illustrated in Figure 1 below. As can also be seen in Table 4, the three sub-categories of KPI-2 are further sub-divided based on the initial Sentinel-1 product timeliness categories - referred to as **NRT-3h** and **FAST-24h** - which indicate the expected publication delay on an ESA data hub after a Sentinel-1 image acquisition.

Table 4: Definition of KPIs used for quarterly reporting of product timeliness of the GFM product, including for Sentinel-1 NRT-3h and Fast-24h products.

TIMELINESS MEASURED	*KPI*	*DESCRIPTION*
From image acquisition to user	***KPI-2a***	Percentage of all products delivered in up to 8 hours, measured between sensing and accessibility by user.
	KPI-2a-NRT-3h	Percentage of all 3H-NRT products delivered in up to 8 hours, measured between sensing and accessibility by user.
	KPI-2a-FAST-24h	Percentage of all FAST-24h products delivered in up to 8 hours, measured between sensing and accessibility by user.
From ESA to user	***KPI-2b***	Percentage of all products delivered in up to 8 hours, measured between availability on ESA Hubs and accessibility by user.
	KPI-2b-NRT-3h	Percentage of all 3H-NRT products delivered in up to 8 hours, measured between availability on ESA Hubs and accessibility by user.
	KPI-2b-FAST-24h	Percentage of all FAST-24h products delivered in up to 8 hours, measured between availability on ESA Hubs and accessibility by user.
From EODC to user	***KPI-2c***	Percentage of all products delivered in up to 8 hours, measured between availability on ESA Hubs and accessibility by user.
	KPI-2c-NRT-3h	Percentage of all 3H-NRT products delivered in up to 8 hours, measured between availability on ESA Hubs and accessibility by user.
	KPI-2c-FAST-24h	Percentage of all FAST-24h products delivered in up to 8 hours, measured between availability on ESA Hubs and accessibility by user.

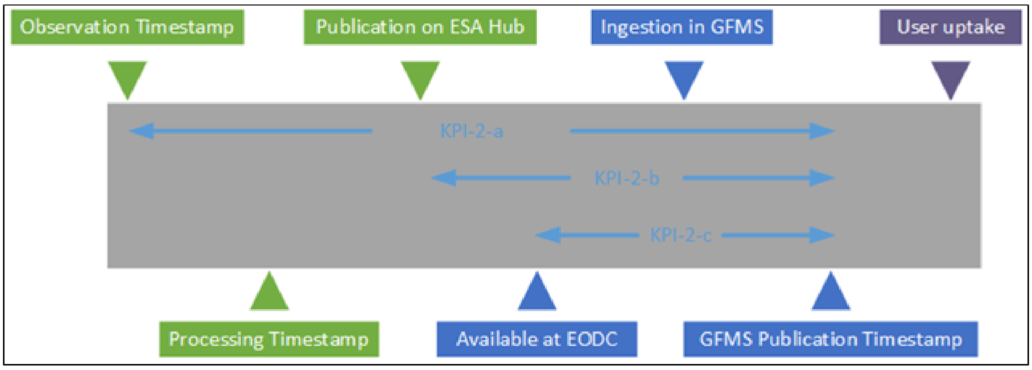

Figure 1: Illustration of end-to-end data flow of Sentinel-1 datasets, used to compute GFM product timeliness (KPI-2). Timestamps are the responsibility of ESA (in green), the contractor (in blue), and the user (in purple).

3.1.2 Sub-categories of KPI-3 (Thematic Accuracy) used for GFM quality assessment

During 2023, the **thematic accuracy** of the GFM product was assessed and reported for 12 Use Cases of worldwide flood events (described in Section 3.2 below). The thematic accuracy assessment of the Observed Flood Extent (for example) is based on the 2x2 **error matrix** that compares "observed" FLOOD and NO FLOOD sample points in an independent reference dataset, with those classified by the GFM product. The error matrix is illustrated in Figure 2. The accuracy metrics computed from the error matrix are defined in Table 5.

		Observed	
		FLOOD	NO FLOOD
Detected	FLOOD	A	B
	NO FLOOD	C	D

Figure 2: 2-by-2 error matrix used to compute the thematic accuracy of the GFM product, by comparing observed and detected sample points (total number = A+B+C+D), for each Use Case.

Table 5: Definition of KPIs used for thematic accuracy assessment of the GFM product (computed based on the 2-by-2 error matrix shown in Figure 2).

KPI	*NAME*	*DESCRIPTION*	*FORMULA (see Figure 1)*	*TARGET VALUE*
KPI-3a	**Critical Success Index**	Proportion of the observed and detected FLOOD pixels correctly classified.	***[A] / [A + B + C]***	*70-80 %*
KPI-3b	**Bias**	Ratio of detected to observed FLOOD and NO FLOOD pixels. Over-detection: > 1. Under-detection: < 1. Neutral errors: = 1.0.	***[A + B] / [A + C]***	*1.0*
KPI-3c	**Overall Accuracy**	Proportion of the total number of sample points (FLOOD and NO FLOOD) correctly classified.	***[A + D] / [A + B + C + D]***	*> 95 %*
KPI-3d	**Commission Error** (over-detection; false positive)	Proportion of detected FLOOD pixels that are NO FLOOD in the observed pixels.	***[B] / [A + B]***	*< 5 %*
-	**User's Accuracy** (complement of KPI-3d)	Proportion of detected FLOOD pixels that are FLOOD in the observed pixels.	***[A] / [A + B]***	*> 95 %*
KPI-3e	**Omission Error** (under-detection; false negative)	Proportion of observed FLOOD pixels that are NO FLOOD in the detected pixels.	***[C] / [A + C]***	*<5 %*
-	**Producer's Accuracy** (complement of KPI-3e)	Proportion of observed FLOOD pixels that are FLOOD in the detected pixels.	***[A] / [A + C]***	*> 95 %*

Accuracy estimations are improved using stratified or post-stratified estimators (Card, 1982); (Olofsson et al., 2013). Estimation of overall and per class accuracy of the GFM output layers should in theory include the known class areas, to improve estimation of the proportion of correctly mapped samples. However, for this Use Case evaluation, no stratification or weighting was needed, as the pixel-level validation is equivalent to a very dense random sampling scheme.

Once the Overall, Producer's and User's Accuracies are correctly estimated, the **confidence intervals** for those estimates are calculated (Olofsson, et al., 2014). The objective is to state the true accuracy of a product, i.e. to claim a certain target accuracy with a certain level of confidence (e.g. a minimum 85% accuracy at a 95% confidence level). A complementary aspect of such an approach is that the error matrix and class proportions can produce unbiased area estimates for each class with associated confidence intervals.

The above error measures satisfy the principles of equivalence of events, i.e. FLOOD and NO FLOOD cases, are equally important. However, the latter class is usually dominant outside the flood extent, so many reported measures might indicate a biased result (towards NO FLOOD accuracy). In this context, the **Critical Success Index** (CSI) is particularly useful where classified events occur much less frequently than the non-occurrence of the event.

Another useful measure is the **bias** (or bias ratio). A bias of 1.0 means that the measured errors are "neutral", with Commission Errors (false positives) and Omission Errors (false negatives) at equal magnitude. When bias < 1.0 or bias > 1.0, an under- or over-detection of events will be observed, respectively. Bias thus combines both Commission and Omission Errors in a single metric, and also helps to find an optimal solution between both cases.

3.2 Use Cases of worldwide flood events, used for quality assessment of Observed Flood Extent, Reference Water Mask, and Exclusion Mask

In order to validate the Observed Flood Extent and Reference Water Mask, a carefully designed sampling scheme is required, since the number of pixels is too large for a complete survey. A proper and efficient sampling scheme must adhere to procedures that ensure statistical rigor, and accommodate practical realities in terms of cost and time constraints.

As stated in the Technical Specifications (European Commission, 2020), the thematic accuracy of the GFM product must be assessed through regular off-line interpretations of the same Sentinel-1 scenes for selected Use Cases of worldwide flood events that are representative of different environments and geographic locations throughout the world.

In order to ensure that the selected Use Cases are well distributed, the Global Environmental Stratification (Metzger et al., 2013; Metzger, 2018) is used. This approach distinguishes 125 strata with relatively homogeneous bioclimatic conditions, aggregated into 18 environmental zones. Use of this dataset enables the grouping of sample points into meaningful categories (strata), and identification of particular issues within regions of similar environmental conditions. Furthermore, this stratification ensures that (a) the evaluation of the Use Cases is more systematic than if Use Cases are selected randomly, and (b) the detailed analysis of the flood events will encompass various environmental zones.

For each reporting quarter of the 2023 GFM product and service quality assessment, Use Cases of worldwide flood events were selected based on the following steps:

- An initial check is made for flood events occurring during the reporting quarter, based on news reports, on-line resources for monitoring flood events (e.g. Floodlist[11]), and the Copernicus Emergency Management Service's Rapid Mapping activations[12].
- A check is then made of whether identified flood events were covered with a Sentinel-1 satellite image acquisition, based on the GFM product output layer "Sentinel-1 Footprint and Metadata" (see Table 1), accessible via the GloFAS Map Viewer[7].
- Continuous checks during the year ensure that selected Use Cases are well distributed, both globally and considering Metzger's Global Environmental Stratification.

[11] https://floodlist.com/
[12] https://emergency.copernicus.eu/mapping/list-of-activations-rapid

- A final check is made that the selected Use Cases satisfy the above factors, while also considering past flood events covered by the GFM product and any recent flood events.

The main details of the 12 Use Cases of worldwide flood events that were selected for the quarterly monitoring and reporting of the thematic accuracy of the GFM product, including their distribution in Metzger's Global Environmental Stratification, are summarized in both Table 6 and Figure 3 below. Further information on the 12 Use Cases, including descriptions of the flood events, an overview of the areas of interest (and the Exclusion Mask), and their distribution within the 18 global environmental zones of Metzger, are provided in **Annex 2**.

As can be seen in Table 6, five of the selected Use Cases were flood events that occurred during 2023, which were mapped by the operational, near real-time GFM product generation, while seven of the Use Cases were flood events that occurred during the period 2017-2021, which are included in the GFM re-processed Sentinel-1 archive of worldwide observed flood events and water extent.

Table 6: Overview of the 12 Use Cases of worldwide flood events that were used for the quarterly thematic accuracy assessment of the GFM product during 2023.

QUARTER	*USE CASE*	*LOCATION OF FLOOD EVENT*	*DATE OF FLOOD EVENT*	*GEOGRAPHIC REGION*	*GLOBAL ENVIRONMENTAL STRATIFICATION*
Q1	*1*	**USA - Texas**: College Station; Brazos County; Texas.	29.08.2017	*North America*	N – Hot and dry
	2	**Morocco**: Souss River, southern Morocco.	09.01.2021	*North Africa*	N – Hot and dry
	3	**Myanmar**: Delta of Irrawaddy (also Ayeyarwady) River, Myanmar.	21.07.2021	*Southeast Asia*	R – Extremely hot and moist
Q2	*4*	**France**: River Aude, Aude department.	16.10.2018	*Europe*	K – Warm temperate and mesic
	5	**Indonesia**: Barito River, South Kalimantan.	29.03.2023	*Southeast Asia*	R – Extremely hot and moist
	6	**Italy**: Lavezzola, Ravenna, Emilia-Romagna.	16.05.2023	*Europe*	K – Warm temperate and mesic
Q3	*7*	**Venezuela**: Llanos (grassland plains), Rio Apure / Rio Arauca.	29.07.2017	*South America*	Q – Extremely hot and xeric
	8	**Bangladesh**: Chattogram Division, around Chittagong.	10.08.2023	*South Asia*	R – Extremely hot and moist
	9	**Greece**: Palamas, Karditsa.	07.09.2023	*Europe*	L – Warm temperate and xeric
Q4	*10*	**Portugal**: Coimbra, Mondego River Basin.	23.12.2019	*Europe*	K – Warm temperate and mesic
	11	**India**: West Bengal and Odisha.	22.05.2020	*South Asia*	Q – Extremely hot and xeric; R – Extremely hot and moist
	12	**Dominican Republic**: near Arenoso, Duarte / María Trinidad Sánchez.	23.11.2023	*Caribbean*	R – Extremely hot and moist

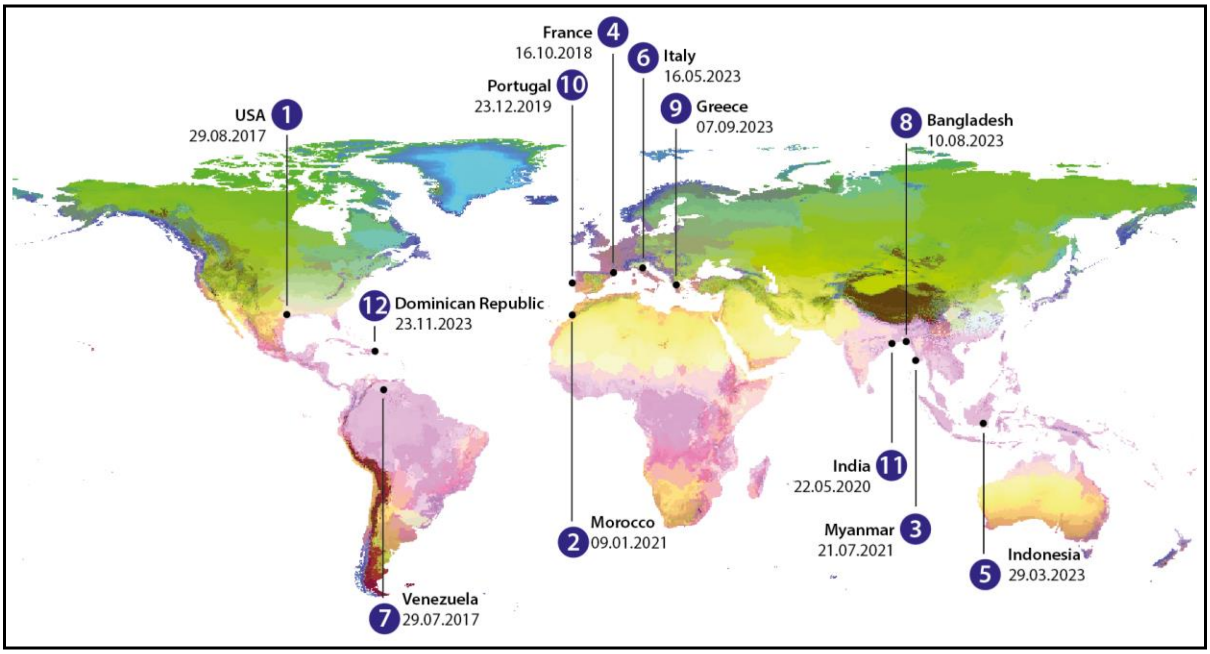

Figure 3: Spatial distribution of the 12 Use Cases of worldwide flood events within the Global Environmental Stratification (Metzger et al., 2013).

3.3 Reference datasets for Observed Flood Extent and Reference Water Mask

The thematic accuracy assessment of the GFM output layers Observed Flood Extent and Reference Water Mask (as well as the Exclusion Mask) has been carried out using an approach based on 12 Use Cases. In accordance with good practice guidelines (e.g. Olofsson, Foody, Stehman, and Woodcock, 2013; Olofsson et al., 2014), product validation can be based either on independent and higher quality reference data, or (if such data is not available) on an independent higher quality production methodology. Since independent, higher quality reference data are not available for any of the 12 Use Cases, the quality assessment applied here uses the GFM production data and applying a higher-quality methodology.

A semi-automated approach was therefore used, as described below, that was tuned to the context of the Use Cases, and visually controlled (and adjusted where required) to create the reference datasets of the best-possible quality. However, due to the large areas covered by the Use Cases, we cannot claim that the reference raster datasets contain no errors. Nonetheless, we denote the reference raster dataset as "ground truth" which means that potential errors stemming from the semi-automated approach will contribute to the analysed errors, thus lowering the values of the KPIs (i.e. correctly detected flood or water in the GFM product that has not been correctly mapped in the reference raster).

Clearly, a fully manual mapping of the presented Use Cases is not feasible, due to the large areas covered and the uncertainty of exact delineation of contiguous flooded regions based on the Sentinel-1 backscatter data. Therefore, a complete picture of the estimated thematic accuracy will be obtained using a validation approach based on sample points.

In the thematic accuracy assessment, for each Use Case the Observed Flood Extent and Reference Water Mask are compared with locally trained and manually enhanced flood / water masks (i.e. the reference datasets).

For each Use Case, the reference datasets were created by regular off-line interpretations of the GFM production data (i.e. Sentinel-1 imagery) and other data (e.g. optical and radar images, and in situ data, where available). The resulting flood and water masks were thus created independently of the methods used for the GFM flood and water maps. For each Use Case, the date and geographic area of the reference and GFM datasets were the same.

For each Use Case area, the thematic accuracy metrics listed in Table 5 are derived by comparing selected sample points (grid-cells) in independently created reference datasets, with those classified by the GFM flood and water mapping algorithms. The main accuracy metric is the Critical Success Index, a commonly used verification measure that combines hit rate and false alarm ratio into one score for low frequency events (such as floods).

The accuracy assessment was conducted by comparing, at a pixel level, the reference datasets with the FLOOD / NO FLOOD maps (for Observed Flood Extent) and the WATER / NO WATER maps (for the Reference Water Mask). All datasets were re-sampled to a dense, regular grid of 100x100 metres, and including the following further steps:

- All pixels with "No Data" values were excluded from the validation.
- All pixels included in the Exclusion Mask (see Table 1) were not considered.
- The Likelihood Values of pixels (see Table 1) were not considered.

The creation of the independent reference datasets is described below.

3.3.1 Reference datasets for Observed Flood Extent

To create reference datasets for the Observed Flood Extent, a high-quality flood mask was created using an independent semi-automated method, with visual enhancement. Dynamic local thresholding methods, mainly following those described in Ludwig et al. (2019) and Twele et al. (2016), were applied to Sentinel-1 data (see GFM Product Definition Document[9]).

The threshold between water and non-water pixels is derived by tiling the Sentinel-1 images into 100x100 pixel patches, each of which is further tiled into four sub-patches. Tiles with permanent water bodies - i.e. compared with an occurrence > 75% in the JRC's Global Surface Water Layer dataset (Pekel et al., 2016) are removed from the threshold computation so that only flooded pixels are considered. Tiles that potentially contain water are selected by analysing statistical relations between tiles and sub-tiles (Twele et al., 2016).

Additionally, the value for each patch in the Height Above Nearest Drainage (HAND) terrain model (a DEM normalized using the nearest drainage) is derived. The HAND index is used to exclude patches from tile selection that cannot be flooded based on physical considerations. Only patches with at least 20% of pixels with a HAND value < 15 are considered.

The water / non-water threshold is computed by applying the Otsu algorithm (Otsu, 1979) to each selected 100x100 pixel tile. Finally, Hartigan's "dip test" values are calculated for each tile to measure the bi- / uni-modality per tile (Hartigan and Hartigan, 1985). The thresholds are then filtered by comparing the tile statistics with the statistics of the whole image and the Dip test values with a threshold that indicates high bimodality.

The 10 most viable tile thresholds are then averaged to get the final global threshold ultimately applied to the input backscatter image.

To facilitate the comparability of the predicted and reference flood masks, the reference water datasets are masked with the same layers (i.e. Exclusion Mask, permanent / seasonal water, topographic shadows) as the ensemble product. Manual enhancement is performed using Sentinel-2 imagery to remove false positives from the reference datasets. From July 2023 onwards, we were able to access data from the Copernicus Contributing Missions that are used in the Rapid Mapping Activations by the Joint Research Centre (JRC). This further facilitates the manual enhancement wherever an activation overlaps with our Use Cases.

3.3.2 Reference datasets for Reference Water Mask

The reference datasets for the Reference Water Mask are generated by dynamic thresholding of optical and SAR imagery separately (Ludwig et al., 2019; Martinis et al., 2009), using pre-processed Sentinel-1 (S-1) and Sentinel-2 (S-2) images. S-2 L1C data are atmospherically corrected using the Sen2Cor Processor (v2.8). Clouds and cloud shadows are masked with the Sen2Cor Scene Classification (SCL). A cloud-shadow detection is also applied to the time series to remove Omission Errors due to similar appearance of cloud-shadow and water (Ludwig et al., 2019). Seeded region-growing is used to fill gaps in incompletely detected shadows. Commission errors are removed with the Cloud Displacement Index (Frantz et al., 2018).

Monthly images are combined with composites calculated by the geometric median (Roberts et al., 2017). Depending on environmental conditions, the quality of the Sen2Cor classification can vary, leading to artefacts in the resulting composites due to undetected clouds.

Depending on the land cover of the area of interest, multispectral indices (i.e. Normalized Difference Water Index or NDWI; Modified NDWI, and Multi-Band Water Index) are derived from monthly image composites or single scenes. Optical water detection is applied on equal-sized tiles (e.g. 100x100 pixels) of the aggregated multispectral indices. Only tiles with meaningful HAND values and variances above the 95th percentile of all tiles are used to determine the global threshold using the median. The global threshold is then adapted for each tile by weighting it with the mean of the neighbouring local thresholds.

The SAR water detection uses monthly VV-polarised backscatter statistics. S-1 images are pre-processed using SNAP (Sentinel Application Platform)[13] Version 8, to carry out the following tasks: orbit corrections; thermal / border and custom border noise removal (if needed); radiometric calibration to backscatter coefficient (i.e. Sigma Nought or σ^0); terrain correction; and speckle noise reduction. The SAR water detection algorithm combines global and local image thresholding, seeded region-growing and fuzzy logic post-processing. Thresholding is done as described above, except that instead of local Otsu thresholding, an adaptive thresholding is used (Bradley and Roth, 2007). Omitted water pixels are added to the water masks using a seeded region-growing algorithm, applied to each water body separately. A post-processing procedure (Martinis et al., 2009) is used to remove Commission Errors (e.g. terrain shadows). The S-1 and S-2 water masks are fused by combining all water pixels.

[13] https://step.esa.int/main/download/snap-download/

The algorithm for processing the surface water (and flood) reference datasets was developed as part of a round robin exercise organized within the ESA-funded WorldWater project (Tottrup, et al., 2022). Results of this initiative show that a dual sensor approach (combining optical and radar satellite data) - as was used for the generation of the reference datasets for this quality assessment activity - is the most effective way to perform large-scale national and regional surface water mapping across bio-climatic gradients.

3.4 Computation of KPIs for service availability, product timeliness, and user uptake and experience

In flood emergencies, near real-time flood extent observation is needed to support decision-making, and for timely definition of evacuation plans and routes. Time is crucial in global flood monitoring, to facilitate early warning and systematic mapping. For emergency response services and other stakeholders, timely access to a global flood monitoring product is a major requirement. A high quality and timely product, with 24/7 service availability, will foster user uptake and "just-in-time" flood detection, aimed at reducing the socio-economic impact.

As outlined in Section 3.1 above, in addition to KPI-3 (**Thematic Accuracy**), the following KPIs are used for the GFM product and service quality assessment: KPI-1 (**Service Availability**); KPI-2 (**Product Timeliness**); KPI-4 (**Unique Visitors**); KPI-5 (**Total Visitors**); KPI-6 (**Total Downloads**); and KPI-7 (**Service Performance Experience**).

Service availability (KPI-1) is considered with reference to the API, WMS-T and front-end application that are the user-facing components of the GFM product. Availability is measured as the percentage of successful requests returned from the individual service components over the reporting quarter, ensuring the healthiness and functionality of the component.

Product timeliness (KPI-2) refers to the percentage of the near real-time GFM output datasets that are delivered within 8 hours, measured from the actual observation of a Sentinel-1 scene to the availability of the GFM output datasets for access and dissemination to users. The information used to calculate KPI-2 and its sub-categories is retrieved via metadata accompanying the initial Sentinel-1 scene, or the Sentinel-1 Level-1 IW GRDH metadata or generated by the GFM production system itself. The metadata used to compute the KPIs for product timeliness, are summarized in Table 7.

As already mentioned, actual user uptake and experience of the service are measured based on the **total number of unique service users** (KPI-4), **total number of users** (KPI-5), **number and volume of data downloads** (KPI-6), and the **service performance experience** (KPI-7).

KPI-4, KPI-5 and KPI-6 describe user uptake (visitors and downloads) via the API / WMS-T / web download (front-end application), and are pure metrics each representing a total number over the reporting period. Anonymous user information is used to differentiate individual users provided by the CEMS identity-provider. Each individual user's service request is logged, to aggregate and report via the specific KPIs. The data volume accessed or downloaded via provided service endpoints (KPI-6) is reported based on the actively maintained metadata infrastructure for the corresponding information of the GFM product.

KPI-7 delineates the user experience exposed by the service (via the GFM dedicated single-page web application[8]), by utilising automated Web User Interface (WebUI) tests simulating user interactions with the browser. The objective of this KPI is to demonstrate and offer a consistent response behaviour of the service over time to the user, and to anticipate potential bottlenecks to ensure user satisfaction.

Table 7: Variables and metadata sources used to compute the product timeliness (KPI-2) of the GFM product.

#	*VARIABLE*	*METADATA SOURCE*	*ATTRIBUTE*
1	***Image observation timestamp***	Sentinel-1 Level-1 IW GRDH metadata exposed by the Copernicus Hub and included in the manifest file of the Sentinel-1 data file (SAFE).	*time_begin*
2	***Published on ESA Hub***	Metadata exposed by the Copernicus Hub.	*insert_date*
3	***Available at EODC***	Metadata retrieved after downloading of Sentinel-1 Level-1 IW GRDH data at EODC and ingesting metadata in GFM metadata database.	*db_insert_date*
4	***Accessible via GFM product***	Metadata created and stored by GFM production system, indicating completion of the production workflow of a Sentinel-1 scene.	*creation_date*
5	***Total no. of Sentinel-1 scenes***	Metadata database used to store metadata of downloaded Sentinel-1 Level-1 metadata, representing a count of all inserted scenes.	*scenes_total*

4. Thematic accuracy assessment of the GFM product

The thematic accuracy results for the GFM output layers Observed Flood Extent and Reference Water Mask, for the 12 Use Cases of worldwide flood events, are presented in Section 4.1 below. The results are discussed separately for each Use Case in Section 4.2 below. In addition to the thematic accuracy assessment of the 12 Use Cases, a qualitative assessment of the GFM results for the flood disaster caused by the destruction of the Kakhovka hydroelectric dam in the Kherson region of southern Ukraine, on 6 June 2023, is presented in Section 4.3 below.

4.1 Thematic accuracy results for Observed Flood Extent and Reference Water Mask

The thematic accuracies for the Observed Flood Extent and Reference Water Mask, for the 12 Use Cases, are summarized in Table 8 and Table 9. Note that the results presented in Table 9 are only for the **permanent water**, and not the **seasonal water**, of the Reference Water Mask. This is due to the major discrepancies that exist between the seasonal water extent in the GFM product and the reference datasets. One reason for this is that the GFM product only uses SAR data to detect water, while the reference datasets use SAR and optical data. Substantial intra-annual variability is also observed for some rivers, giving "salt-and-pepper" differences along the water / non-water border, between the GFM and reference seasonal water. Finally, due to the ephemeral nature of seasonal water, finding reference satellite images that coincide with the seasonal water extent is often not possible.

Table 8: Thematic accuracy of Observed Flood Extent ,for the 12 Use Cases, based on CSI (KPI-3a, target = 70%), Bias (KPI-3b, target = 1.0), Overall Accuracy (KPI-3c, target > 95%), Commission Error (KPI-3d, target < 5%), and Omission Error (KPI-3e, target < 5%). Commission and Omission Errors for NO FLOOD are shown in square brackets.

#	*USE CASE*	*KPI-3a (%)*	*KPI-3b*	*KPI-3c (%)*	*KPI-3d (%)*	*KPI-3e (%)*
1	**USA – Texas** (29.08.2017)	*61.6*	*0.642*	*99.1*	*2.5 [0.9]*	*37.4 [0.0]*
2	**Morocco** (09.01.2021)	*18.1*	*0.211*	*99.9*	*12.1 [0.1]*	*81.4 [0.0]*
3	**Myanmar** (21.07.2021)	*11.0*	*0.121*	*95.0*	*7.7 [5.0]*	*88.9 [0.1]*
4	**France** (16.10.2018)	*71*	*0.756*	*99.6*	*3.6 [0.4]*	*27.1 [0.0]*
5	**Indonesia** (29.03.2023)	*69.9*	*0.929*	*99.6*	*14.6 [0.3]*	*20.6 [0.2]*
6	**Italy** (16.05.2023)	*82*	*0.852*	*99.7*	*2.0 [0.3]*	*16.6 [0.0]*
7	**Venezuela** (29.07.2017)	*71.0*	*0.91*	*97.5*	*13.0 [1.7]*	*20.6 [1.0]*
8	**Bangladesh** (10.08.2023)	*77.8*	*0.99*	*99.2*	*12.2 [0.4]*	*12.8 [0.4]*
9	**Greece** (07.09.2023)	*82.1*	*0.9*	*97.3*	*4.8 [2.4]*	*14.3 [0.7]*
10	**Portugal** (23.12.2019)	*70.0*	*0.793*	*96.6*	*6.9 [2.0]*	*26,1 [0.4]*
11	**India** (22.05.2020)	*70.9*	*0.894*	*97.9*	*12.2 [1.5]*	*21.4 [0.8]*
12	**Dominican Republic** (23.11.2023)	*64.1*	*0.789*	*96.6*	*11.5 [2.8]*	*30.1 [0.9]*

Table 9: Thematic accuracy of Reference Water Mask (permanent water), for the 12 Use Cases, based on CSI (KPI-3a, target = 70%), Bias (KPI-3b, target = 1.0), Overall Accuracy (KPI-3c, target > 95%), Commission Error (KPI-3d, target < 5%), and Omission Error (KPI-3e, target < 5%). Commission and Omission Errors for NO FLOOD are shown in square brackets.

#	USE CASE	KPI-3a (%)	KPI-3b	KPI-3c (%)	KPI-3d (%)	KPI-3e (%)
1	**USA – Texas** (29.08.2017)	61.9	0.644	97.7	2.5 [2.3]	37.2 [0.1]
2	**Morocco** (09.01.2021)	81.6	1.212	99.9	18.0 [0.0]	0.6 [0.1]
3	**Myanmar** (21.07.2021)	83.5	0.910	99.1	4.5 [0.7]	13.1 [0.2]
4	**France** (16.10.2018)	86.0	1.137	99.8	13.1 [0.0]	1.2 [0.2]
5	**Indonesia** (29.03.2023)	32.8	2.566	97.9	65.7 [0.1]	1.9 [1.9]
6	**Italy** (16.05.2023)	86.3	1.077	99.3	10.7 [0.2]	3.7 [0.6]
7	**Venezuela** (29.07.2017)	67.5	1.345	97.9	29.7 [0.3]	5.5 [2.0]
8	**Bangladesh** (10.08.2023)	73.8	1.149	97.7	20.6 [0.7]	8.8 [1.8]
9	**Greece** (07.09.2023)	72.4	1.380	99.9	27.6 [0.0]	0.1 [0.1]
10	**Portugal** (23.12.2019)	74.2	1.107	99.7	18.9 [0.1]	10.3 [0.2]
11	**India** (22.05.2020)	62.4	0.745	98.4	10.0 [1.3]	33.0 [0.3]
12	**Dominican Republic** (23.11.2023)	60.0	1.059	99.7	11.5 [2.8]	30.1 [0.9]

4.2 Discussion of thematic accuracy results for Observed Flood Extent and Reference Water Mask

The thematic accuracy results for the Observed Flood Extent and Reference Water Mask, for each Use Case, are discussed below. Of the accuracy metrics that are reported in Table 8 and Table 9, the analysis and discussion focuses on the CSI (KPI-3a) and - for completeness and due to their frequent usage for other mapping products - Errors of Commission (KPI-3d) and Omission (i.e. KPI-3e). Clearly, Overall Accuracy (i.e. KPI-3c) is not very meaningful in the context of detecting rare flood events and water, as non-flood and non-water areas dominate the results. Note that for each Use Case, the permanent water class of the Reference Water Mask was computed across all Sentinel-1 images available in 2020-2021. An overview of each Use Case, and the associated flood event, is provided in **Annex 2**.

4.2.1 Use Case 1 (USA – Texas, 29.08.2017) - Discussion of results for Observed Flood Extent and Reference Water Mask

As can be seen in Figure 4 and Figure 5 below, the Observed Flood Extent shows good agreement with the reference dataset. The CSI value is 61.9%, with an overall accuracy of 97.7%. The Commission Error (2.5%) is below the target, indicating that over-detection by the GFM product occurs rarely. The Omission Error is much higher (37.1%), meaning that the GFM product substantially under-estimates the true flood extent in this case. These Omission Errors arise because the flood extent of the reference dataset is often slightly larger than that of the GFM product, and the reference dataset also identifies more flooded areas.

For the Q1 Use Cases, the performance of the GFM individual algorithms was also assessed. This showed that some algorithms detected flooding well, but due to the majority ranking of the ensemble algorithm, the final Observed Flood Extent did not contain these floods.

For Use Case 1, one peculiarity was that one algorithm did not cover the full area, so flooding was only detected when the results from the other two algorithms matched.

Similar to the Observed Flood Extent, as shown in Figure 6, for the Reference Water Mask there are discrepancies between the permanent water of the GFM product and of the reference dataset. The Omission Error (23.1%) is also higher than the Commission Error (15.3%). This is especially prominent in the continuous detection of rivers. Some rivers are not captured by the GFM product, but they are present in the respective months assessed. The reference dataset contains these rivers, as shown in the difference map in Figure 6.

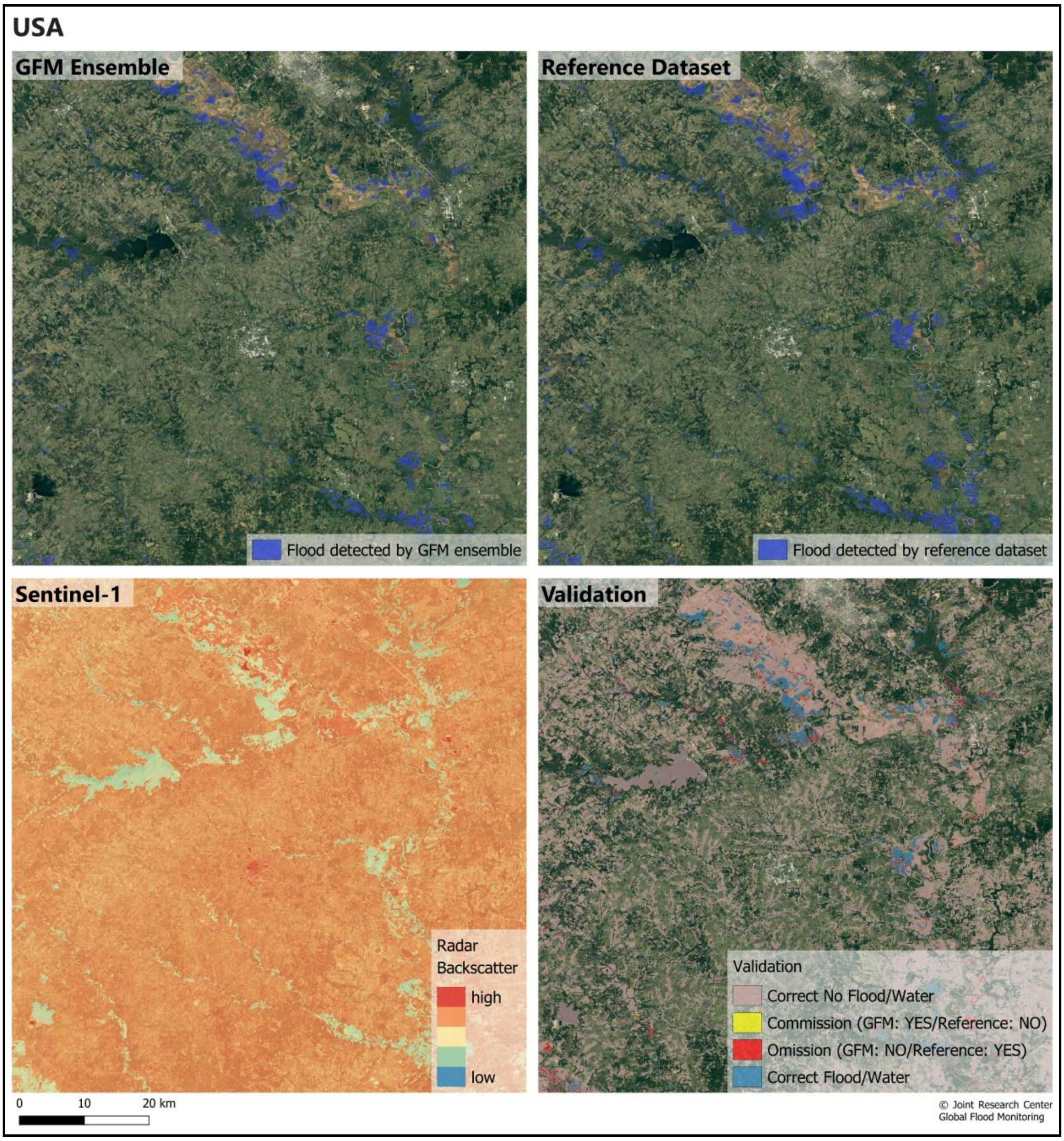

Figure 4: Use Case 1 – Observed Flood Extent from the GFM (top-left) and the reference dataset (top-right); Sentinel-1 SAR data (bottom left); difference map (bottom-right).

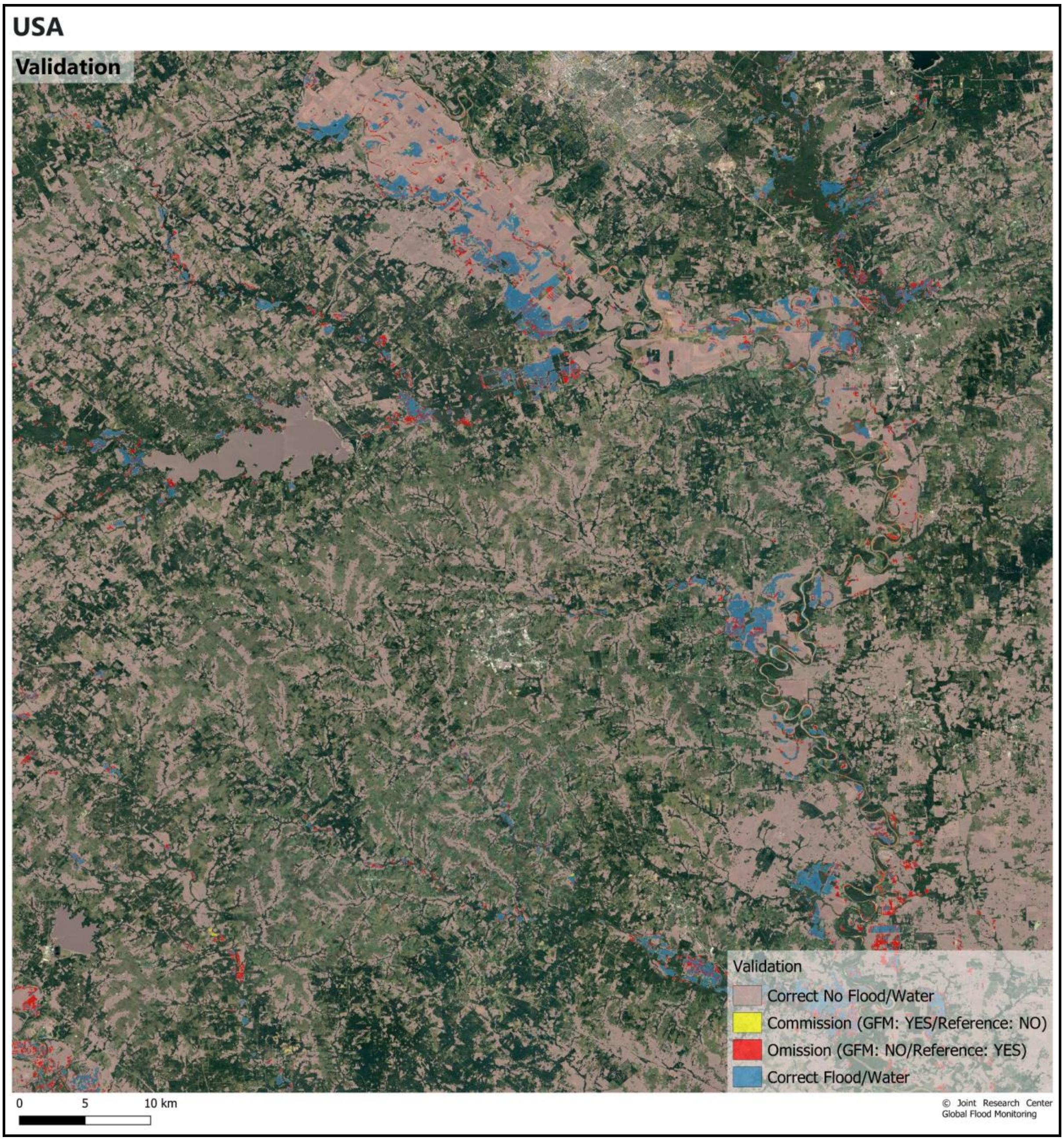

Figure 5: Use Case 1 – Difference map between Observed Flood Extent of the GFM and the reference dataset, showing the highly agreeing results (in blue), and slight under-estimation (in red) by the GFM compared with the reference dataset.

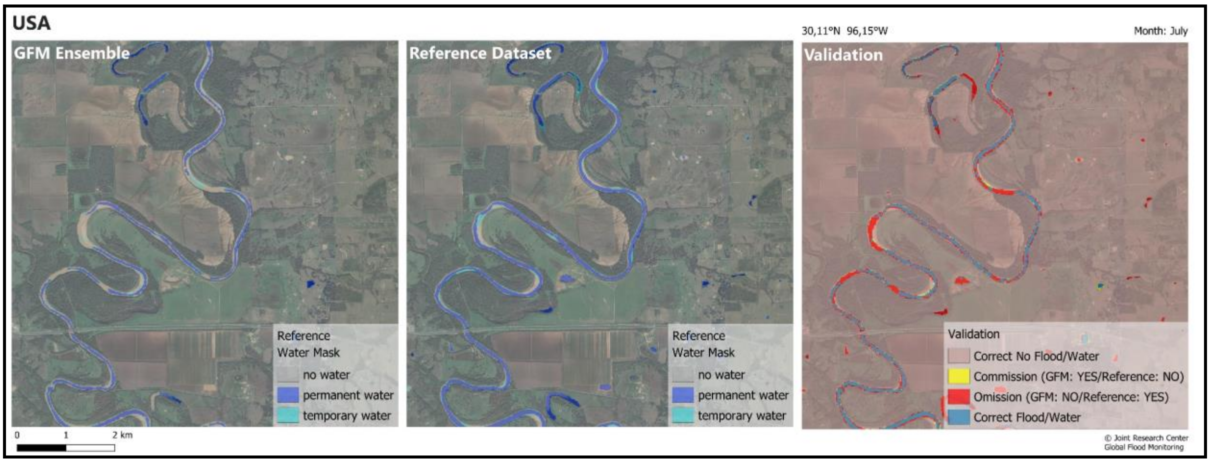

Figure 6: Use Case 1 – Reference Water Mask of the GFM (left) and the reference dataset (middle), and the difference map (right), showing significant omissions (in red) by the GFM product, as river courses are not fully detected.

4.2.2 Use Case 2 (Morocco, 09.01.2021) - Discussion of results for Observed Flood Extent and Reference Water Mask

Heavy rainfall affected parts of Morocco in early 2021. Some areas, such as Casablanca and the region of the Souss River (one of the longest rivers in Southern Morocco), experienced intense rainfall that started on 6 January 2021, and caused flash floods. According to media reports, one person died and four were injured in Casablanca. Several houses were damaged and a number of roads were not accessible due to floodwaters[14].

Flash floods occurred along the Souss River, which is characterized by a large basin. This suggests that during flood events, the majority of water is contained within the riverbed, minimizing flooding in adjacent areas along the river. Also for this flood event, the majority of the flood water remained in the "dry" river bed.

As can be seen in see Figure 7 and Figure 8, the Observed Flood Extent of the GFM product and of the reference dataset shows a limited amount of overlap. The GFM product detected much less water than the reference dataset, which resulted in a very low CSI value (18.1%). Whereas the reference dataset captured flooded areas in the riverbed, the GFM product almost did not map any water extent. The Sentinel-1 radar image shows that several areas in the river bed along the whole lower stream of the Souss River contain water after rainfalls.

The Commission Errors (12.1%) indicates that the GFM product sometimes detected water, where the reference dataset did not. The Omission Error (81.4%) is significantly higher, which is the main cause for the low CSI. The bias is also very low (0.211; target 1).

As for Use Case 1, the GFM individual algorithms were also compared. One algorithm detected almost no water, which strongly affected the ensemble result as it contains only the matching areas of the other two algorithms. Hence, the flood area detected by the GFM product was much lower than the reference dataset.

[14] https://erccportal.jrc.ec.europa.eu/ECHO-Products/Echo-Flash#/echo-flash-items/20243

The permanent water of the Reference Water Mask of the GFM product and of the reference dataset, fit better than the Observed Flood Extent, as reflected by the high CSI value (81.6%). Both datasets include the Souss River, a seasonal river which only has water intermittently. Therefore, the permanent water does not include the river basin, except for the river-mouth (at the Atlantic Ocean), where the river basin is more or less permanently water-covered. However, there are also some differences in this area between the GFM product and the reference dataset, as the former classifies as permanent water areas that seem to be sand-dunes (see Figure 9). In this region, the river basin and its single estuaries change considerably from year to year, so detecting permanent water is very challenging.

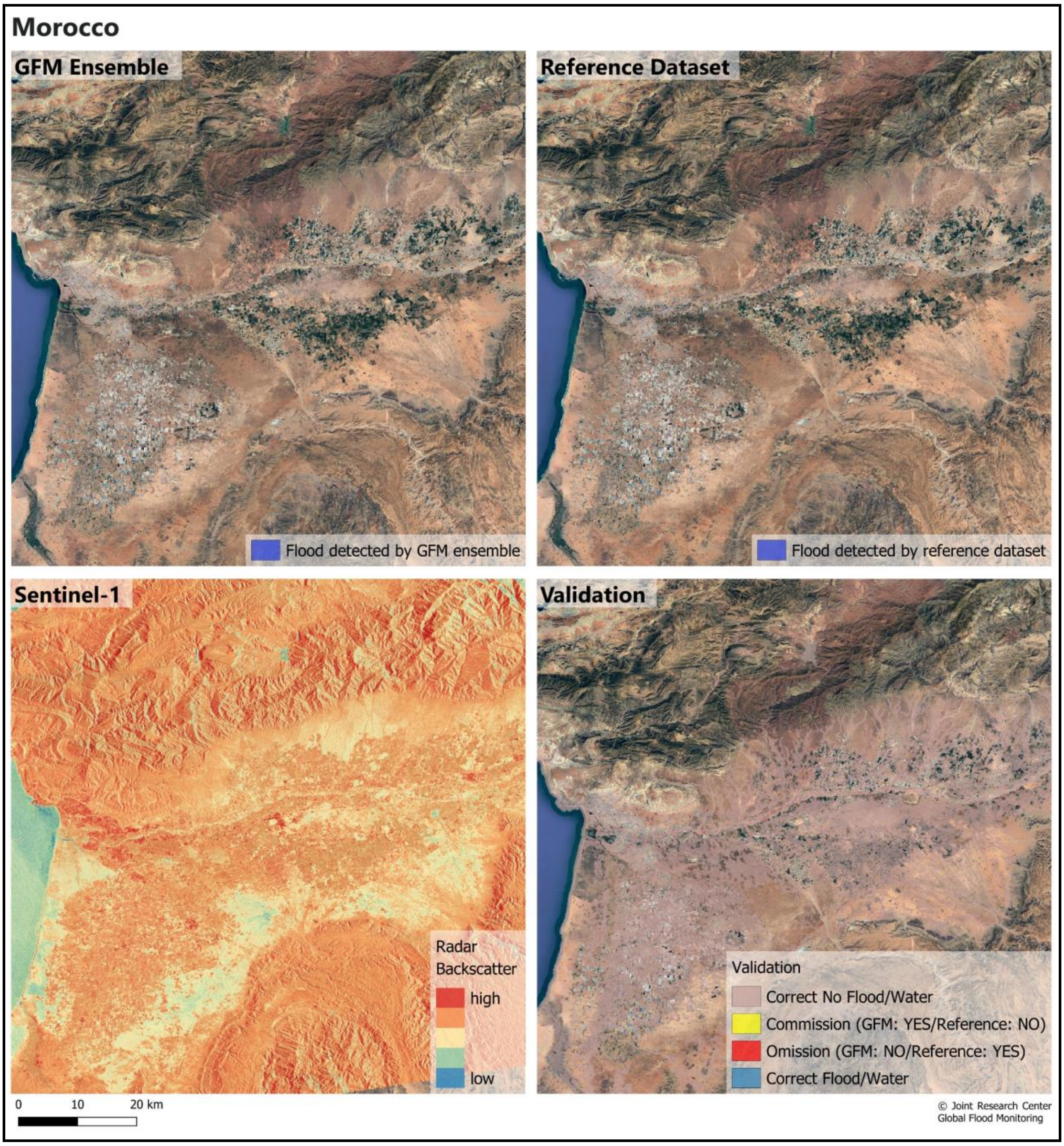

Figure 7: Use Case 2 – Observed Flood Extent from the GFM (top-left) and the reference dataset (top-right); Sentinel-1 SAR data (bottom left); difference map (bottom-right).

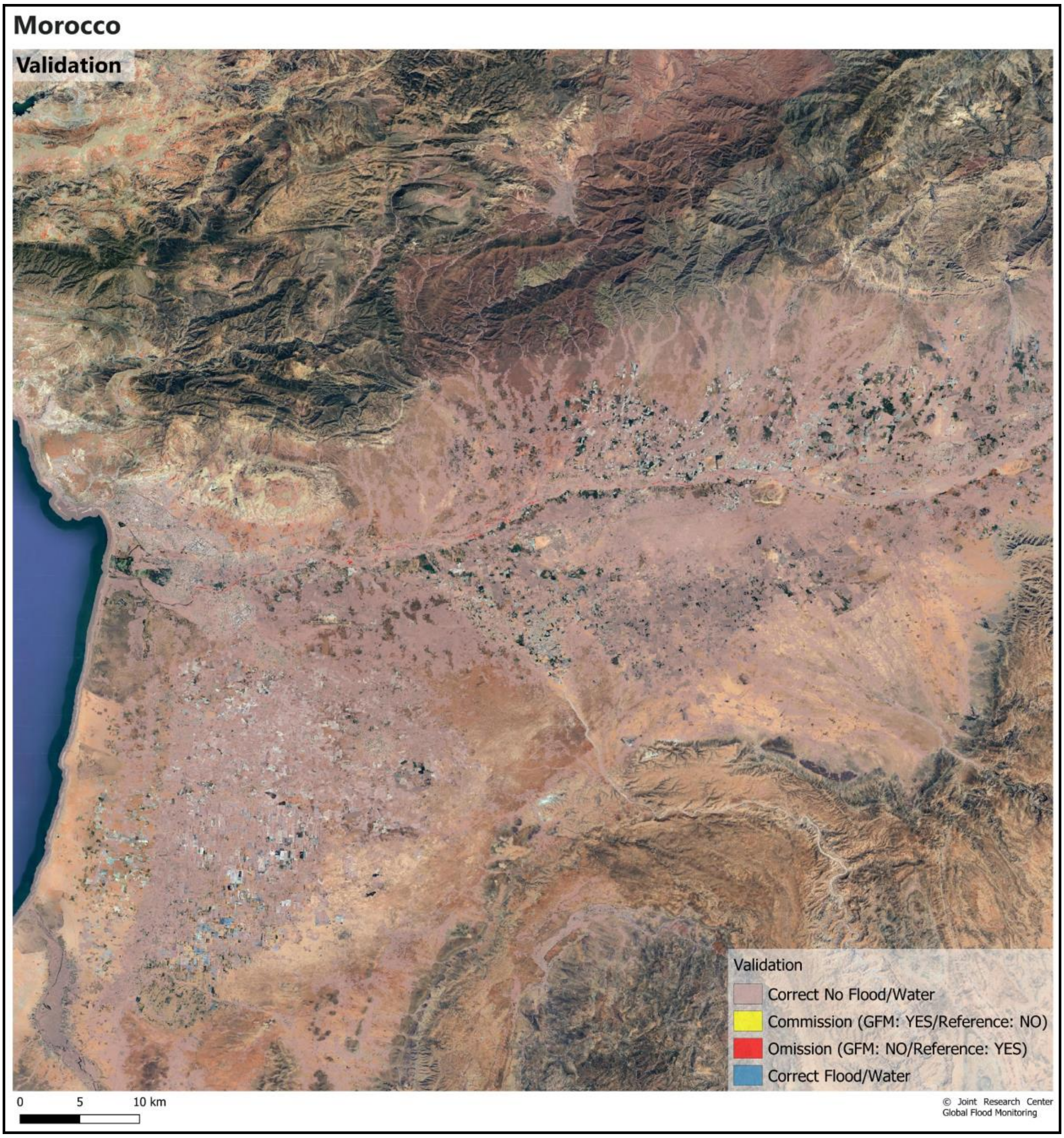

Figure 8: Use Case 2 – Difference map between Observed Flood Extent of the GFM and the reference dataset, showing the highly agreeing results (in blue), and slight under-estimation (in red) by the GFM product compared with the reference dataset.

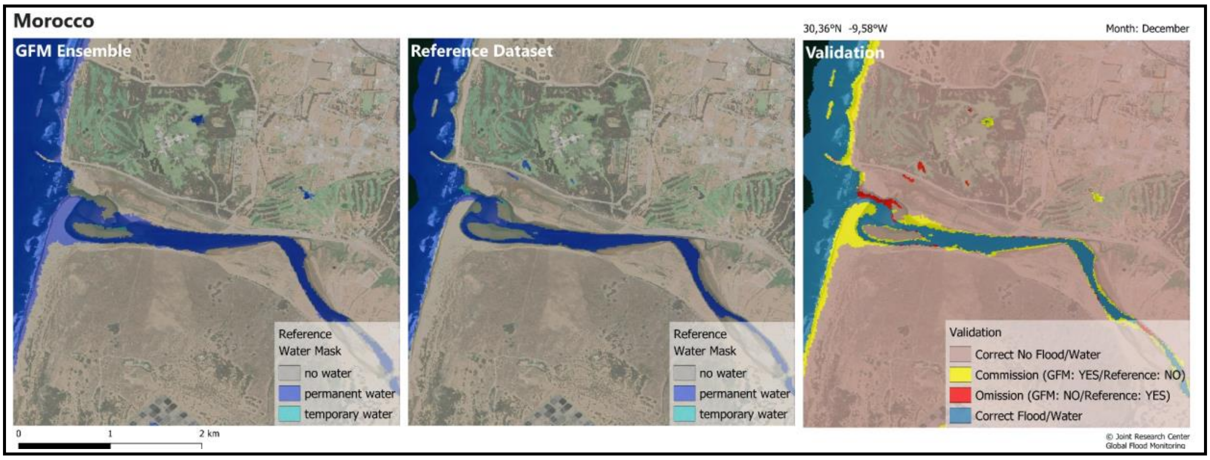

Figure 9: Use Case 2 – Reference Water Mask of the GFM (left) and the reference dataset (middle), and the difference map (right), showing similar permanent water in the upstream river region, and larger differences at the river mouth and the coastline.

4.2.3 Use Case 3 (Myanmar, 21.07.2021) - Discussion of results for Observed Flood Extent and Reference Water Mask

Heavy rains and floods resulting from a monsoon weather system affected southeastern parts of Myanmar, in July 2021. The heavy rainfalls caused a rise in river levels, and danger-levels of some major rivers and dams were exceeded. The floods led to crop damage, especially within paddy fields.

As can be seen in Figure 10, for this Use Case the Observed Flood Extent of the GFM product and of the reference dataset differ significantly, similar to Use Case 2. The CSI value (11.0%) is very low, with the major problem again being a substantial under-detection of flooded areas, leading to a very high Omission Error (88.9%) for this Use Case.

In order to investigate the root cause of the high Omission Error, the performance of the GFM individual algorithms was assessed. No single algorithm had exceptional outliers (e.g. no data, incomplete coverage), but all detected less water than the reference dataset. Some algorithms were closer to the reference dataset, but due to other algorithms detecting less flooding, the ensemble majority rule resulted in larger deviations from the reference dataset.

As can be seen in Figure 12, the permanent water of the Reference Water Mask detected by the GFM product and by the reference dataset, match very well (CSI = 83.5%). Rivers and permanent water areas are well mapped in both datasets.

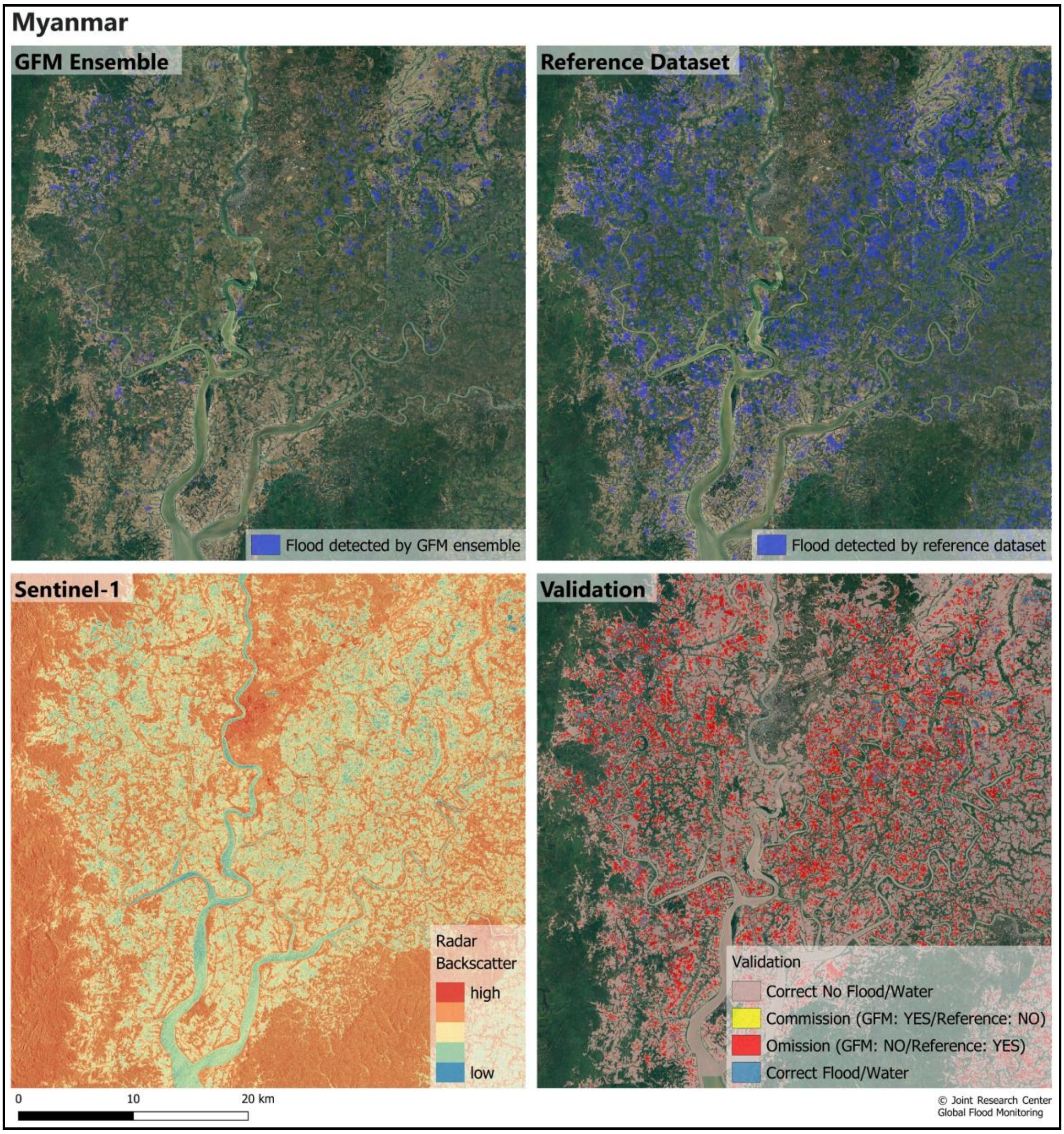

Figure 10: Use Case 3 – Observed Flood Extent from the GFM (top-left) and the reference dataset (top-right); Sentinel-1 SAR data (bottom left); difference map (bottom-right).

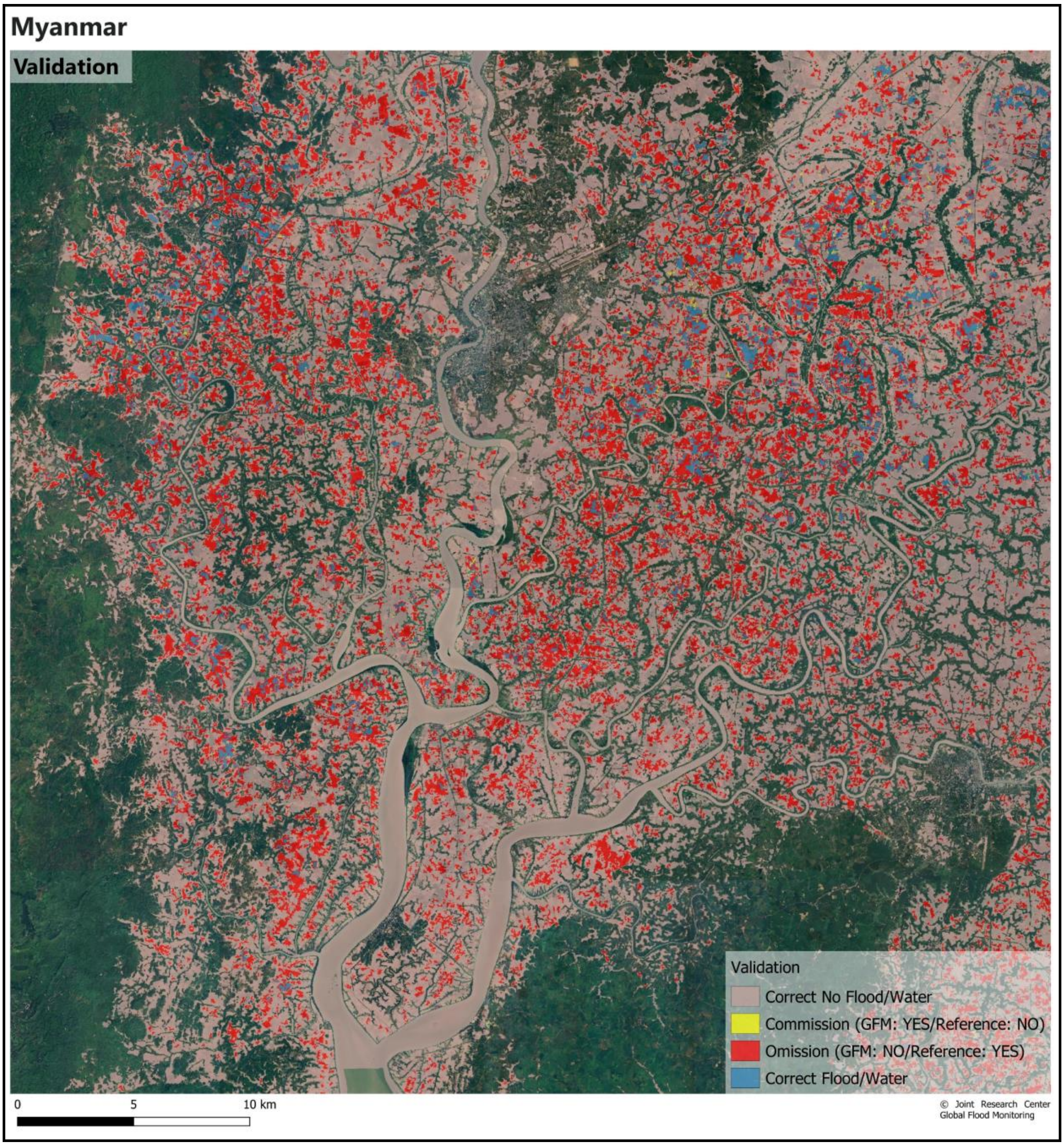

Figure 11: Use Case 3 – Difference map between Observed Flood Extent of the GFM and the reference dataset, showing the agreeing results (in blue), and high under-estimation (in red) by the GFM product compared with the reference dataset.

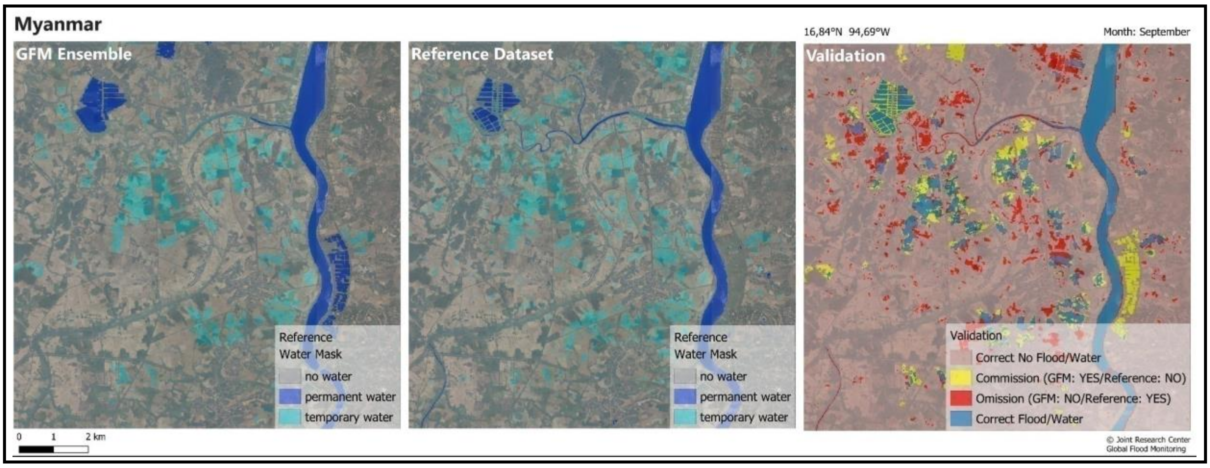

Figure 12: Use Case 2 – Reference Water Mask of the GFM (left) and the reference dataset (middle) and the difference map (right), highlighting differences of seasonal water detection in cropland.

4.2.4 Use Case 4 (France, 16.10.2018) - Discussion of results for Observed Flood Extent and Reference Water Mask

As shown in Table 8, for Use Case 4 the CSI value (71%) for the Observed Flood Extent is satisfactory, while the bias (0.76) indicates an under-detection compared with the reference dataset. As shown in Table 9, for the permanent water of the Reference Water Mask, the CSI (86 %) is high, while the bias (1.14) indicates that the permanent water extent is slightly over-estimated.

Overall, for this Use Case the GFM product and the reference dataset are in good agreement. Figure 13 and Figure 14 show that the main differences are due to under-estimation of the Observed Flood Extent by the GFM product. This concerns mainly agricultural fields, which are not captured in the GFM product. As can be seen in Figure 15, for the Reference Water Mask, the GFM product and reference dataset agree in most parts. The GFM product tends to over-estimate the water extent as compared with the reference dataset. This can mainly be attributed to border pixels around the water bodies in the port area, and to fishponds that are rather seasonal in nature. Additionally, some areas that are denoted as seasonal water in the reference dataset are classified as permanent water in the GFM product.

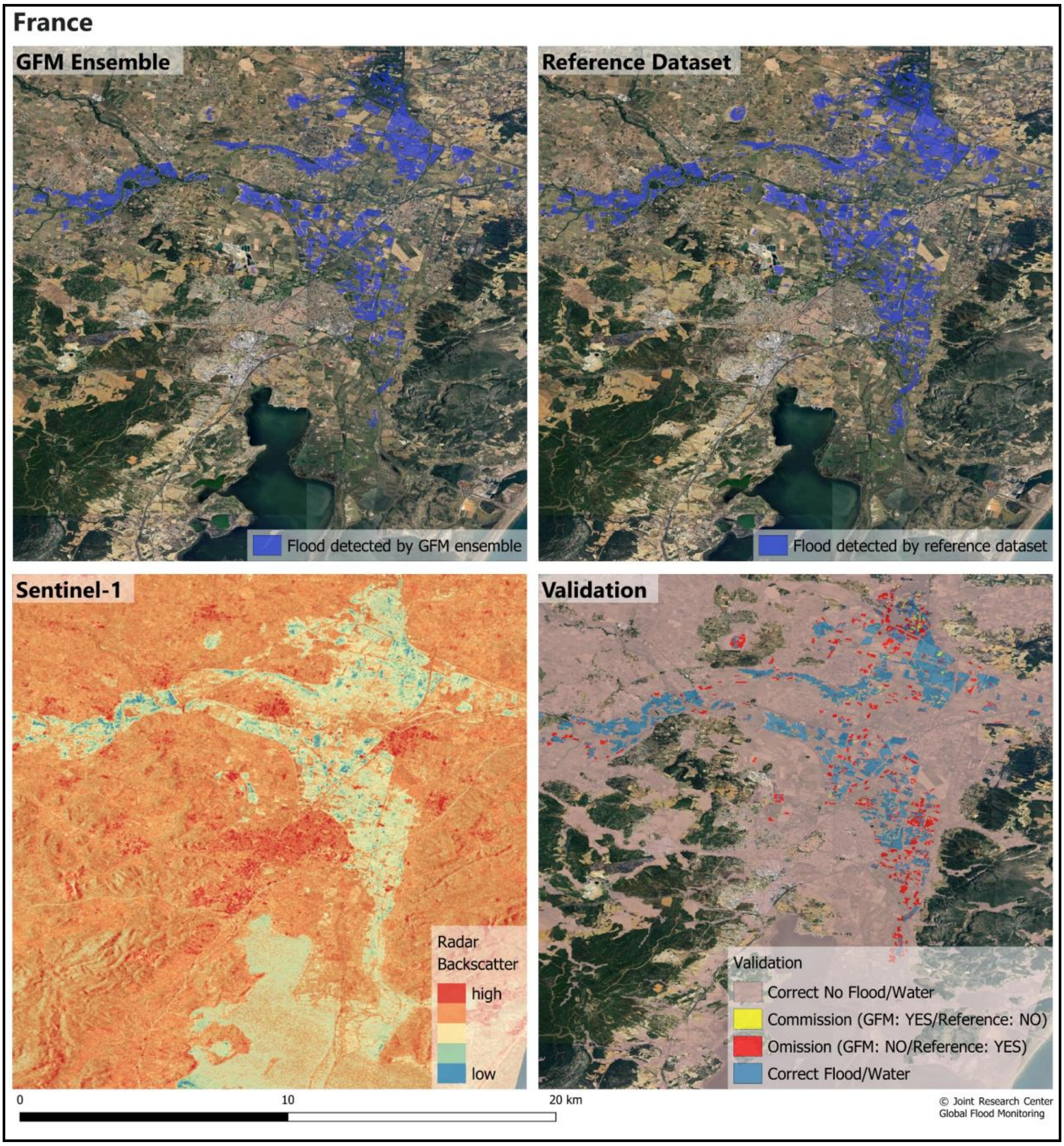

Figure 13: Use Case 4 – Observed Flood Extent from the GFM (top-left) and the reference dataset (top-right); Sentinel-1 SAR data (bottom left); difference map (bottom-right).

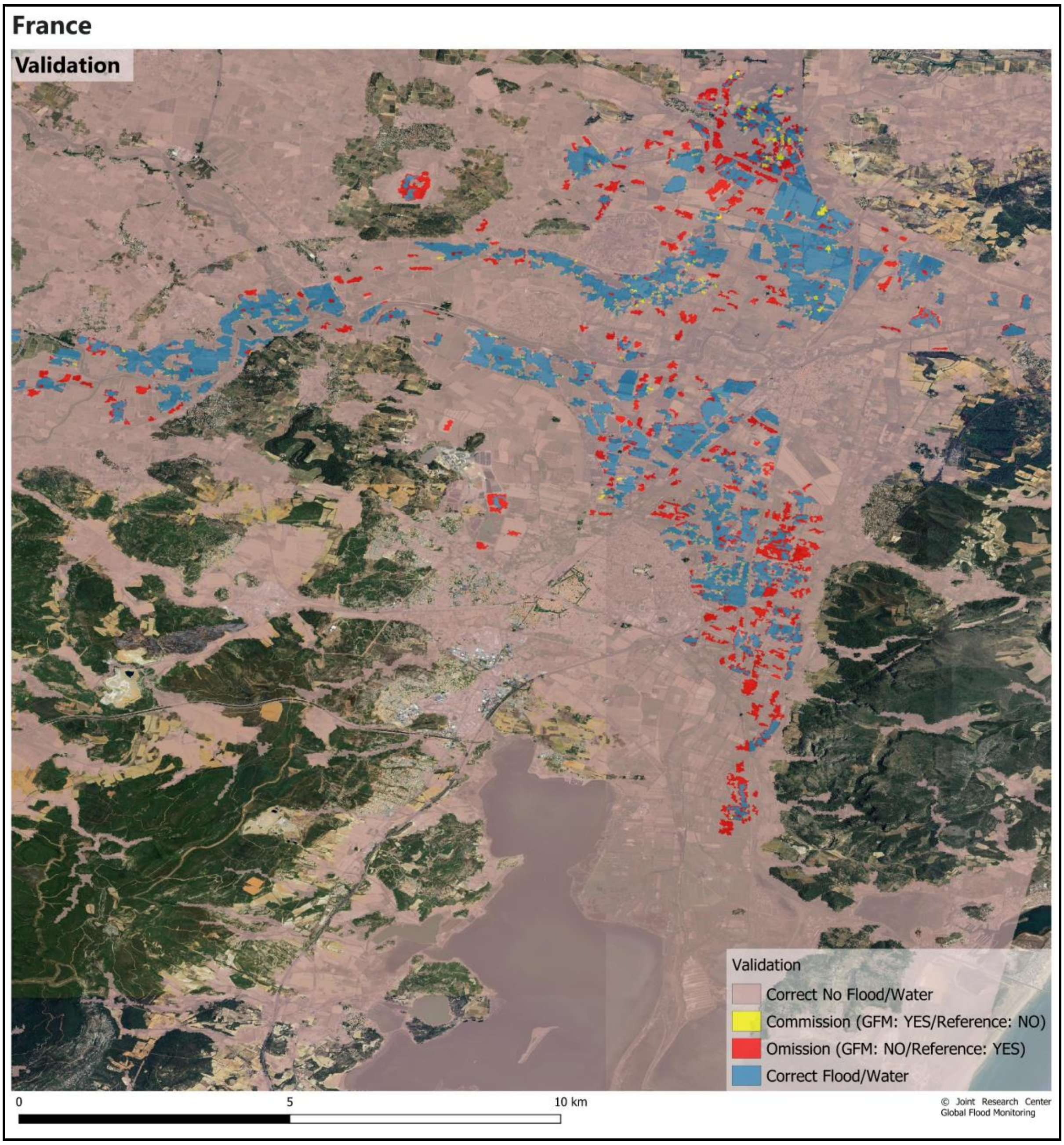

Figure 14: Use Case 4 – Difference map between Observed Flood Extent of the GFM and the reference dataset, showing the highly agreeing results (in blue), and slight under-estimation (in red) by the GFM product compared with the reference dataset.

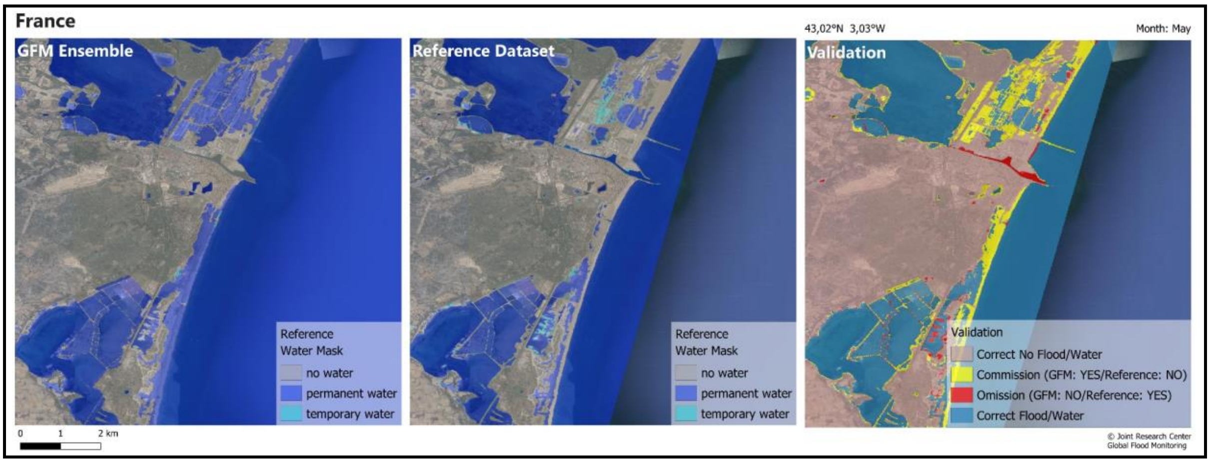

Figure 15: Use Case 4 – Reference Water Mask of the GFM (left) and the reference dataset (middle), and the difference map (right), highlighting over-estimations (in yellow) by the GFM product near an artificial reservoir.

4.2.5 Use Case 5 (Indonesia, 29.03.2023) - Discussion of results for Observed Flood Extent and Reference Water Mask

As can be seen in Table 8, for Use Case 5 the CSI value (69.9%) for the Observed Flood Extent is satisfactory, while a bias of 0.93 indicates a slight under-estimation compared with the reference dataset. As can be seen in Table 9, for the permanent water of the Reference Water Mask, the CSI value (32.8 %) is low, while a bias of 2.57 suggests that the permanent water is over-estimated.

As can be seen in Figure 16 and Figure 17, a visual check of the GFM product and the reference datasets shows a large agreement (as suggested by the accuracy results). The smaller red and yellow patches in the difference map indicate over- and under-estimations of the flood extent from the GFM product compared with the reference dataset.

For the Reference Water Mask, for this Use Case the detection of rivers is in good agreement between both datasets, with slight over- and under-estimations due to border effects. The high over-estimation indicated by the bias value for the permanent water can be attributed to a wetland area. As can be seen in Figure 18, the GFM product classifies this as permanent water, whereas the reference dataset delineates a much smaller area as permanent water and partially as seasonal water.

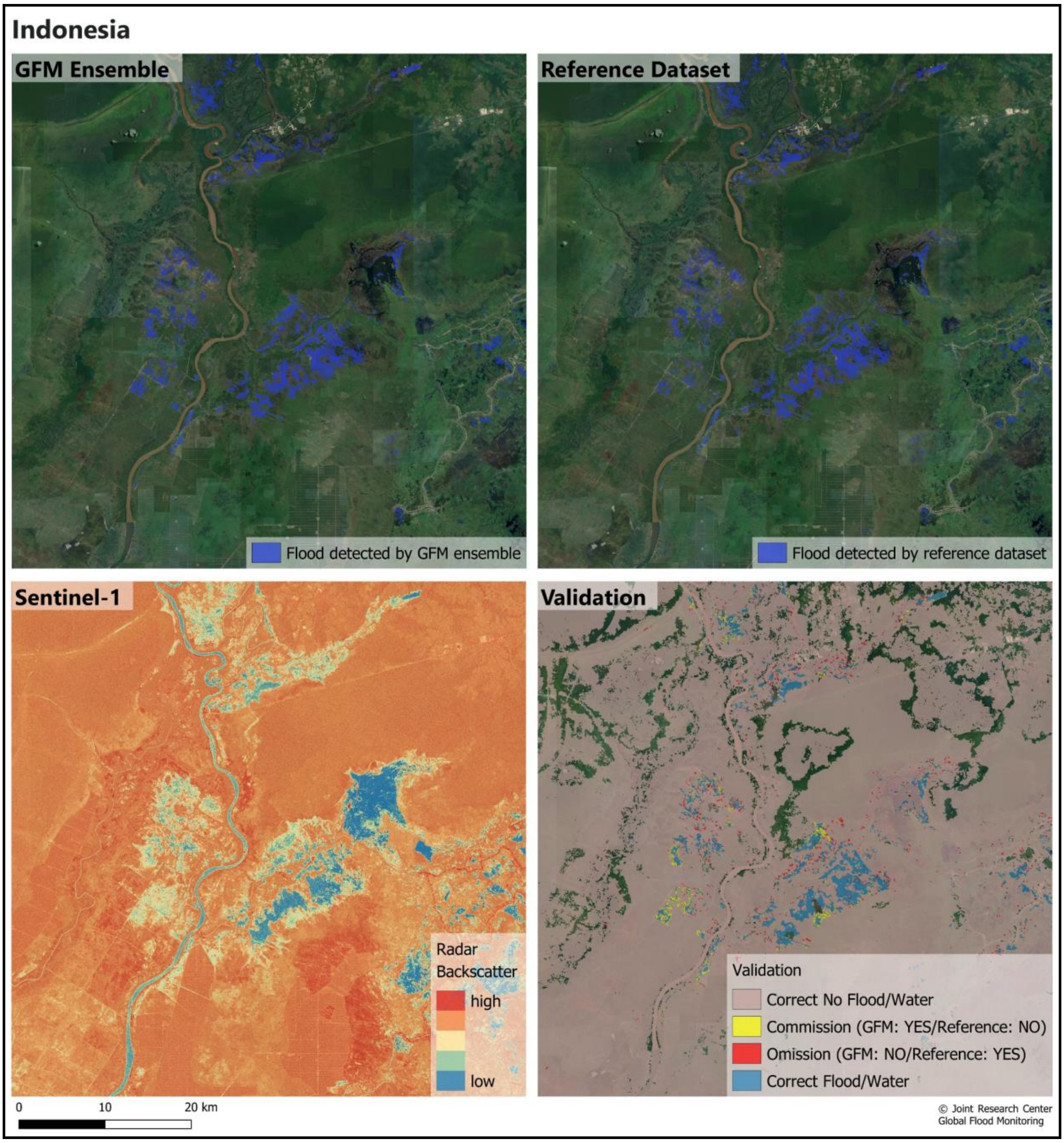

Figure 16: Use Case 5 – Observed Flood Extent from the GFM (top-left) and the reference dataset (top-right); Sentinel-1 SAR data (bottom left); difference map (bottom-right).

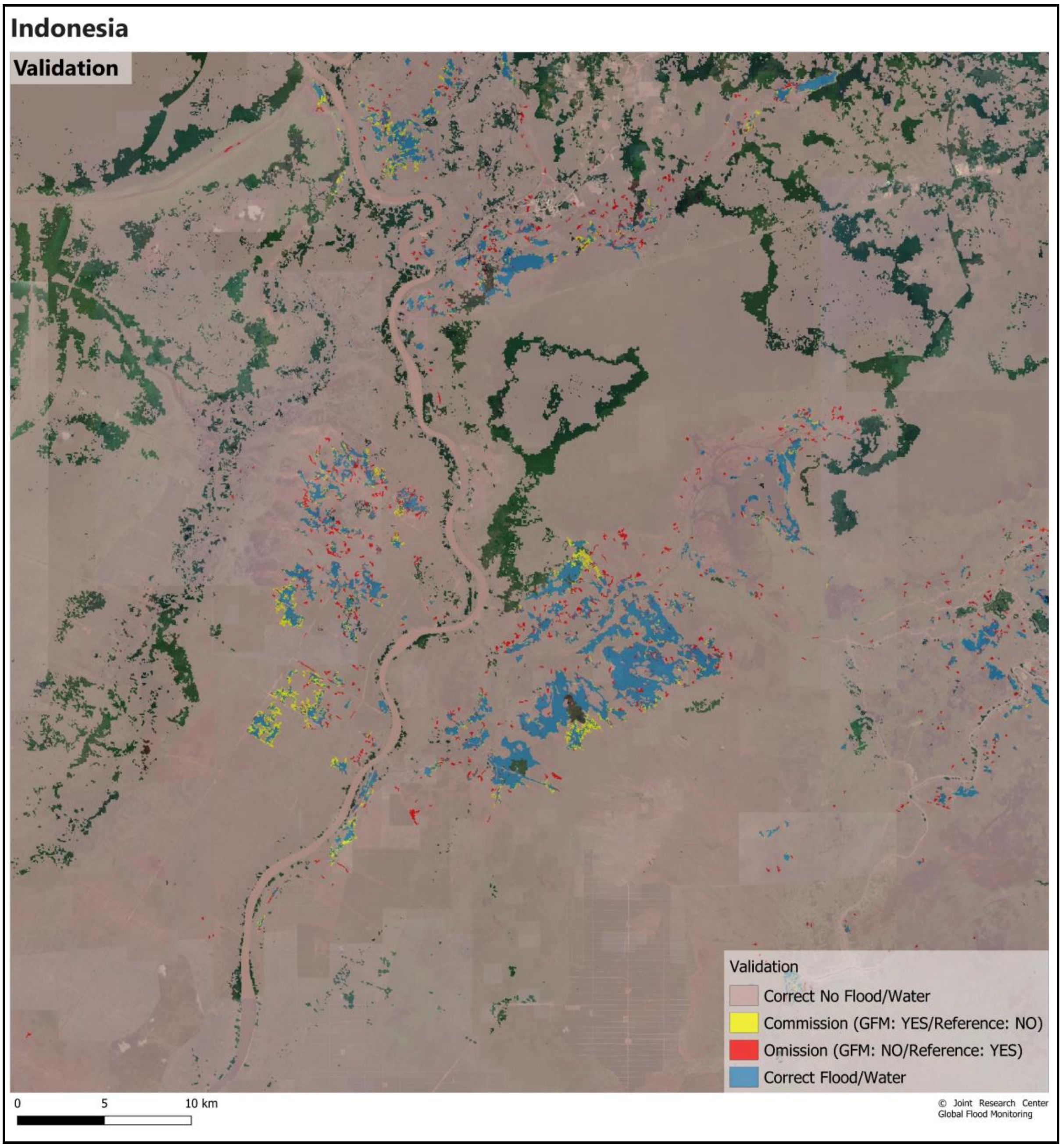

Figure 17: Use Case 5 – Difference map between Observed Flood Extent of the GFM and the reference dataset, showing the highly agreeing results (in blue), and over- (in yellow) and under-estimations (in red) by the GFM product compared with the reference dataset.

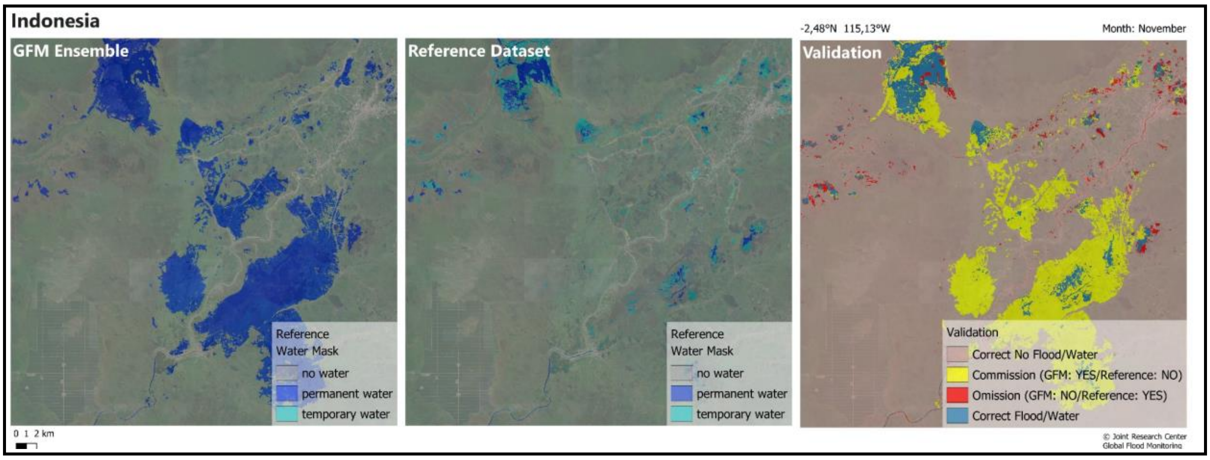

Figure 18: Use Case 5 – Reference Water Mask of the GFM (left) and the reference dataset (middle), and the difference map (right), highlighting over-estimation (in yellow) by the GFM product for wetland areas.

4.2.6 Use Case 6 (Italy, 16.05.2023) - Discussion of results for Observed Flood Extent and Reference Water Mask

As can be seen in Table 8, the Observed Flood Extent of the GFM product and of the reference dataset shows remarkable agreement (CSI = 82%), despite a significant amount of under-estimation (Omission Error = 16.6%). This under-estimation is primarily due to individual agricultural fields dispersed around the periphery of main floodwater clusters, and seems to be randomly distributed. On the other hand, Commission Errors (2%) are low. These differences are highlighted in the difference map in Figure 19 and Figure 20.

In the case of the permanent water of the Reference Water Mask, the agreement between the GFM product and the reference dataset is similarly very high (CSI = 86.3%, bias = 1.077). Here, the differences are characterized by over-estimation (Commission Error = 10.7%), rather than under-estimation (Omission Error = 3.7%) by the GFM product. Many of these errors are classification discrepancies: the GFM product appears to include seasonal water in its permanent water. Nonetheless, as shown in Figure 21, the overall agreement between the permanent water of the GFM product and of the reference dataset, is remarkably high.

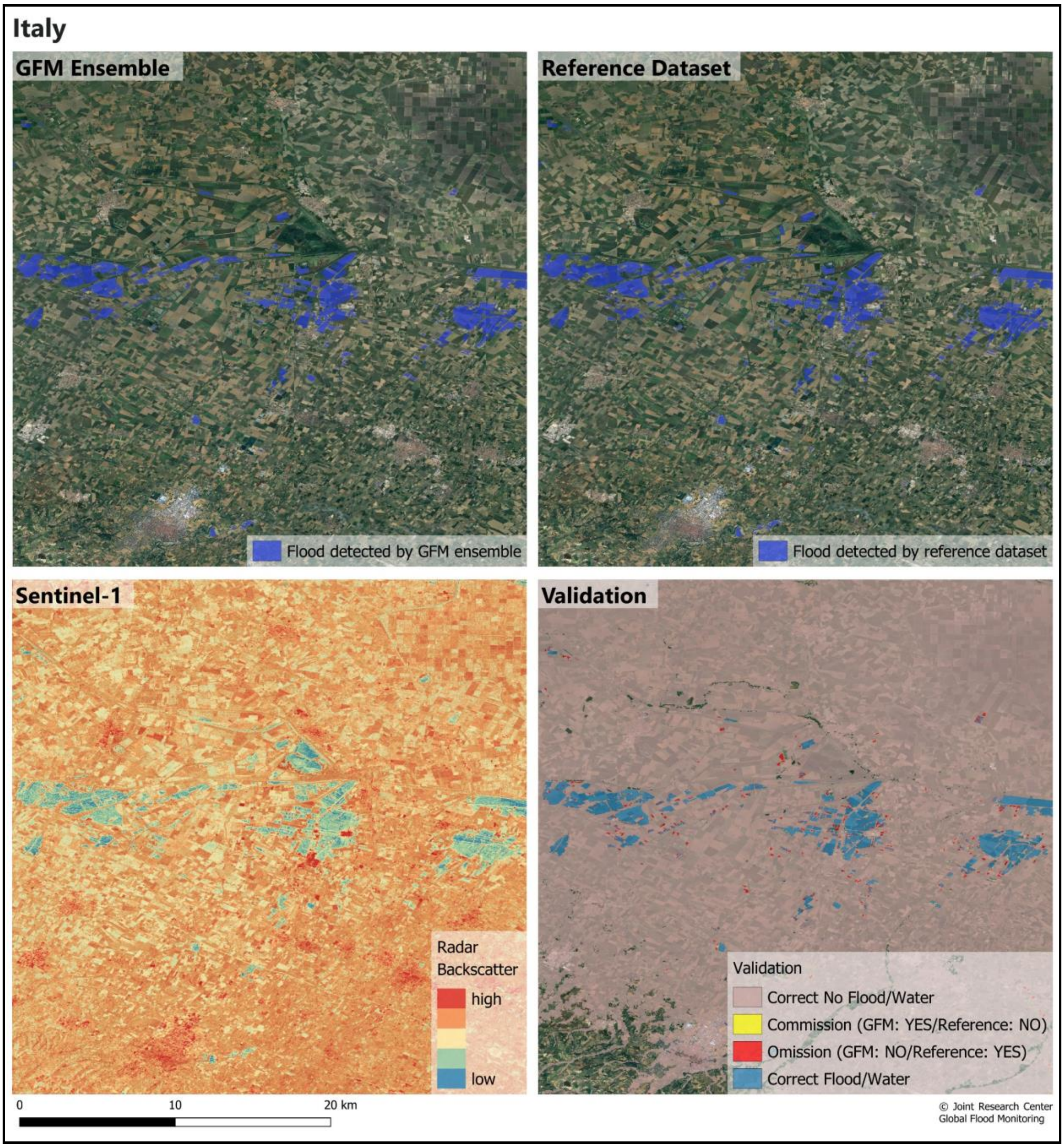

Figure 19: Use Case 6 – Observed Flood Extent from the GFM (top-left) and the reference dataset (top-right); Sentinel-1 SAR data (bottom left); difference map (bottom-right).

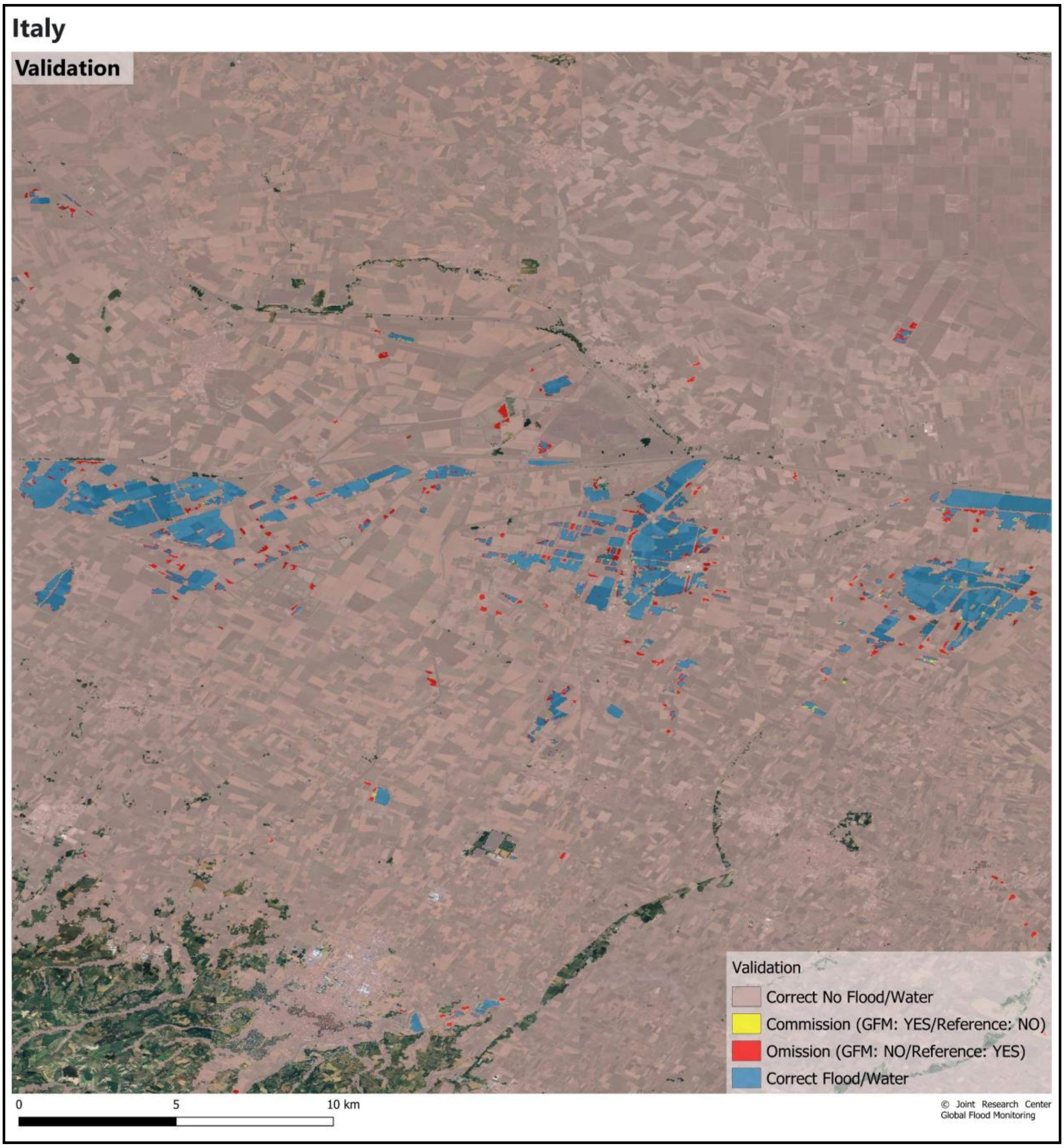

Figure 20: Use Case 6 – Difference map between Observed Flood Extent of the GFM and the reference dataset, showing the highly agreeing results (in blue), and slight under-estimations (in red) by the GFM product compared with the reference dataset.

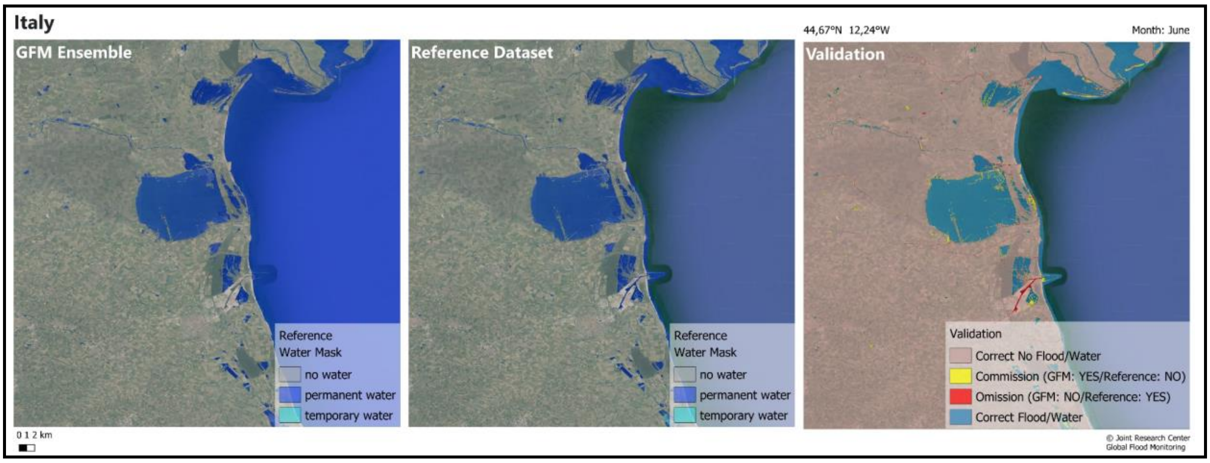

Figure 21: Use Case 6 - Reference Water Mask of the GFM (left) and the reference dataset (middle), and the difference map (right).

4.2.7 Use Case 7 (Venezuela, 29.07.2017) - Discussion of results for Observed Flood Extent and Reference Water Mask

As can be seen in Table 8, for this Use Case the Observed Flood Extent is in good agreement with the reference dataset (CSI = 71%). As can be seen in Figure 22 and Figure 23, the main flooded areas and floodwater pools and clusters are accurately identified, although a significant amount of both false positives (Commission Error = 13%) and false negatives (Omission Error = 20.6%) are present. False positives are mainly attached to areas for which the permanent / seasonal water extent has been estimated too conservatively, and are thus resulting in extensively detected flood water areas. False negatives are typically not adjacent to correctly identified pixels, but rather stand-alone features speckled across the area of interest. The higher Omission Error results in an overall slight under-estimation by the GFM product, reflected in the bias value of 0.91 (target = 1).

The main difference between the permanent water of the Reference Water Mask of the GFM product and of the reference dataset, is a significant over-estimation by the GFM product (Commission Error = 29.7%, bias = 1.345). Nevertheless, overall agreement is reasonable (CSI = 67.5%). As can be seen in Figure 24, in many cases over-estimation appears to be a classification issue. Especially on the western bank of the Orinoko River, between its tributaries Arichuna and Apure, various water bodies are classified as permanent water by the GFM product, while in the reference dataset many of these appear as seasonal water.

As can also be seen in Figure 24, overall agreement between the permanent water of the Reference Water Mask is satisfactory. The vast areas omitted by the GFM product (right; in red) are in fact seasonal water areas in the reference dataset (for October, in this case). Agreement in seasonal water extent is much more difficult to achieve.

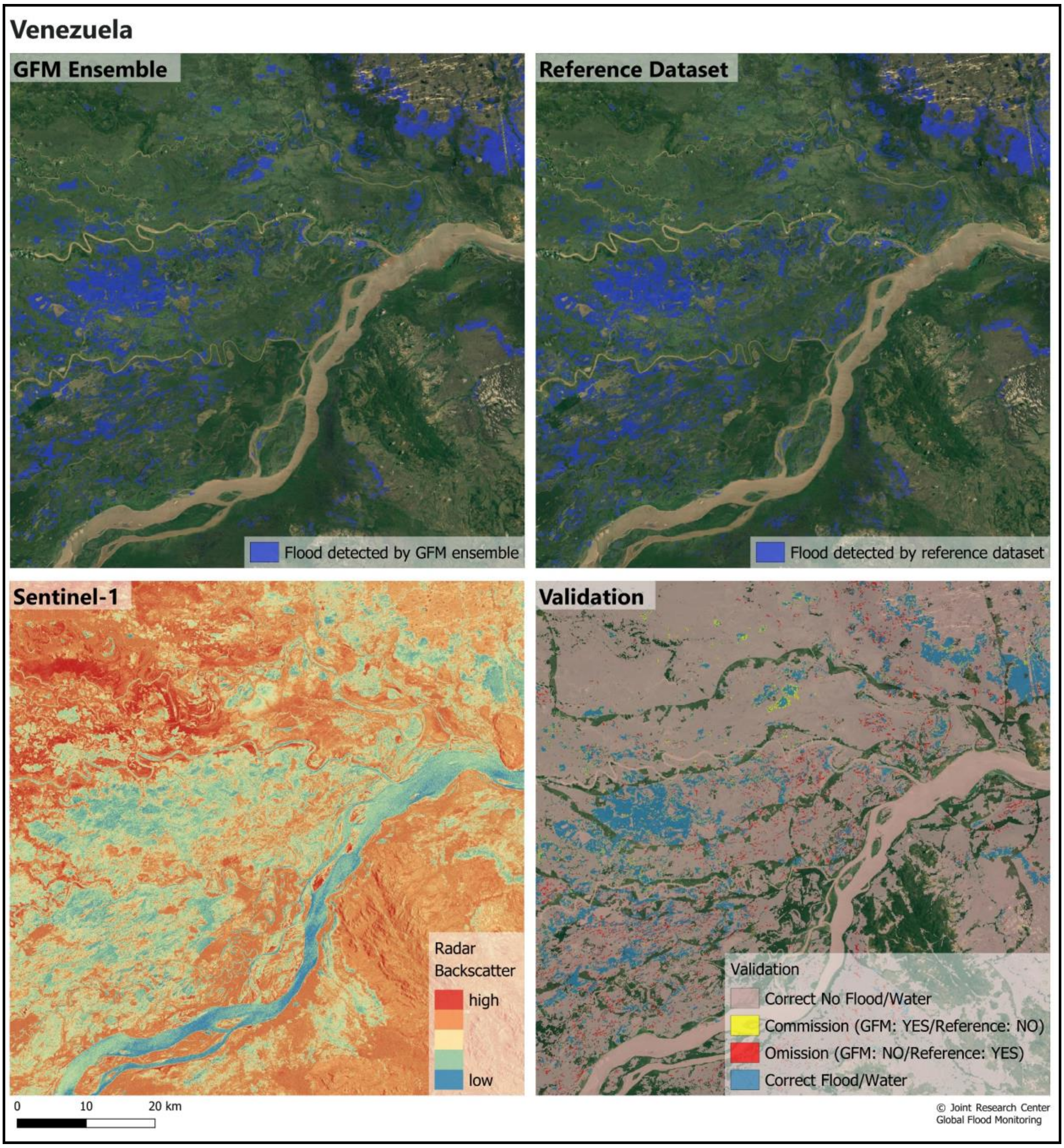

Figure 22: Use Case 7 – Observed Flood Extent from the GFM (top-left) and the reference dataset (top-right); Sentinel-1 SAR data (bottom left); difference map (bottom-right).

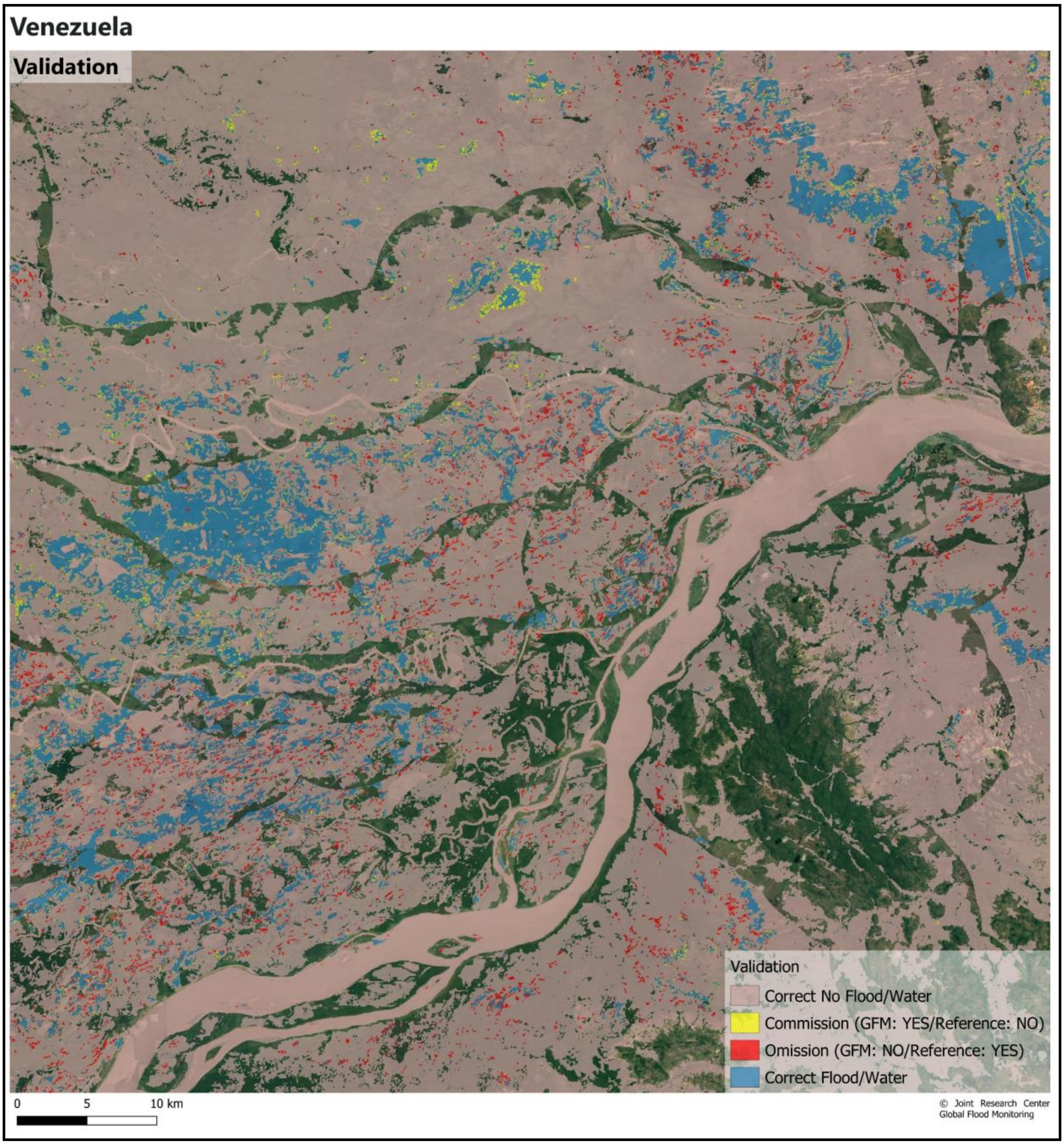

Figure 23: Use Case 7 – Difference map between Observed Flood Extent of the GFM and the reference dataset, showing the agreeing results (in blue), and under- (in red) and over-estimations (in yellow) by the GFM product compared with the reference dataset.

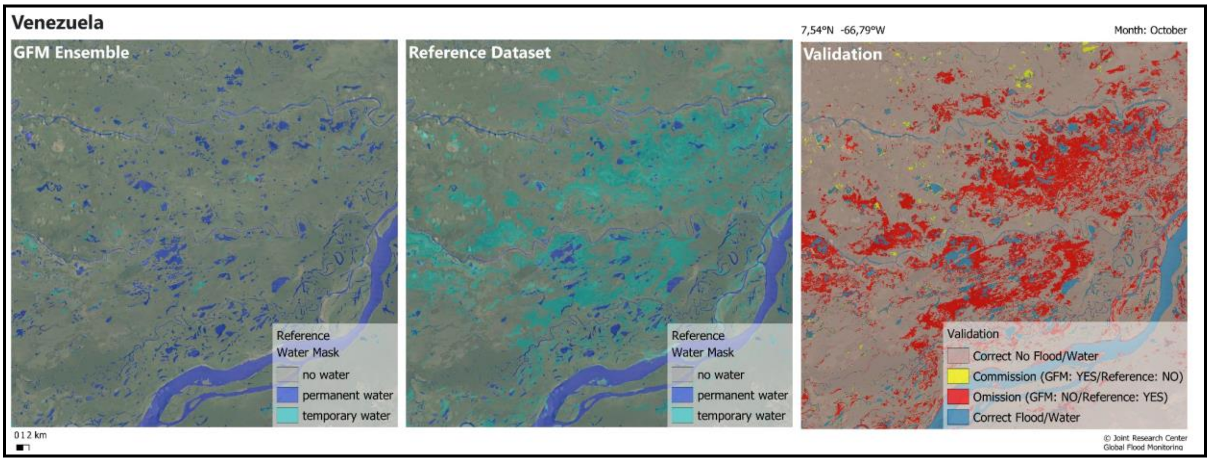

Figure 24: Use Case 7 – Reference Water Mask of the GFM (left) and the reference dataset (middle), and the difference map (right), highlighting significant under-estimation (in red) by the GFM product, mainly of seasonal water.

4.2.8 Use Case 8 (Bangladesh, 10.08.2023) - Discussion of results for Observed Flood Extent and Reference Water Mask

As can be seen in Table 8, Figure 25 and Figure 26, for this Use Case, the Observed Flood Extent of the GFM product and the reference dataset show very high agreement (CSI value = 77.8%), correctly identifying each of several flood-affected areas. As can be seen in Figure 26, there is an apparent "salt and pepper" pattern of both Commission Errors (12.2%) and Omission Errors (12.8%). The dispersed pattern of these misclassifications indicates that they are likely to be random noise rather than a systematic error. The similarity of both errors gives a bias value (0.99) that is very close to the target (1.0), indicating no systematic error.

As can be seen in Table 9, the permanent water of the Reference Water Mask also achieved good accuracy (CSI = 73.8%, bias = 1.15), despite a considerable number of false positives (20.6%) and false negatives (8.8%). As can be seen in Figure 27, the differences occur mainly (a) along the coastline, where the GFM product appears to over-estimate the water extent by a significant margin, and (b) in the Karnaphuli River, where a whole section of the river is missed by the GFM product (shown in red, on the right of Figure 27), interestingly not at the river mouth but mid-stream and where it is very broad.

Significant discrepancies in the seasonal water occur along the coastlines. The GFM product generally over-estimates coastal water extent, and does not show any month-to-month variation in delineation of the coast. In the reference dataset, there is a buffer of pixels classified as seasonal water along the coast. As the Reference Water Mask is constructed from multiple scenes and uses a threshold approach to classify water as either permanent or seasonal, the stage of the tidal cycle at the time of scene capture could influence the results. Further discrepancies are present on the Karnaphuli River, at the height of the Chittagong City, where small clusters of pixels classified as "non-water" or "seasonal water" are present in the middle of the river. This is due to the presence of many large ships and barges on the water. Interestingly, this section of the river is entirely missed by the GFM product.

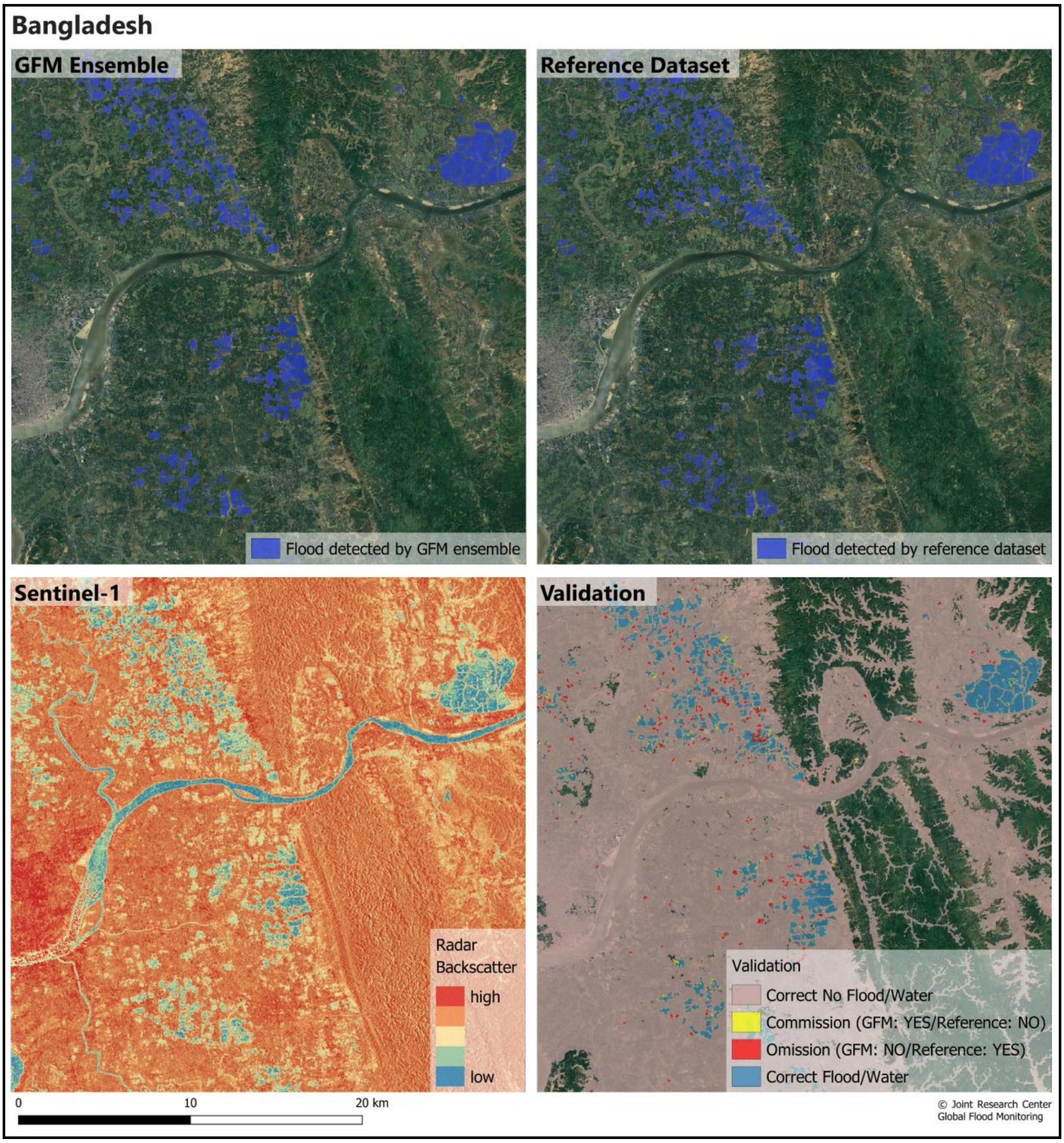

Figure 25: Use Case 8 – Observed Flood Extent from the GFM (top-left) and the reference dataset (top-right); Sentinel-1 SAR data (bottom left); difference map (bottom-right).

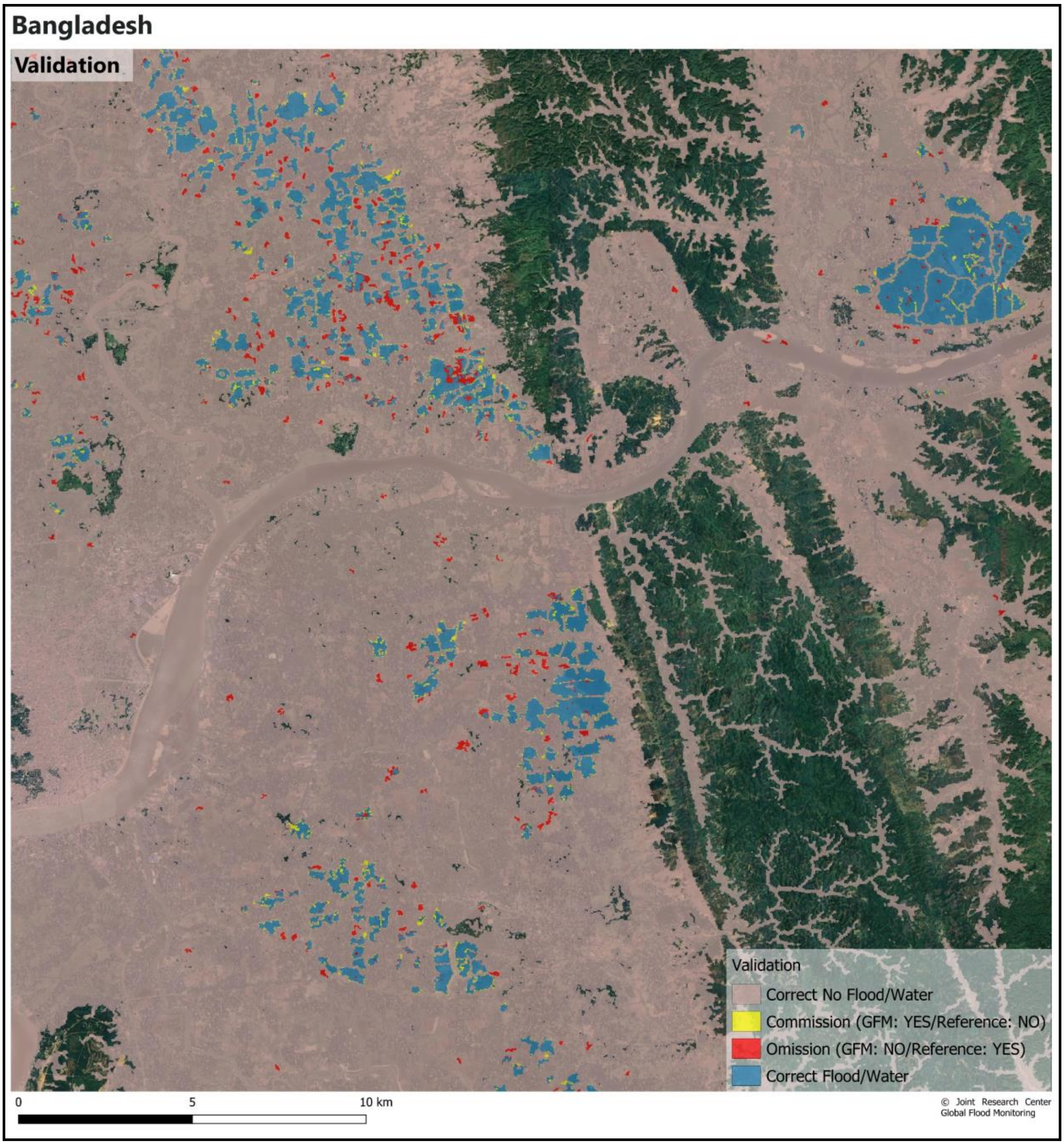

Figure 26: Use Case 8 – Difference map between Observed Flood Extent of the GFM and the reference dataset, showing the agreeing results (in blue), and under- (in red) and over-estimations (in yellow) by the GFM product compared with the reference dataset.

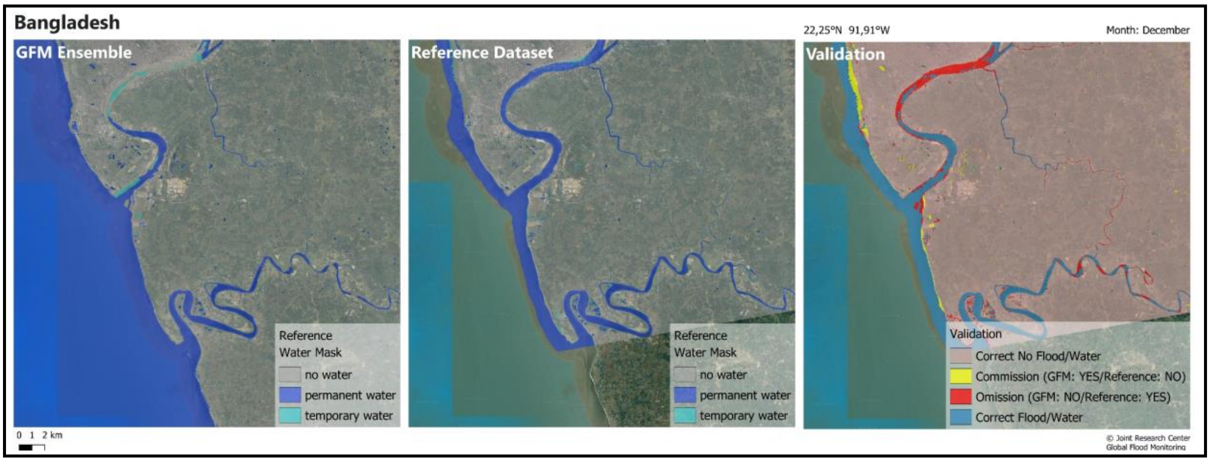

Figure 27: Use Case 8 – Reference Water Mask of the GFM (left) and of the reference dataset (middle), and the difference map (right).

4.2.9 Use Case 9 (Greece, 07.09.2023) - Discussion of results for Observed Flood Extent and Reference Water Mask

As can be seen in Table 8, for this Use Case, the Observed Flood Extent of the GFM product agrees very well with the reference dataset (CSI value = 82.1%). The bias value (0.9) indicates slight under-estimation, also reflected in the Omission Error (14.3%). The false positive rate (Commission Error = 4.8%) is satisfactory.

The spatial extent of the Observed Flood Extent of the GFM product and of the reference dataset, as well as the differences between the two, are presented in Figure 28 and Figure 29. As can be seen, the main flood-affected areas are accurately identified, and only smaller floodwater pools on the periphery are omitted (Figure 29, in red). The vast majority of the omitted flood extent occurred in agricultural fields.

As can be seen in Table 9, the agreement between the permanent water of the Reference Water Mask of the GFM product and of the reference dataset, is similarly satisfactory (CSI value = 72.4%), despite a significant over-estimation (Commission Error = 27.6%, bias = 1.380). As can be seen in Figure 30, this discrepancy comes almost exclusively from the GFM product's over-estimation of the extent of Lake Smokovo, the only significant water body in the area. As the area of interest is very dry, the extent of Lake Smokovo is well captured by the GFM product, with respect to the reference dataset (middle), albeit with a string of false positive classifications (right, in yellow) around the perimeter. As this lake is some distance from the flood-affected area, the accuracy of its delineation had no impact on the Observed Flood Extent. Omission Errors (0.1%) are very low.

The results for this Use Case are very satisfactory, and the key statistical targets are met and even exceeded. Regarding the Observed Flood Extent, while Omission Errors (14.3%) are rather high, these concern dispersed agricultural fields and do not form significant clusters.

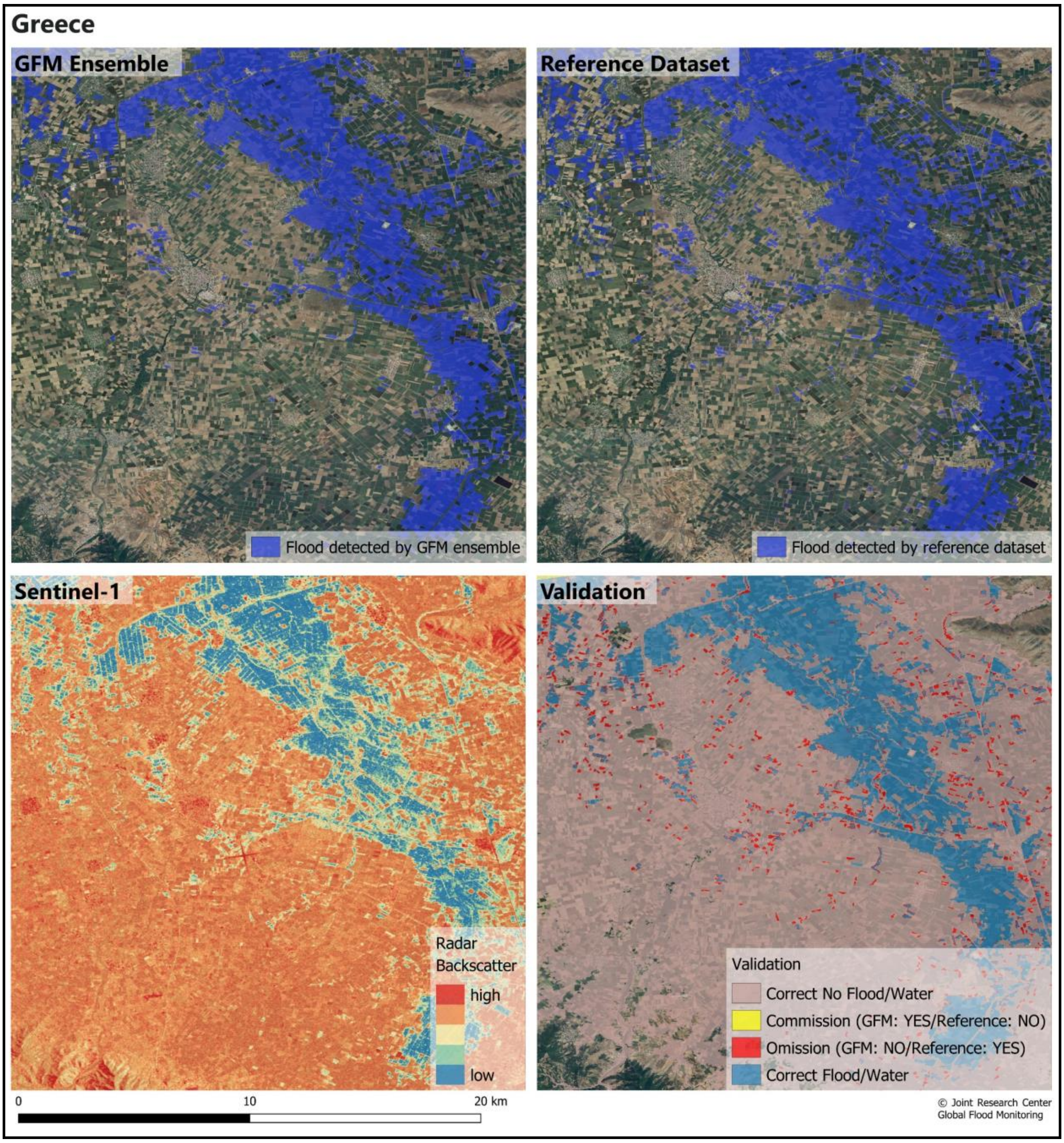

Figure 28: Use Case 9 – Observed Flood Extent from the GFM (top-left) and the reference dataset (top-right); Sentinel-1 SAR data (bottom left); difference map (bottom-right).

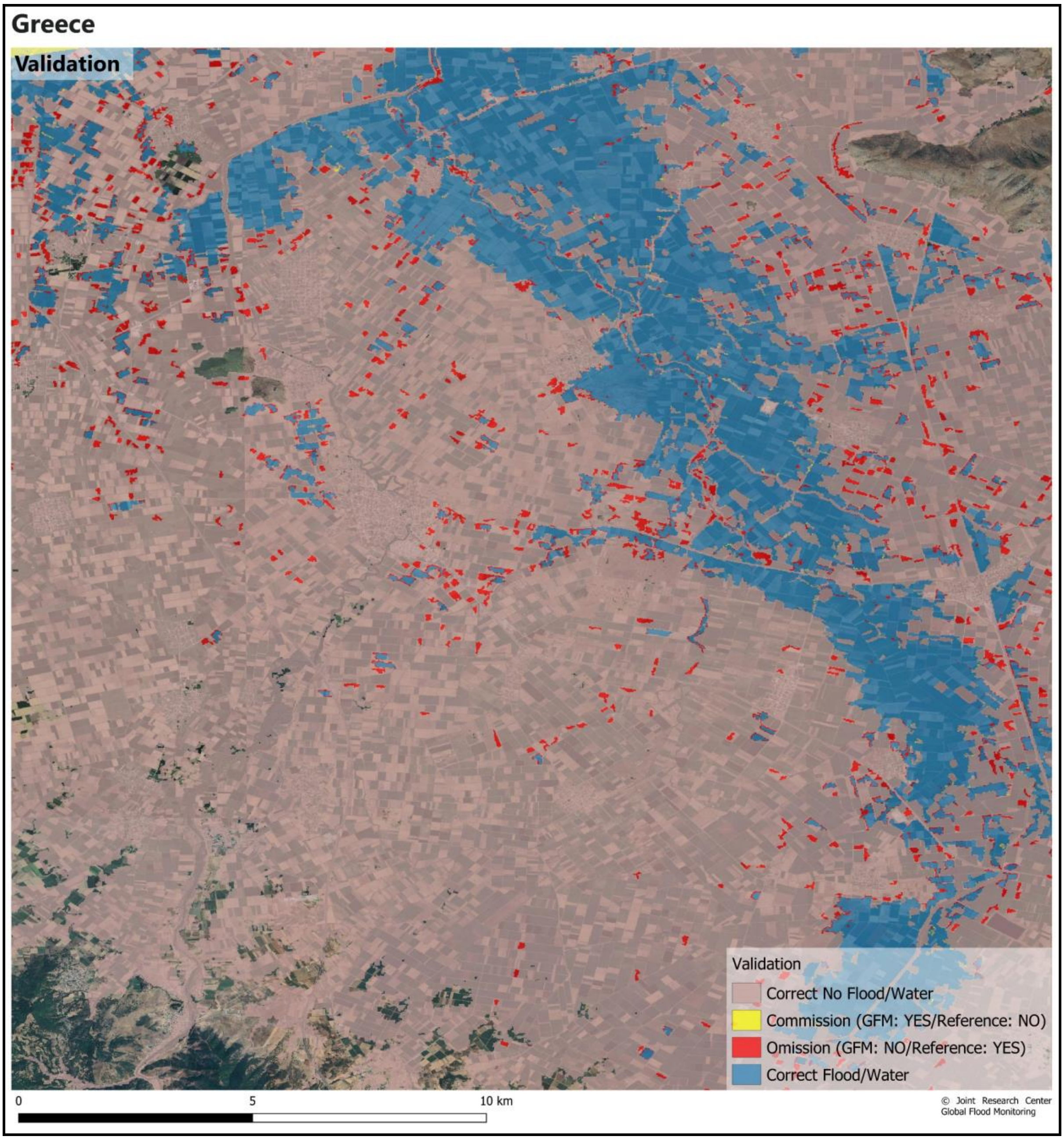

Figure 29: Use Case 9 – Difference map between Observed Flood Extent of the GFM and the reference dataset, showing agreeing results (in blue), and dispersed pattern of agricultural fields omitted (in red) by the GFM product compared with the reference dataset.

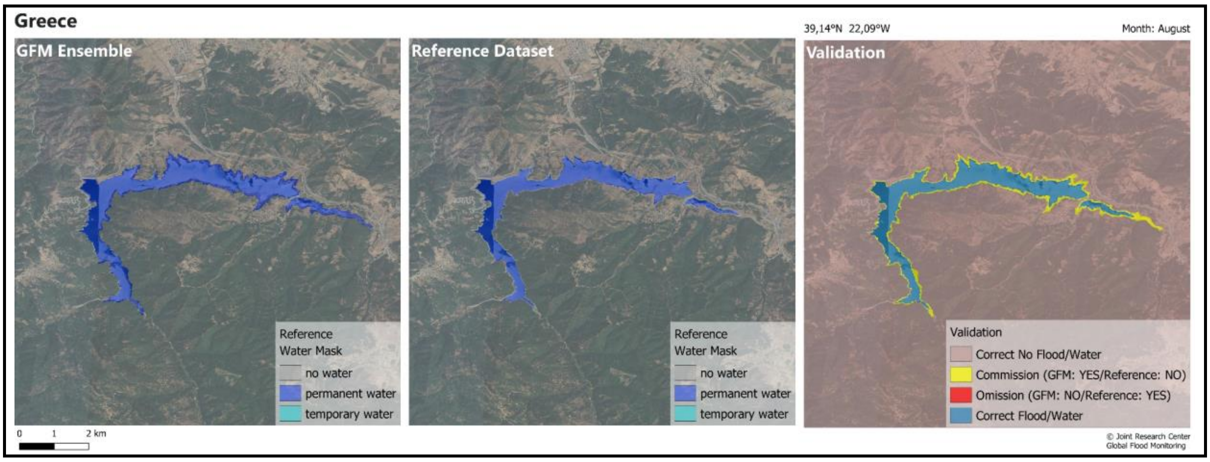

Figure 30: Use Case 9 – Reference Water Mask of the GFM (left) and of the reference dataset (middle), and the difference map (right).

4.2.10 Use Case 10 (Portugal, 23.12.2019) - Discussion of results for Observed Flood Extent and Reference Water Mask

As can be seen in Table 8, the Observed Flood Extent of the GFM product and of the reference dataset are in good agreement (CSI = 70%), except for significant (but localized) under-estimation (Omission Errors = 26.1%; bias = 0.793) in two areas. Both of the flooded areas not detected by the GFM product are seasonally inundated rice fields (arrozais). Figure 31 and Figure 32 show the main flood-affected area (where the river Mondego has overflowed, between the city of Figuera da Foz on the coast and Coimbra further upstream), and the differences between flooding detected by the GFM product and by the reference dataset.

As can be seen in Table 9 and Figure 32, the agreement between the permanent water of the Reference Water Mask of the GFM product and the reference dataset is also satisfactory (CSI = 74.2%), despite a slight over-estimation by the GFM product (Commission Error = 18.9%, bias = 1.107). The main differences in permanent water appear to be mainly in the extent of rivers and reservoirs, in areas not relevant to the flood event.

Regarding the seasonal water of the Reference Water Mask, it should be noted that the total number of pixels classified as seasonal water (in December, the month of the flood event) is very small, and their detection was based on a limited number of available scenes, and a much smaller sample size than in the case of permanent water detection. In the main area affected by flooding (upstream from the coastal city of Figuera da Foz) the differences again are clustered in fields under rice cultivation.

For this Use Case, the performance of the flood detection by the GFM product is satisfactory. Nevertheless, in the main affected area, there are two separate clusters of undetected inundated fields, resulting in a rather high Omission Error (26.1%).

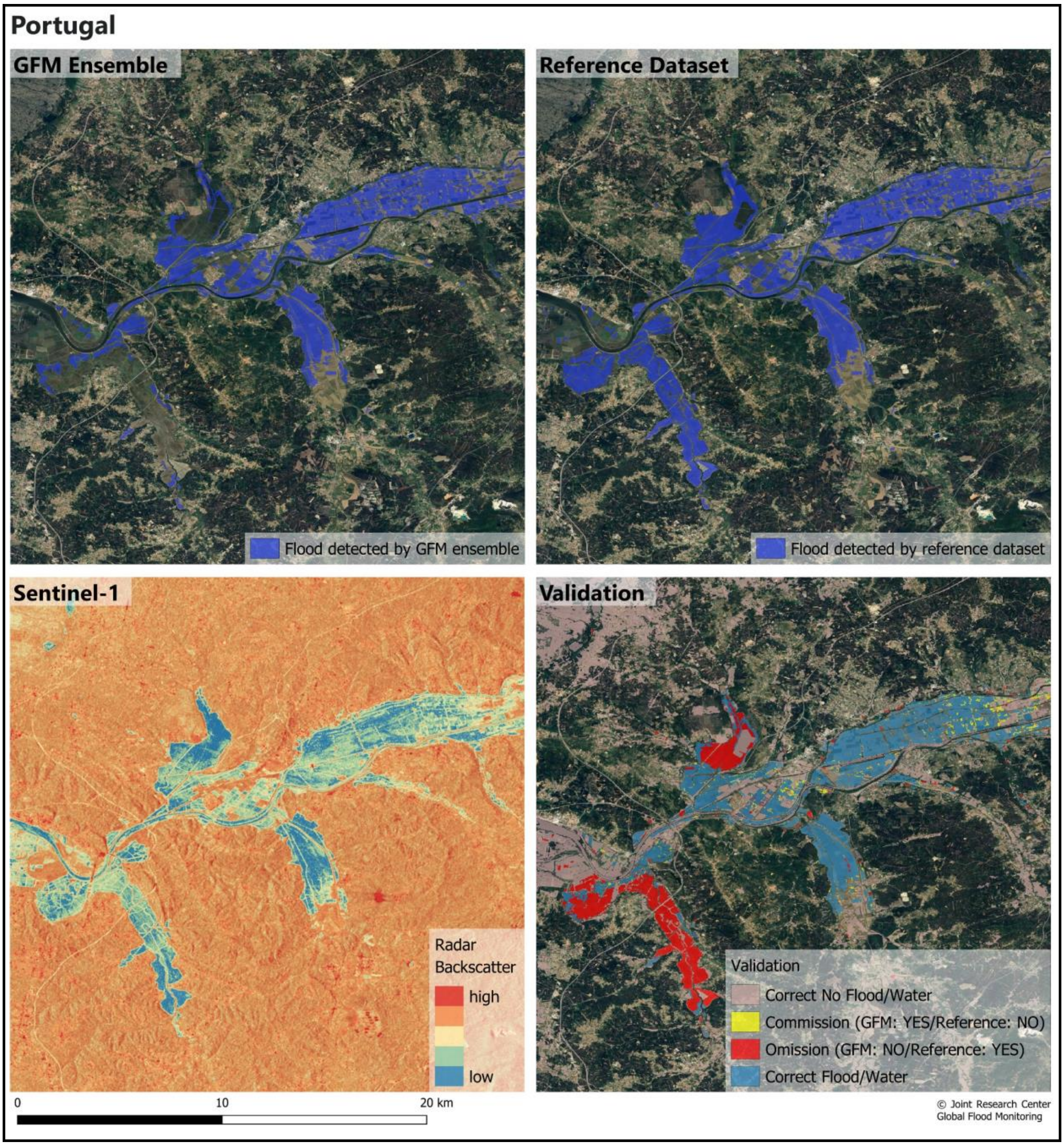

Figure 31: Use Case 10 – Observed Flood Extent from the GFM (top-left) and the reference dataset (top-right); Sentinel-1 SAR data (bottom left); difference map (bottom-right).

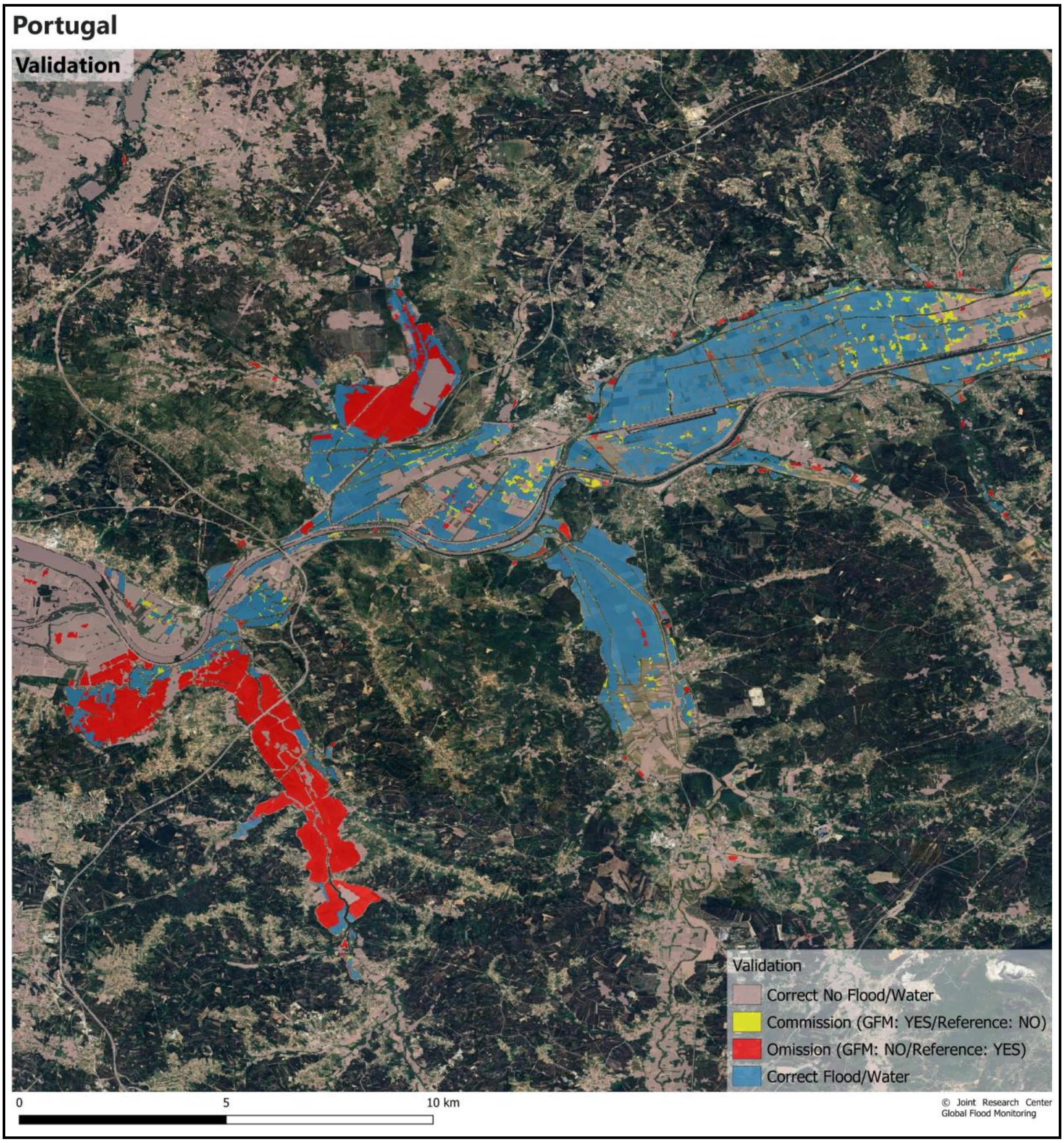

Figure 32: Use Case 10 – Difference map between Observed Flood Extent of the GFM and the reference dataset, showing the agreeing results (in blue), and under-estimations (in red) by the GFM product compared with the reference dataset.

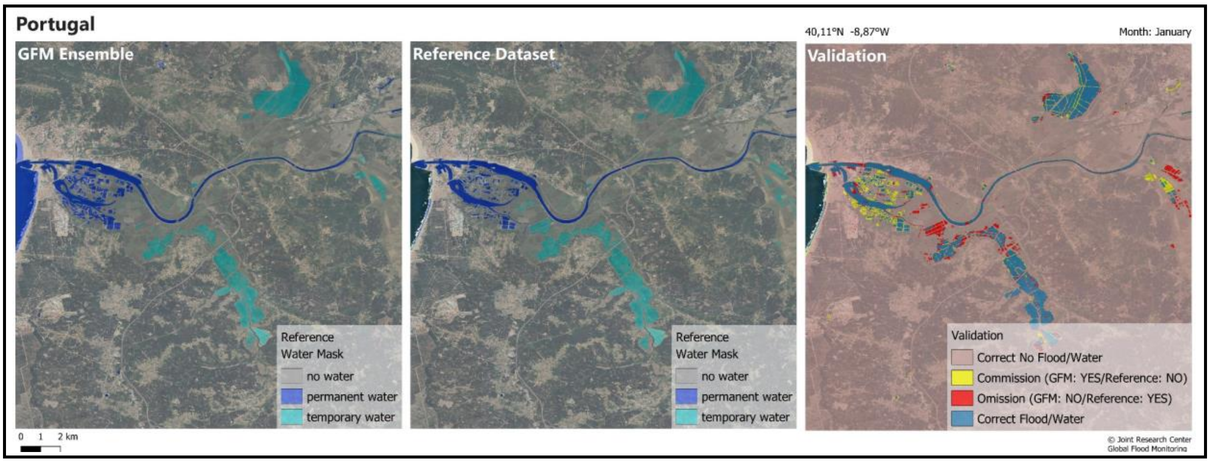

Figure 33: Use Case 10 - Reference Water Mask of the GFM (left) and of the reference dataset (middle), and the difference map (right).

4.2.11 Use Case 11 (India, 22.05.2020) - Discussion of results for Observed Flood Extent and Reference Water Mask

As can be seen in Table 8, Figure 34, and Figure 35, the Observed Flood Extent of the GFM product and the reference dataset are in good agreement (CSI value = 70.9%), despite considerable Commission Errors (12.2%) and Omission Errors (21.4%). The bias value (0.894) indicates slight under-estimation.

As can be seen in Figure 35, in the main flood-affected area on the western bank of the Hooghly river, most large floodwater pools are accurately detected (in blue), albeit with over-estimation (in yellow). Commission Errors (i.e. over-estimations) are primarily present on the fringes of accurately detected flood extent, and much less frequently as stand-alone detections. The contrary is true for Omission Errors, which are more typically present as self-standing pixel clusters where the GFM product failed to identify inundated areas in their entirety (in red). A significant part of the flood-affected area is dedicated to aquaculture and rice cultivation, with aquaculture ponds and rice fields often interspersed with each other. Many of the Omission Errors appear in rice-cultivated fields, and much less often, in aquaculture ponds. Omission Errors are dispersed over the area, rather than forming clusters.

As can be seen in Table 9 and Figure 36, for this Use Case the differences in the permanent water of the Reference Water Mask of the GFM product and the reference dataset are characterized by an under-estimation by the GFM product. This is reflected in a bias value of 0.745. Despite a satisfactory overall agreement (CSI = 62.4%), the GFM product does not correctly classify many additional aquaculture ponds captured in the reference dataset, either by under-estimating their extent or failing to detect them (Omission Error = 33%). Moreover, only the major rivers in their widest parts are detected by the GFM product, with many of the smaller waterways missing entirely.

In the example of August (the month of the flooding event), the extent of the seasonal water detected by the GFM product (apart from the rivers and waterways), is confined to a very small number of individual fields dispersed throughout the area. On the contrary, in the reference dataset, vast amounts of land, primarily under rice cultivation, are classified as seasonal water. Additionally, many of the aquaculture ponds, typically entirely missed by the GFM product, were classified as seasonal water in the reference dataset.

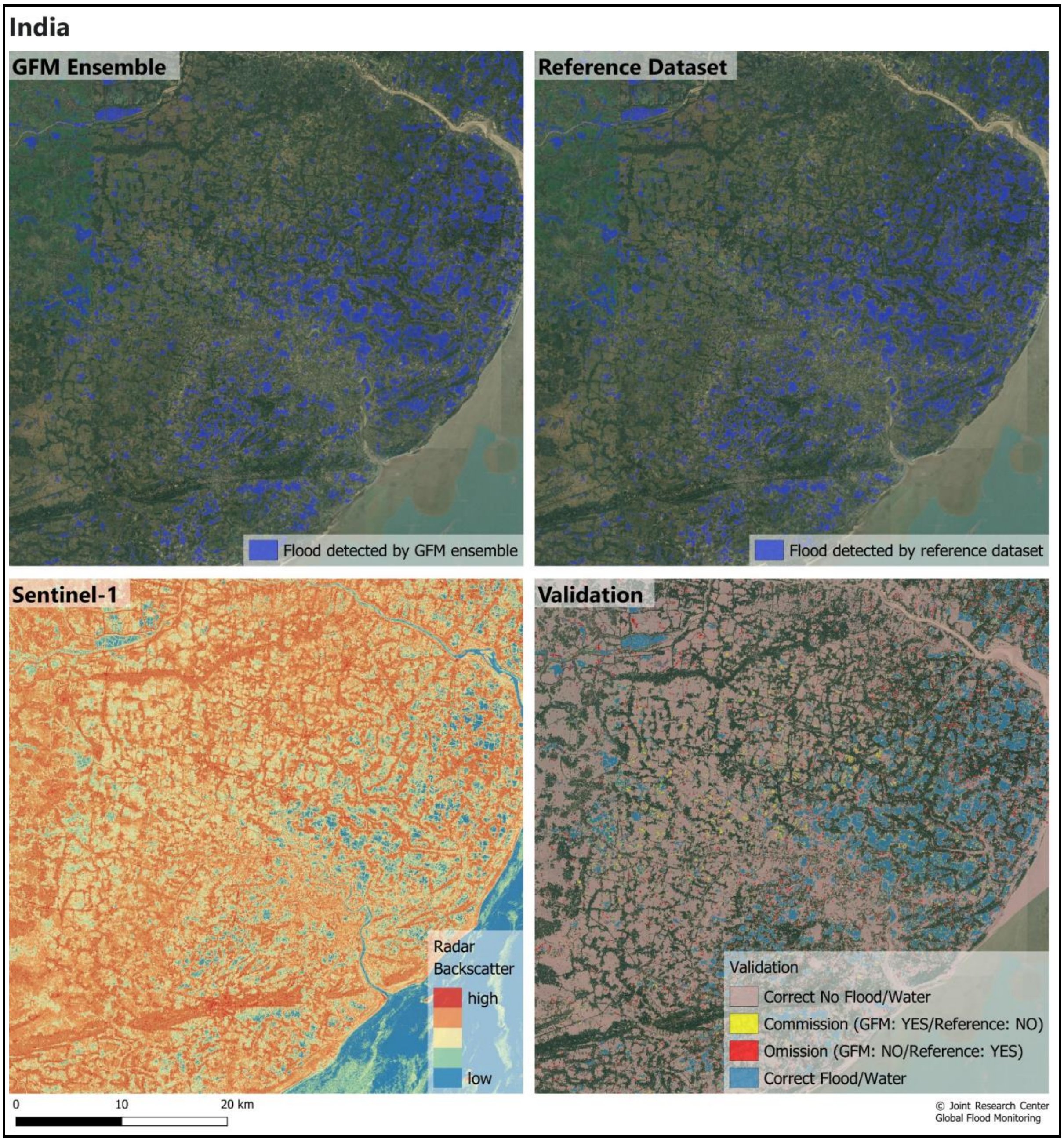

Figure 34: Use Case 11 – Observed Flood Extent from the GFM (top-left) and the reference dataset (top-right); Sentinel-1 SAR data (bottom left); difference map (bottom-right).

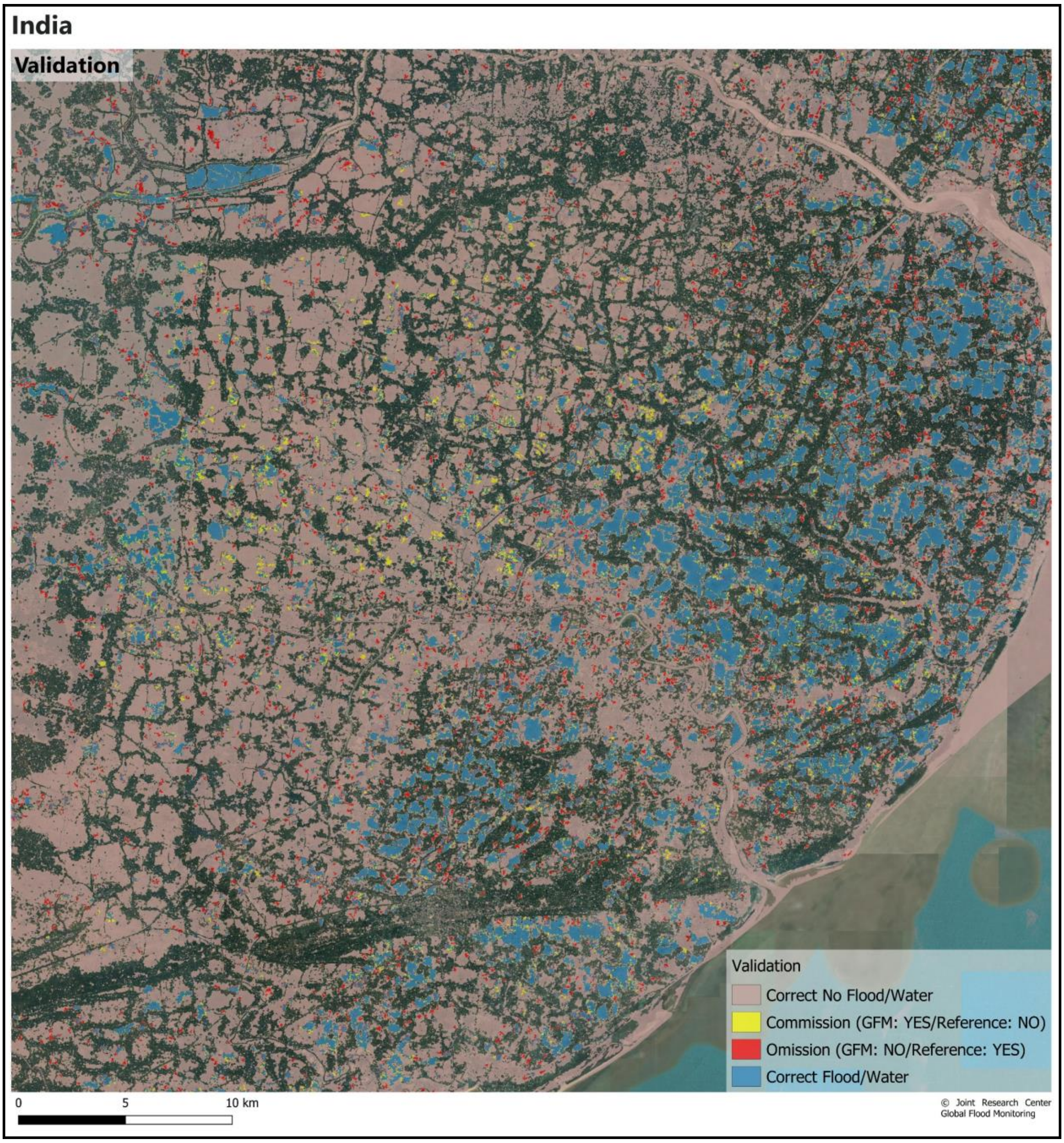

Figure 35: Use Case 11 – Difference map between Observed Flood Extent of the GFM and the reference dataset, showing correctly detected results (in blue), and under- (in red) and over-estimations (in yellow) by the GFM product compared with the reference dataset.

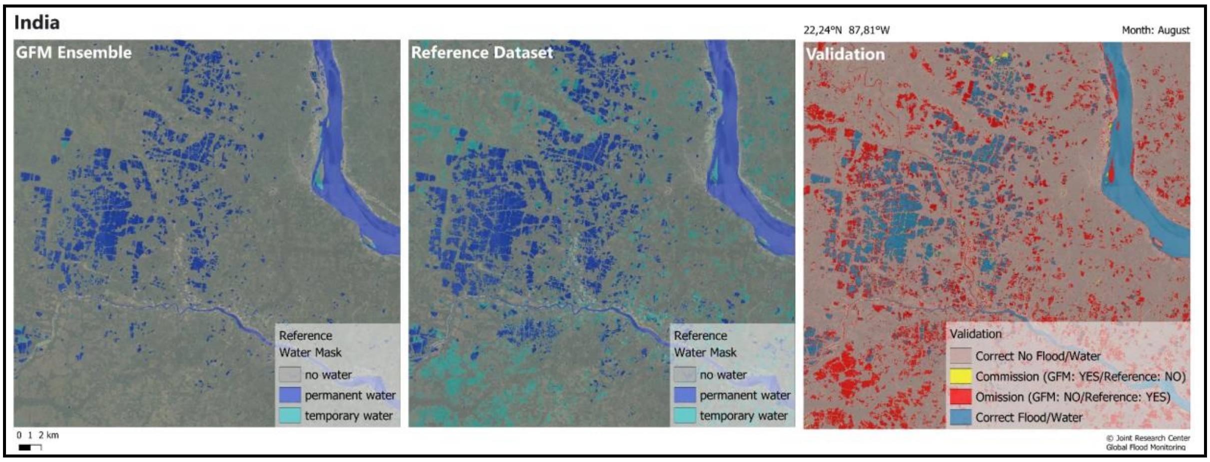

Figure 36: Use Case 11 – Reference Water Mask of the GFM (left) and the reference dataset (middle), and the difference map (right), highlighting significant omissions (in red) by the GFM product of (for example) aquaculture ponds.

4.2.12 Use Case 12 (Dominican Republic, 23.11.2023) - Discussion of results for Observed Flood Extent and Reference Water Mask

As can be seen in Table 8, the Observed Flood Extent of the GFM product and of the reference show reasonable agreement (CSI value = 64.1%), although slightly below the target value. This is influenced by a significant number of Omission Errors (30.1%), reflected in the bias value (0.79), and indicates under-estimation of flood extent by the GFM product. As can be seen in Figure 37 and Figure 38, a significant cluster of Omission Errors is present in agricultural fields where the river Nagua passes, just south of the town of Nagua. The remaining Omission Errors are more widely dispersed through the affected area, and appear to be present only in agricultural fields. Commission errors (11.5%) are instead present as a buffer around the correctly identified flooded areas.

Overall, the results for this Use Case, although short of the targets, are reasonably satisfying. Despite the under-estimation by the GFM product, the main flood-affected areas and the largest pools of floodwater show good agreement with the reference dataset (see Figure 38).

As can be seen in Table 9, for this Use Case, the permanent water of the Reference Water Class shows a reasonable thematic accuracy (60%), although again below the target value. The bias value (1.059) is very good. As can be seen in Figure 39, the most notable Omission Error by the GFM product is the complete absence of the river Yuna, whose overflow caused the flooding (see). Other discrepancies, which are a mixture of Commission and Omission Errors, occur primarily around the coastline, and have no relevance or impact for this event.

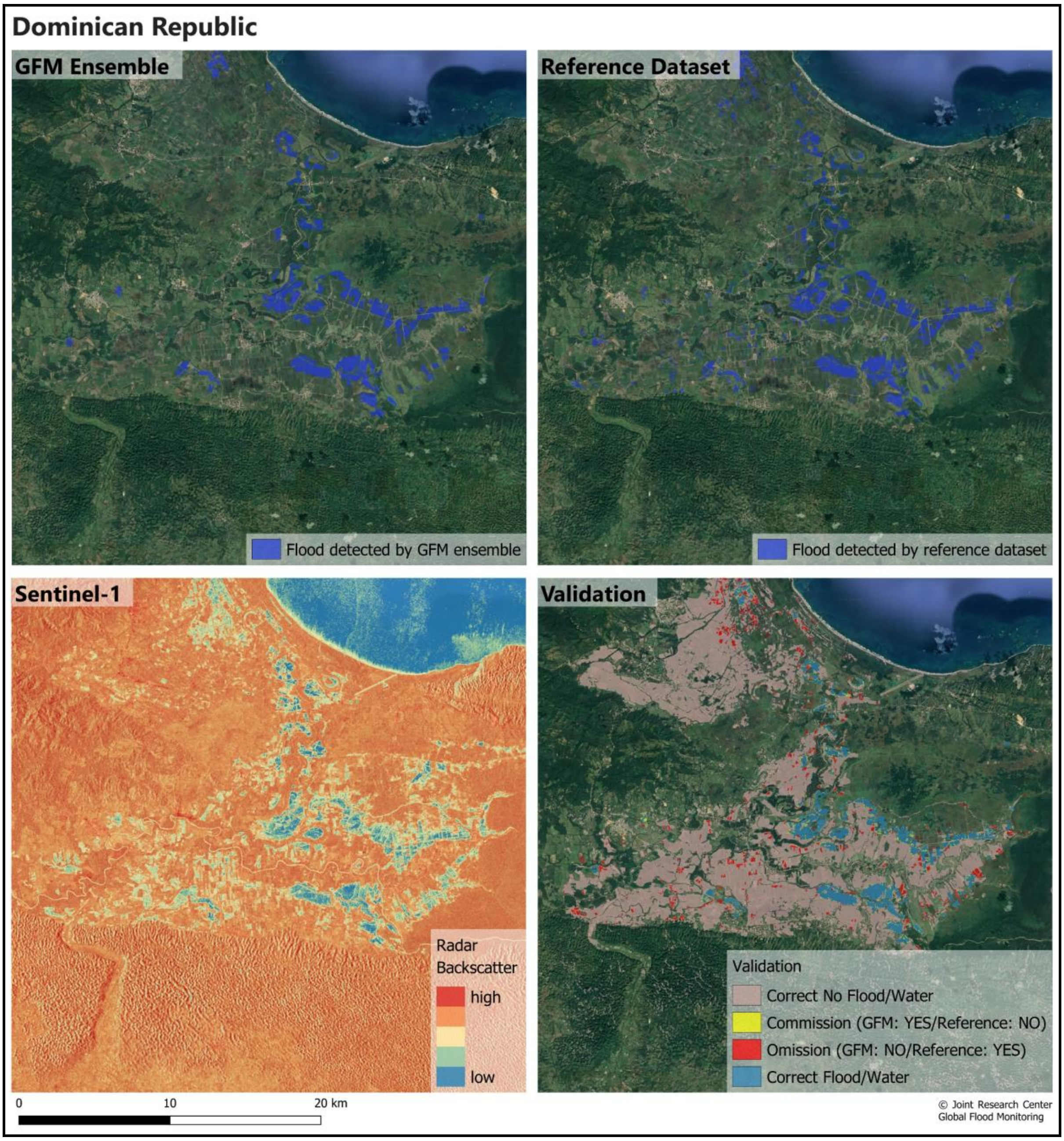

Figure 37: Use Case 12 – Observed Flood Extent from the GFM (top-left) and the reference dataset (top-right); Sentinel-1 SAR data (bottom left); difference map (bottom-right).

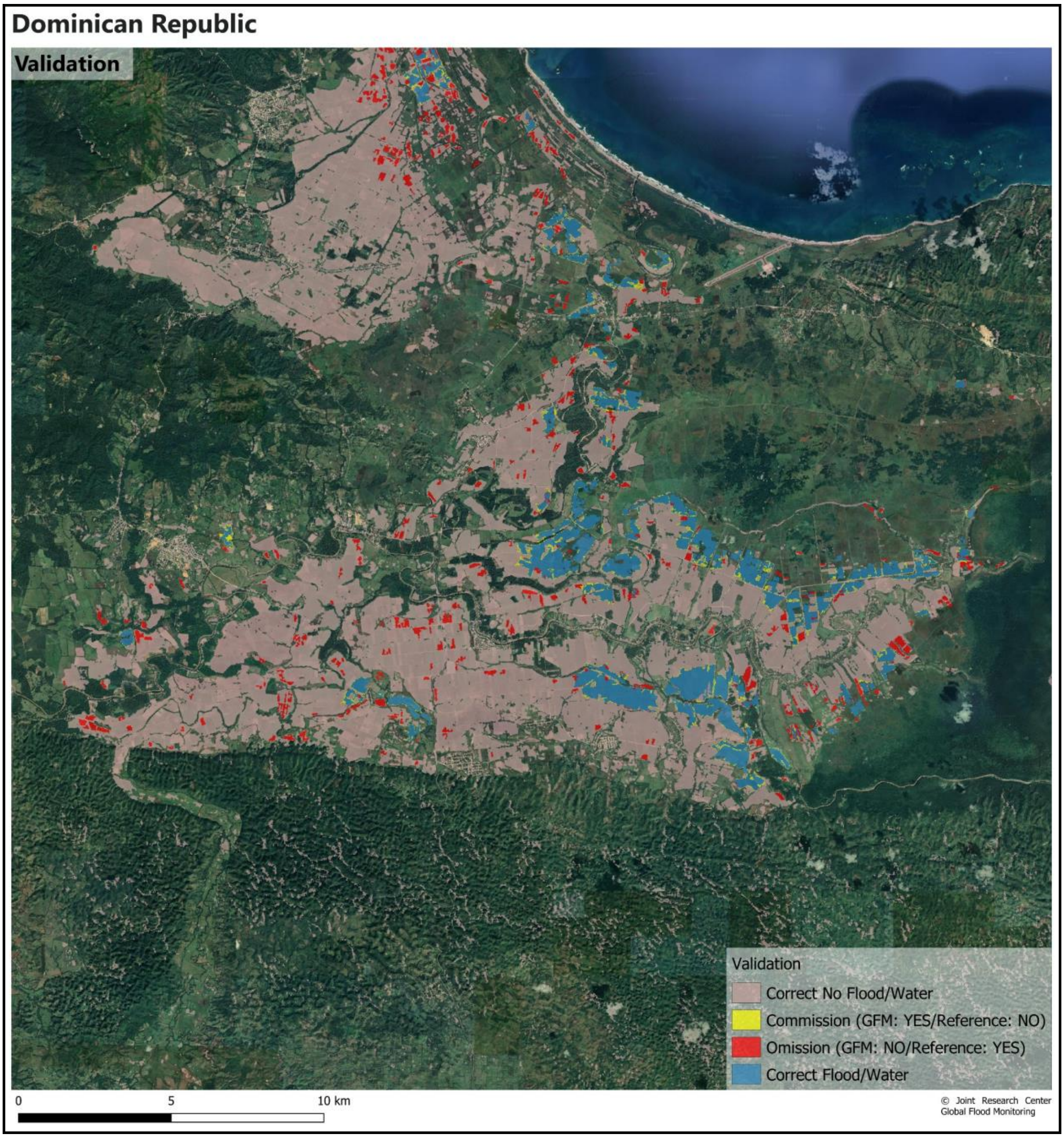

Figure 38: Use Case 12 – Difference map between Observed Flood Extent of the GFM and the reference dataset, showing the agreeing results (in blue), and omissions (in red) by the GFM product of inundated agricultural fields, compared with the reference dataset.

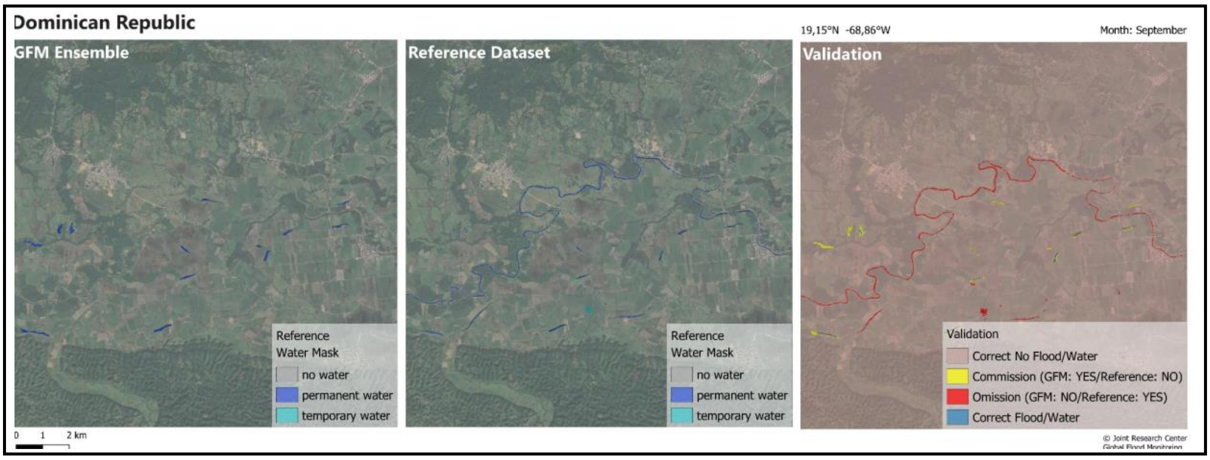

Figure 39: Use Case 12 – Reference Water Mask of the GFM (left) and of the reference dataset (middle), and the difference map (right), highlighting the omission (in red) by the GFM product of the river.

4.3 Qualitative assessment of GFM results for the Kakhovka Dam flood disaster in Kherson region, southern Ukraine, in June 2023

The destruction of the Kakhovka Dam, on the Dnipro River in southern Ukraine, on 6 June 2023, resulted in extensive flooding in the Kherson province (oblast).[15,16] As can be seen in Figure 40, the flood event was captured by the Observed Flood Extent of the GFM product, based on the Sentinel-1 SAR image acquisition of 9 June 2023.

A comparison of the spatial extent of the flooding delineated by the GFM product with international media reports, as well as with floods maps based on optical satellite imagery, indicated that, for this event, the GFM product had under-estimated the actual flood extent. Figure 41 shows the Sentinel-2 images that were acquired before (i.e. on 3 June 2023) and after (i.e. on 8 June 2023 and 13 June 2023) the flood event. Figure 42 shows the Sentinel-1 images of the corresponding area that were captured before (i.e. on 2 June 2023) and after (i.e. on 9 June 2023 and 13 June 2023) the flood event. It is clear that that the flood extent is more conspicuous in the Sentinel-2 optical images than in the Sentinel-1 SAR images.

A detailed qualitative analysis of the GFM outputs for this flood event led to the conclusion that there were in fact three separate issues that contributed to the under-estimation of the extent of the flood event in Kherson province:

- The GFM product uses **co-polarised VV** (i.e. Vertical Transmit, Vertical Receive) Sentinel-1 SAR backscatter images. Scientific studies (e.g. Tran et al., 2022) have highlighted the advantages of **cross-polarised VH** (i.e. Vertical Transmit, Horizontal Receive) Sentinel-1 SAR backscatter images for mapping flooded vegetation areas, such as those that typify this flood event. In such areas, which are characterized by mixed soil, water and vegetation conditions, “double-bounce” scattering significantly increases the backscatter intensity of VV polarisation, but has an insignificant impact on VH polarisation.

[15] https://www.bbc.com/news/world-europe-65818705
[16] https://www.theguardian.com/world/2023/jun/09/visual-guide-ukraine-nova-kakhovka-dam-collapse

- Some of the areas affected by this flood event were masked from the analysis by the **Exclusion Mask**, in particular the layer of the Exclusion Mask that delineates **no sensitivity areas** (e.g. urban areas, dense vegetation), where Sentinel-1 SAR is not sensitive to flooding (or any other type of change) of the ground surface.

- At the time of the flood event, one **GFM individual flood mapping algorithm (i.e. TUW)** had not been producing results, following an update (on 1 June 2023) of the sigma nought backscatter coefficient values (db) of the Sentinel-1 SAR datacube (on which the TUW algorithm is based). This problem, caused by an error in the TUW algorithm's configuration file, was immediately fixed. The GFM ensemble flood mapping now employs a semi-automatic quality control of the output of the individual flood mapping algorithms. Automatic alerts are generated when the success rate of an algorithm is below a certain threshold in a defined timeframe, enabling the team to react quickly.

Figure 43 shows the individual information layers of the **Exclusion Mask**, namely the layers delineating areas of **topographic distortions**, **low backscatter** and **no sensitivity** of the ground surface. As can be seen, a major factor in the under-estimation of the flood extent in this case was the **no sensitivity layer** of the Exclusion Mask. This underlines the importance of using the best possible and highest resolution maps for masking urban areas and dense vegetation. It is also evident that the Exclusion Mask appears to be plausible, and delineates well (without over-masking) the many problem areas for SAR-based flood detection.

Figure 44 shows the **Observed Flood Extent** for this event, which resulted from the GFM ensemble flood mapping algorithm, but re-calculated to include the output of the **TUW flood mapping algorithm**, which had been erroneously omitted. Inclusion of the output of the TUW flood mapping algorithm clearly improves the final result. Indeed, looking only at the output of the TUW flood mapping algorithm, it is clear that many more areas have been correctly classified as flooded, particularly the river to the north and the wetland area.

On a more general note, it must be said that this flood event occurred in an area that is particularly challenging for Sentinel-1 (or any) SAR imagery, as it includes significant amounts of **urban areas**, **forests**, and most notably, **wetlands**. It is also difficult to compare the flood mapping results of a global, automated, single-sensor approach (such as the GFM product) with those from multi-sensor, human-supervised, and more elaborated processing systems, which can also take advantage of different observations dates and multi-day aggregated data.

Figure 40: Kherson region (Ukraine) - Flood extent captured by the GFM product based on the Sentinel-1 image of 9 June 2023.

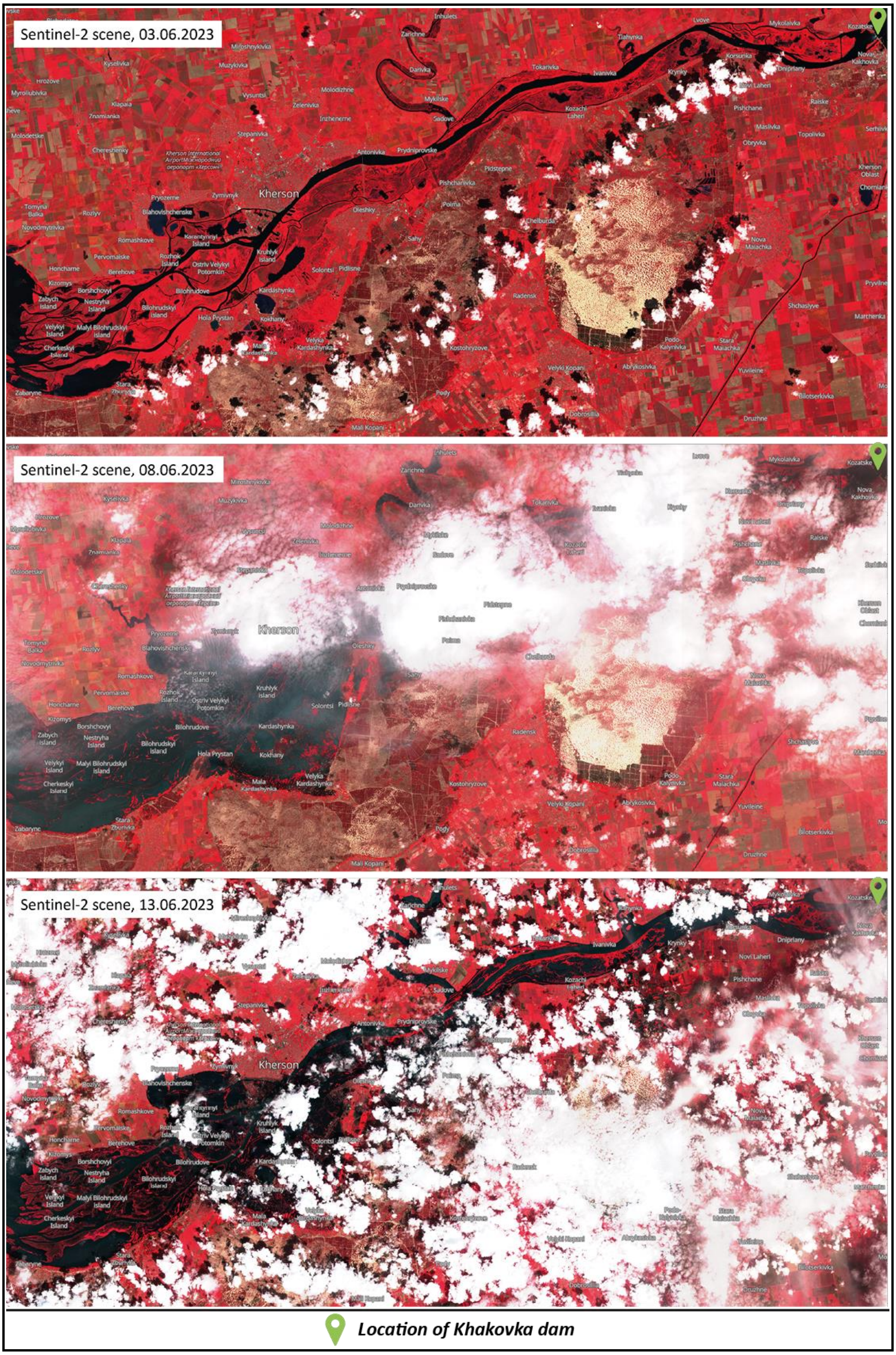

Figure 41: Kherson region (Ukraine) - Sentinel-2 imagery of affected area before (top, 03.06.2023) and after (middle, 08.06.2023; bottom, 13.06.2023) the flood event.

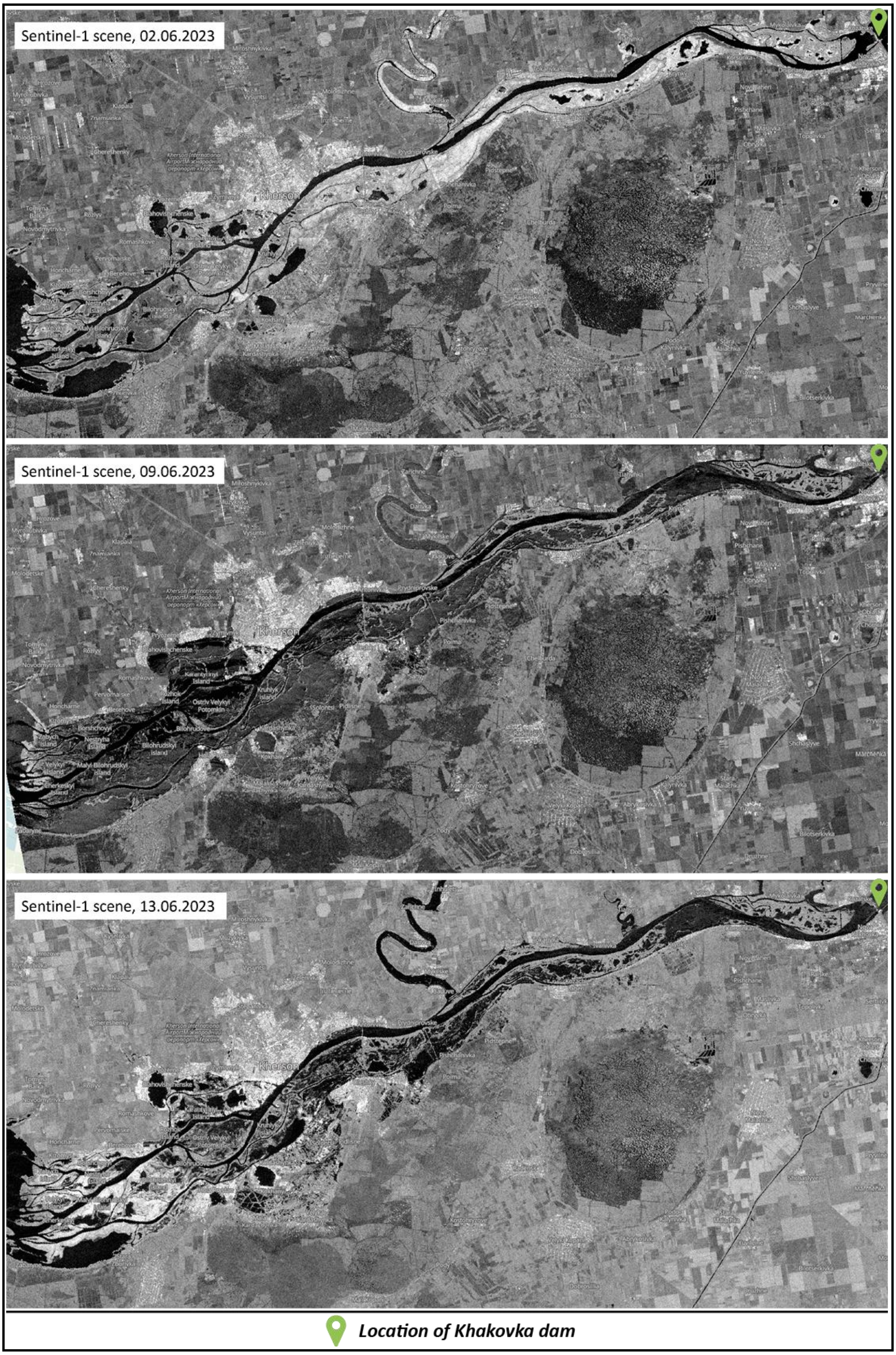

Figure 42: Kherson region (Ukraine) - Sentinel-1 imagery of affected area before (top, 02.06.2023) and after (middle, 09.06.2023; bottom, 13.06.2023) the flood event.

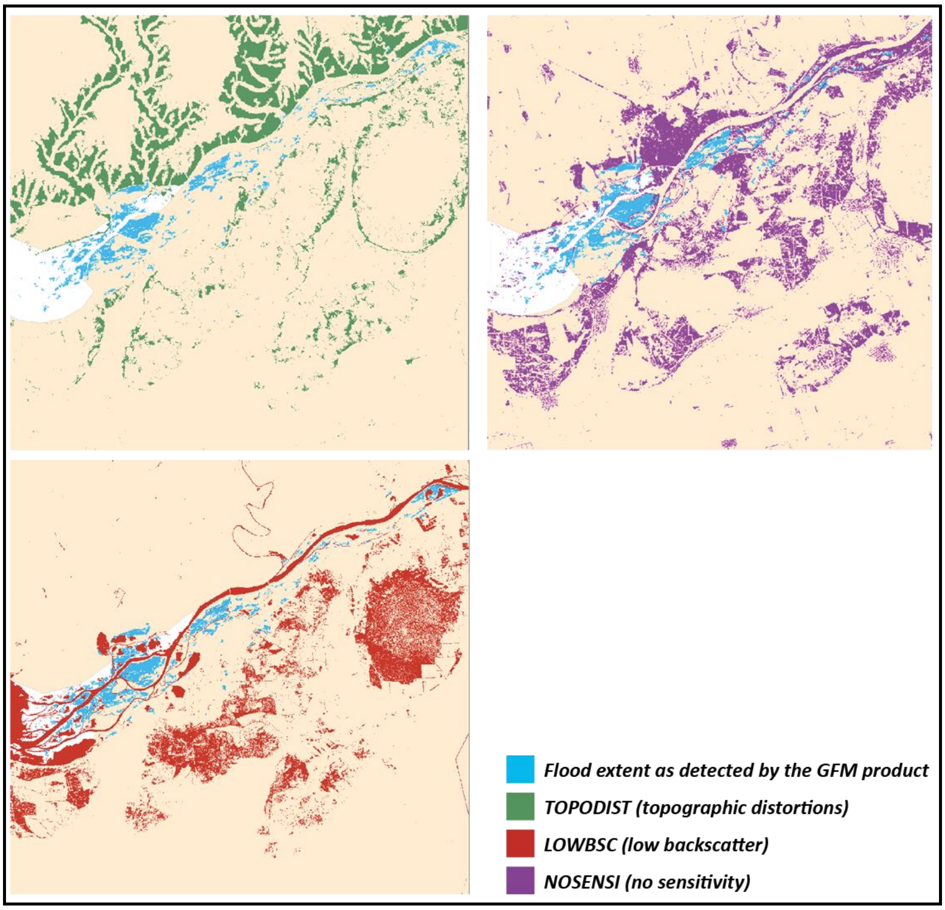

Figure 43: Kherson region (Ukraine) - Individual layers of the Exclusion Mask that most contributed to masking out parts of the flood-affected area.

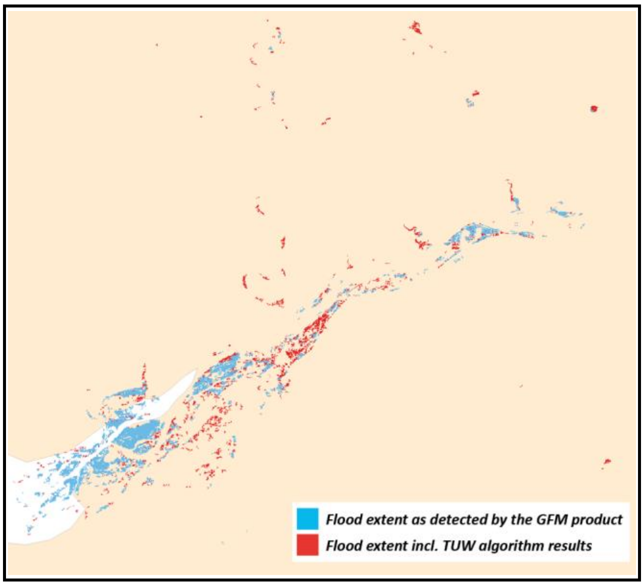

Figure 44: Kherson region (Ukraine) - Observed Flood Extent, re-generated using the GFM ensemble flood detection, including the TUW algorithm.

5. Assessment of service availability, product timeliness, and user uptake and experience

The assessments results for the service availability, product timeliness, and user uptake and experience of the GFM product, are presented and discussed below.

5.1 Assessment results for service availability, product timeliness, and user uptake and experience

The results of the 2023 quality assessment of the service availability, product timeliness, and user uptake of the GFM product, based on the relevant KPIs, are summarized in Table 10. The results for the nine sub-categories of product timeliness (KPI-2) are summarized in Table 11. The descriptions, definitions and expected target values for all KPIs reported in Table 10 and Table 11, were provided earlier in this report (see Sections 3.1 and 3.4 above). The expected target values for the KPIs are **>= 99%** for Service Availability (i.e. KPI-1), **>= 95%** for Product Timeliness (i.e. KPI-2), and **< 20%** for Service Performance Experience (i.e. KPI-7).

As was mentioned earlier (in Section 3.1), no target values are specified for KPI-4 (Unique Visitors), KPI-5 (Total Visitors) and KPI-6 (Total Downloads). However, the results for these KPIs (Table 10), confirm an increasing or steady uptake and use of the GFM product in 2023.

Table 10: 2023 GFM quality assessment results for Service Availability (KPI-1, target >=99%), Product Timeliness (KPI-2, target >=95%), Unique Visitors (KPI-4, no target), Total Visitors (KPI-5, no target), Total Downloads (KPI-6, no target), and Service Performance Experience (KPI-7, target < 20%).

QUARTER	KPI-1 (%)	KPI-2a (%)	KPI-2b (%)	KPI-2c (%)	KPI-4	KPI-5	KPI-6	KPI-7 (%)
Q1	97,07	0.87	0.98	0.98	2,115	74,447	5,480 / 59,279 MB	22.00
Q2	99.97	0.84	0.97	0.97	2,314	68,728	222,335 / 350,063 MB	68.00
Q3	99.99	0.85	0.96	0.98	2,324	84,754	104,406 / 514,335 MB	106.00
Q4	99.9	0.84	0.96	0.98	2,373	87,786	173,675 / 2,449,210 MB	130.00

Table 11: 2023 GFM quality assessment results for Product Timeliness (KPI-2, target >=95%), measured from image acquisition to user (KPI-2a), ESA to user (KPI-2b), and EODC to user (KPI-2c), and for the NRT-3h and Fast-24h Sentinel-1 products.

QUARTER	KPI-2a (%)			KPI-2b (%)			KPI-2c (%)		
	All	NRT-3h	FAST-24h	All	NRT-3h	FAST-24h	All	NRT-3h	FAST-24h
Q1	86.6%	97.3	83.7	97.8	98.5	97.6	97.9	98.6	97.7
Q2	83.9%	96.4	80.5	96.9	98.2	96.6	97.4	98.7	97.0
Q3	85.1%	95.1	82.3	96.0	95.7	96.0	97.6	97.5	97.6
Q4	84.1%	93.4	81.6	95.5	94.3	95.8	98.5	97.7	98.6

5.2 Discussion of assessment results for service availability, product timeliness, and user uptake and experience

Firstly regarding the GFM **product timeliness**, the assessment results for the four quarters (i.e. Q1, Q2, Q3, Q4) during 2023, presented in Table 11 above, are briefly discussed below:

- Q1: KPI-2a indicates an under-performance of the GFM. However, when compared with KPI-2b and KPI-2c, it is obvious that this is due to the delayed publication of FAST-24h products of Sentinel-1 on the Copernicus Hub. The production system and dissemination system of the GFM do show a good performance with KPIs greater than the target. Even though, the small differences in KPI-2b and KPI-2c highlight that as soon as data is available on the Copernicus Hub, the service is able to deliver the targeted timeliness.

- Q2: Compared with Q1, we faced a similar situation for Q2. An even further delayed publication of FAST-24h products resulted in an under-performing product timeliness to the user. Reasons for this were several service interruptions with Copernicus hub or Sentinel-1A products, such as satellite manoeuvres or maintenance windows.

- Q3: All values of KPI-2-b and KPI-2-c meet the required >=95% threshold, which indicates that the processing chain worked in a nominal state and produced results in time. However, KPI-2a suggests that the publication of the FAST-24h products from Sentinel-1, as for previous quarters, was too late to meet the 8-hour target. The average publication time (download time minus observation time) for Sentinel-1 products that did not meet the 8-hour target was about 9.4 hours.

- Q4: A complete rework of the download workflow was necessary in the fourth quarter, as the operation of ESA's Copernicus Data Hubs was discontinued. Since the end of October, the new **Copernicus Data Space Ecosystem** (CDSE)[17] became the interface to Copernicus Sentinel Data. Initial problems with download performance and data availability are the reason for the reduced KPIs, which include the time from ESA to EODC (KPI-2-a, KPI-2-b). In the second half of November, the download workflow reached a similar performance as before the changeover. However, all values of KPI-2-b and KPI-2-c (except KPI-2-b-NRT-3h) meet the required >=95% threshold, which indicates that the processing chain worked overall in a nominal state and produced results in time.

- Q4: Splitting KPI-2-b-NRT-3h into the respective months, 100% for October, 87.5% for November and 97.2% for December were reached. Similarly, KPI-2-b-FAST-24h reached 100% for October, 90.5% for November and 97.9% for December. This clearly indicates a reduced availability during the time of the changeover to the CDSE.

When analyzing KPI-2-c, it was found that 1.5% of products were not delivered on time within 8 hours of sensing. In addition to the degradation due to the above-mentioned change in the download workflow, EODC had minor problems with the network storage infrastructure. This led to a temporary restriction in the availability of the products. Corrective actions were carried out as soon as possible to reduce downtime.

[17] https://dataspace.copernicus.eu/

The assessment results for **service availability**, **unique visitors**, **total visitors**, **total downloads**, and **service performance experience** of the GFM product, for the four quarters during 2023, which are presented in Table 10, are briefly discussed below:

- During Q1 of 2023, due to a network infrastructure incident that affected the entire virtualisation layer of the production system, the targeted service availability (KPI-1) was not achieved. Corrective action was taken by the operations team to resume nominal operations as quickly as possible. The faulty component was removed from the virtualisation layer leading to a redeployment of the production system.

- For Q2, Q3 and Q4, the targets for KPI-1 were met.

- The GFM user uptake (KPI-4, KPI-5, and KPI-6) and service performance experience (KPI-7) improved compared to the previous year (2022), due to a significant update at the beginning of 2023. To enhance and speed up the accessibility and visibility of the GFM output layers in the GloFAS (and EFAS) Map Viewers[7] and the GFM single-page web application[8], all data are now converted to Cloud Optimized GeoTiff (COG) raster files. Additional changes in the folder structure and clipping the input files for the WMS-T server to the footprints enabled further improvement of the user experience.

6. Plausibility analysis of the Exclusion Mask for the 12 Use Cases

The Exclusion Mask denotes those areas where SAR-based flood- and water-detection is not feasible, and is created by combining the following information layers describing four types of “static” ground surface characteristics:

- The “**no-sensitivity**” layer delineates all land cover types and areas (e.g. urban areas, dense vegetation), where Sentinel-1 SAR is not sensitive to flooding (or any other type of change) of the ground surface.

- Water look-alikes (e.g. flat impervious areas, sand surfaces), due to a **Low Backscatter** signature of the ground.

- **Topographic distortion** of the Sentinel-1 signals in areas of complex topography.

- So-called “**radar shadows**”, which occur behind vertical features or slopes with steep sides (e.g. mountains, high vegetation canopies, anthropogenic structures).

This Section provides a brief analysis of the general plausibility of the Exclusion Mask, for the areas of interest (AOIs) of the 12 Use Cases (see Section 5) that are used to validate the Observed Flood Extent and Reference Water Mask. An overview of the AOIs for the 12 Use Cases, including the Exclusion Mask, is presented in **Annex 2**.

Regarding the Exclusion Mask and considering all AOIs, generally speaking, the **radar shadows** and **low backscatter** sub-layers seem plausible. In some cases, the **topographic distortion** sub-layer excludes flood-prone areas. Highest uncertainty seems to be evident in the **no-sensitivity** sub-layer. For example, as shown below for Use Case 4 (France) and 12 (Dominican Republic), agricultural areas are partially excluded from the flood detection, even though these are flood-prone areas. Note that in the the following sub-sections, graphical examples are only presented if any issues are observed in the Exclusion Mask for the Use Cases.

<u>Use Case 1 (USA – Texas, 29.08.2017) - Plausibility of Exclusion Mask</u>:

In case of the flood event in the USA - Texas, the Exclusion Mask seems plausible, despite small areas of noticeable errors caused by artifacts in the topographic distortion mask. These have a negative impact on the flood area. An example of this is shown Figure 45, based on the Sentinel-1 image of the flood event.

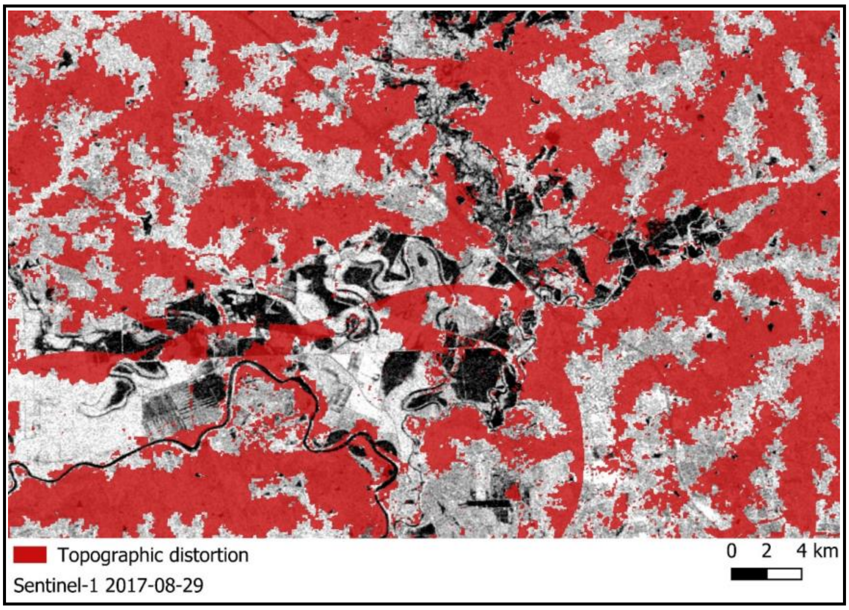

Figure 45: Use Case 1 (USA - Texas, 29.08.2017) – Example of the Topographic distortion mask (in red) covering agricultural fields, excluding flood-prone areas.

Use Case 2 (Morocco, 09.01.2021) - Plausibility of Exclusion Mask:

Regarding the flood event in Morocco, for the defined area, the Exclusion Mask seems plausible and the various input layers do not show bigger inconsistencies.

Use Case 3 (Myanmar, 21.07.2021) - Plausibility of Exclusion Mask:

Regarding the flood event in Myanmar, the Exclusion Mask appears reasonable for the specified area, and no discrepancies in the input sub-layers are seen.

Use Case 4 (France, 16.10.2018) - Plausibility of Exclusion Mask:

Regarding the flood event in France, the Exclusion Mask looks mostly plausible. However, as shown in the example in Figure 46, where the *no sensitivity* sub-layer (in green) is overlaid on a Sentinel-1 image (from 16.10.2018), the *no sensitivity* seems very strict and covers agricultural areas near a small river, thus masking out flood-prone areas.

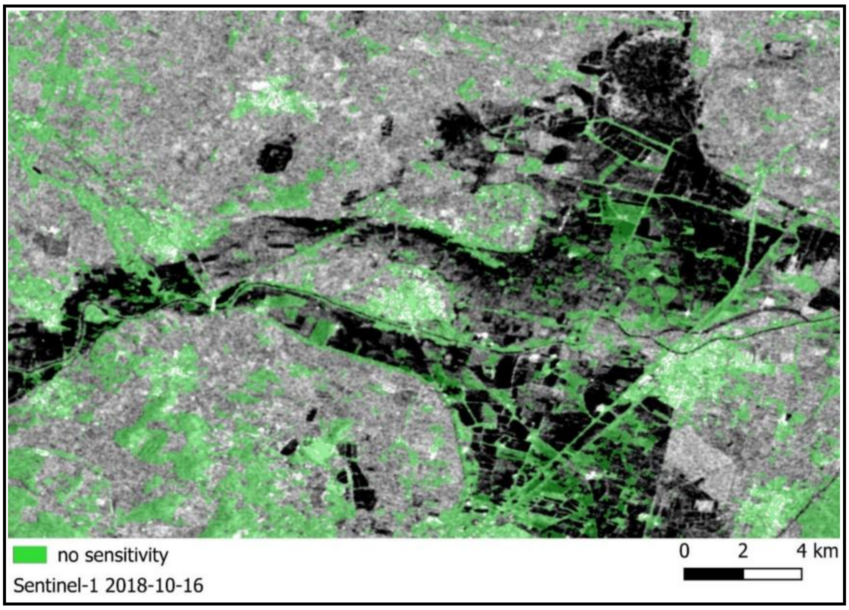

Figure 46: Use Case 4 (France, 16.10.2018) – This example shows the no sensitivity sub-layer (in green) that is responsible for the errors in the Exclusion mask.

Use Case 5 (Indonesia, 29.03.2023) – Plausibility of Exclusion Mask:

Regarding the flood event in Indonesia, for the defined area, the Exclusion Mask seems plausible and the various input layers do not show bigger inconsistencies.

Use Case 6 (Italy, 16.05.2023) – Plausibility of Exclusion Mask:

Regarding the flood event in Italy, no inconsistencies were found.

Use Case 7 (Venezuela, 29.07.2017) – Plausibility of Exclusion Mask:

Regarding the flood event in Venezuela, for the defined area, the Exclusion Mask seems plausible. In some areas, there are noticeable errors caused by artifacts in the topographic distortion mask, which have a negative impact on the flood area.

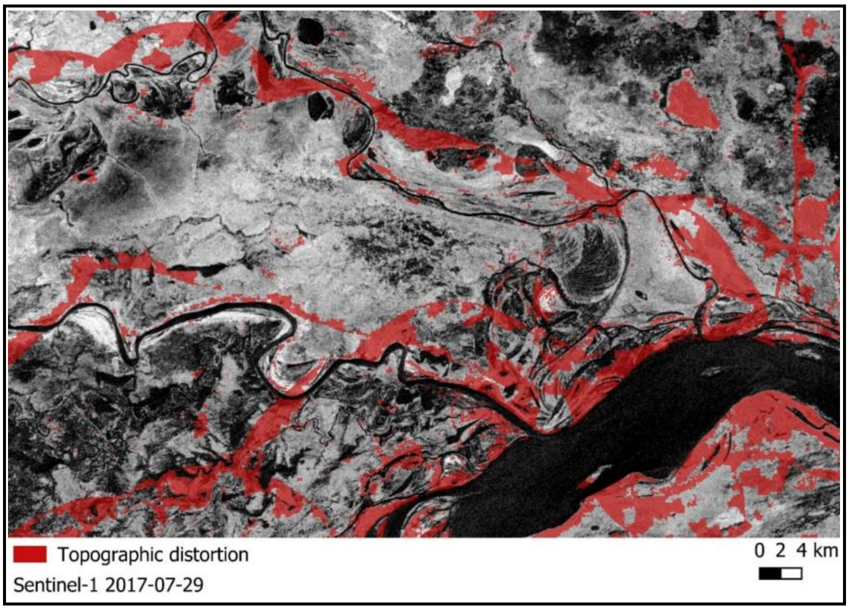

Figure 47: Use Case 7 (Pakistan, 29.07.2017) – In this example, the topographic distortion sub-layer (in red) shows some artefacts in the flood zone, negatively affecting the Exclusion Mask.

Use Case 8 (Bangladesh, 10.08.2023) - Plausibility of Exclusion Mask:

In case of the Bangladesh flood event, inconsistencies in the no-sensitivity layer of the Exclusion Mask cover some smaller flooded areas (Figure 48, in green).

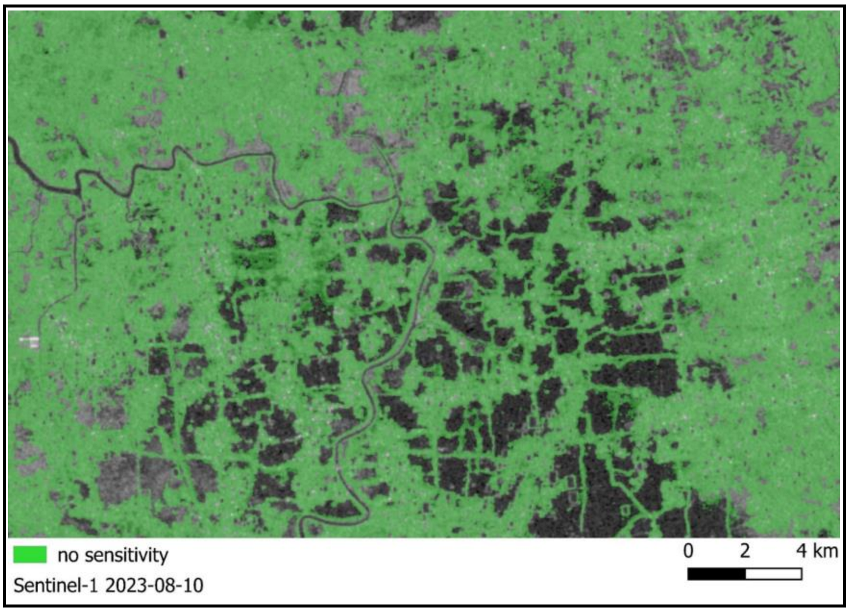

Figure 48: Use Case 8 (Bangladesh, 10.08.2023) – This example shows the no sensitivity sub-layer (in green) that is responsible for the errors in the Exclusion mask.

Use Case 9 (Greece, 07.09.2023) - Plausibility of Exclusion Mask:

Regarding the flood event in Greece, the Exclusion Mask does not show any artefacts or other significant problems.

<u>Use Case 10 (Portugal, 23.12.2019) - Plausibility of Exclusion Mask</u>:

Regarding the flood event in Portugal, the Exclusion Mask is conspicuous. The no-sensitivity layer masks out some flood zones, negatively affecting the Observed Flood Extent.

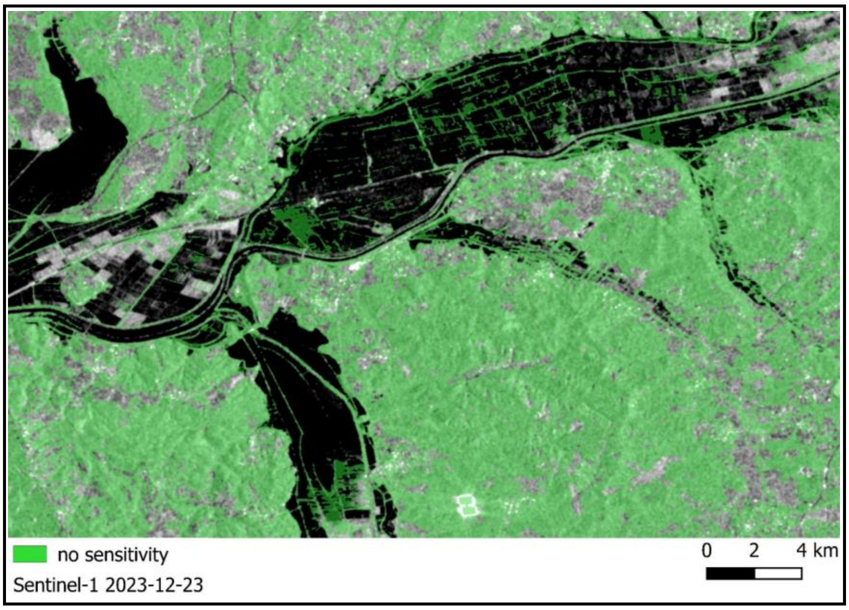

Figure 49: Use Case 10 (Portugal, 23.12.2019) – Flood areas covered by Exclusion Mask based on the no sensitivity sub-layer in green.

<u>Use Case 11 (India, 22.05.2020) - Plausibility of Exclusion Mask</u>:

Regarding the flood event in India, for the defined area, the Exclusion Mask seems plausible and the various input layers do not show major inconsistencies.

<u>Use Case 12 (Dominican Republic, 23.11.2023) - Plausibility of Exclusion Mask</u>:

Regarding the flood event in Dominican Republic, inconsistencies in the no-sensitivity layer of the Exclusion Mask cover some flooded areas.

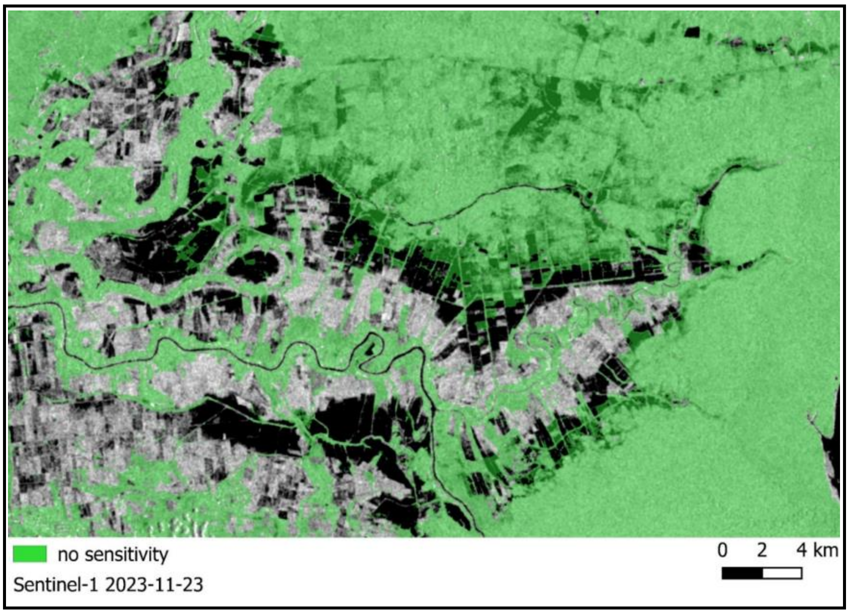

Figure 50: Use Case 6 (Dominican Republic, 23.11.2023) – This example shows the no-sensitivity sub-layer (in green) that is responsible for the errors in the Exclusion mask.

7. Conclusions and Outlook

As part of the 2023 GFM annual product and service quality assessment, the thematic accuracy of the two main outputs of the GFM product of the Copernicus Emergency Management Service (CEMS), namely the Observed Flood Extent and Reference Water Mask, was assessed for 12 Use Cases of worldwide flood events between July 2017 and November 2024 (Table 6). The thematic accuracy of both GFM output layers was assessed by a comparison with independent reference flood and water maps. As required by the Technical Specifications (European Commission, 2020), the target value for the thematic accuracy of the GFM product is 70% or higher, computed based on the Critical Success Index (CSI).

The independent reference flood maps for the 12 Use Cases were generated by a semi-automated processing of the same Sentinel-1 SAR image scenes used by the GFM product, with manual enhancement of the resulting flood masks with optical (i.e. Sentinel-2) imagery. The independent reference water maps were created, by dynamic thresholding of Sentinel-1 SAR and Sentinel-2 images separately, to generate monthly image composites, and fusing the derived water masks by combining all water pixels.

Regarding the Observed Flood Extent's thematic accuracy (Table 8), eight of the 12 Use Cases had CSI values that met or exceeded the target of 70%, while two Use Cases were just below the target (61.6% and 64.1%). Two Use Cases (Morocco and Myanmar) had very low CSI values (18.1% and 11.0%), for reasons outlined in Sections 4.2.2 and 4.2.3 of this report.

Regarding the Reference Water Mask's thematic accuracy (Table 9), seven of the 12 Use Cases met or exceeded the target value, four were between 60.0% and 67.5%, while one Use Case (Indonesia) had a low CSI value (32.8%), for reasons outlined in Section 4.2.5 of this report.

For the thematic accuracy assessment of the Reference Water Mask, only the **permanent water** class, and not the **seasonal water** class, was considered. As was the case in the 2022 GFM product and service quality assessment, the seasonal (i.e. monthly) water generally exhibits very low CSI values (not presented in this report), due to significant under-estimation of seasonal water by the GFM product, for reasons outlined in Section 4.1 of this report.

The 2023 GFM product and service quality assessment also includes a qualitative assessment of the GFM results for the flood disaster due to the destruction of the Kakhovka hydroelectric dam in the Kherson region of southern Ukraine, on 6 June 2023. Considering that this event occurred in an area that is challenging for SAR-based flood mapping (i.e. including significant amounts of urban areas, forests, and wetlands), it was found that the GFM product performed reasonably well also for this flood event, as described in Section 4.3 of this report.

In addition to the thematic accuracy, all other performance-related aspects of the GFM product (i.e. product timeliness, service availability, etc.) were reported on a quarterly basis during 2023, and the results are presented in this report. Furthermore, this report also includes an assessment of the general plausibility of the Exclusion Mask (delineating where SAR-based water mapping is not technically feasible), for the 12 Use Cases.

Operational implementation of the GFM product has continued during 2024. GFM output data are regularly included, for example, in daily maps published by the Emergency Response Coordination Centre (ERCC) of the European Commission's Directorate-General for European Civil Protection and Humanitarian Aid Operations (DG ECHO).[18] The following significant technical improvements to the GFM product were also implemented, on 24 January 2024:[19]

- Improvements to the Reference Water Mask, by extending the reference period of Sentinel-1 data to 5 years (instead of 2 years).

- Improvements to the GFM Product flood and water detection algorithms, including improved harmonic model parameters for the TUW algorithm, reduced over-detection by the LIST algorithm at high incidence angles, flagging newly processed scenes as "flooded" or "not flooded" by anomaly detection based on time-series of water pixel counts, and a general stabilization of all algorithms.

- Preparation of the GFM product systems for ingestion of future Sentinel-1C SAR acquisitions, and integration once the data are available. (See last paragraph below).

- Re-processing of the entire Sentinel-1 data archive using the GFM product, incorporating the latest changes, to re-generate a stable, consistent, harmonized and complete archive of worldwide observed flood events and water extent, from 1 January 2015 until the start of the near real-time GFM product. This evolution is currently under preparation, and will be released during 2024.

- Improved and streamlined post-processing of the results of the GFM ensemble and individual flood mapping algorithms, using the most recent methods and auxiliary data, to reduce the effects of both flood over-detection and flood under-detection.

Further enhancements of the quality of the Observed Flood Extent are foreseen during 2024. For example, in order to reduce the effects of both flood over-detection (e.g. due to backscatter speckle or noise) and flood under-detection (e.g. due to the removal of small flooded areas) , improved, streamlined procedures for postprocessing the results of the GFM individual and ensemble flood mapping algorithms will be implemented.

Finally, as a result of the premature end of the mission of the Copernicus Sentinel-1B satellite, the global coverage of the GFM product is currently based only on the Sentinel-1A satellite. It is expected that the full global coverage of the GFM product (i.e. based on two Sentinel-1 satellites) will be restored later in 2024, with the planned launch of the Sentinel-1C satellite.

[18] https://erccportal.jrc.ec.europa.eu/ECHO-Products/Maps/Maps-Old/Daily-maps
[19] As part of Task 5 (Product evolution and re-processing) of GFM Specific Contract 3.

References

- Bauer-Marschallinger, B., Cao, S., Tupas, M. E., Roth, F., Navacchi, C., Melzer, T., . . . Wagner, W. (2022). Satellite-Based Flood Mapping through Bayesian Inference from a Sentinel-1 SAR Datacube. Remote Sens., 14(3673). https://doi.org/10.3390/rs14153673

- Bradley, D., and Roth, G. (2007). Adaptive Thresholding using the Integral Image. Journal of Graphics Tools, 12(2). https://doi.org/10.1080/2151237X.2007.10129236

- Card, D. (1982). Using known map category marginal frequencies to improve estimates of thematic map accuracy. Photogrammetric Engineering and Remote Sensing, 431-439. https://www.asprs.org/wp-content/uploads/pers/1982journal/mar/1982_mar_431-439.pdf

- Chini, M., Hostache, R., Giustarini, L., and Matgen, P. (2017). A Hierarchical Split-Based Approach for parametric thresholding of SAR images: flood inundation as a test case. IEEE Transactions on Geoscience and Remote Sensing, 55(12), 6975-6988. https://doi.org/10.1109/TGRS.2017.2737664

- Donchyts, G., Winsemius, H., Schellekens, J., Erickson, T., Gao, H., Savenije, H., and van de Giesen, N. (2016). Global 30m Height Above the Nearest Drainage. Conference: European Geosciences Union 2016. http://dx.doi.org/10.13140/RG.2.1.3956.8880

- European Commission. (2020). Call for Tenders JRC/IPR/2020/OP/0551 - Provision of an Automated, Global, Satellite-based Flood Monitoring Product for the Copernicus Emergency Management Service. Technical specifications. https://etendering.ted.europa.eu/cft/cft-display.html?cftId=6052

- Frantz, D., Haß, E., Uhl, A., Stoffels, J., and Hill, J. (2018). Improvement of the Fmask algorithm for Sentinel-2 images: Separating clouds from bright surfaces based on parallax effects. Remote sensing of environment, 215, 471-481. https://doi.org/10.1016/j.rse.2018.04.046

- Hartigan, J. A., and Hartigan, P. M. (1985). The Dip Test of Unimodality. Ann. Statist., 13(1), 70-84. https://doi.org/10.1214/aos/1176346577

- Ludwig, C., Walli, A., Schleicher, C., Weichselbaum, J., and Riffler, M. (2019). A highly automated algorithm for wetland detection using multi-temporal optical satellite data. Remote Sensing of Environment, 224, 333-351. https://doi.org/10.1016/j.rse.2019.01.017

- Martinis, S., Twele, A., and Kersten, K. (2015). A fully automated TerraSAR-X based flood service. ISPRS Journal of Photogrammetry and Remote Sensing, 104, 203-212. http://dx.doi.org/10.1016/j.isprsjprs.2014.07.014

- Martinis, S., Twele, A., and Voigt, S. (2009). Towards operational near real-time flood detection using a split-based automatic thresholding procedure on high-resolution TerraSAR-X data. Nat. Hazards Earth Syst. Sci., 9, 303–314. https://doi.org/10.5194/nhess-9-303-2009

- Matgen, P., Martinis, S., Wagner, W., Freeman, V., Zeil, P., and McCormick, N. (2020). Feasibility assessment of an automated, global, satellite-based flood-monitoring product for the Copernicus Emergency Management Service. Publications Office of the European Union, Luxembourg. https://doi.org/10.2760/653891

- Metzger, M. J. (2018). The Global Environmental Stratification: A high-resolution bioclimate map of the world [dataset]. The University of Edinburgh. https://doi.org/10.7488/ds/2354

- Metzger, M. J., Bunce, R., Jongman, R., Sayre, R., Trabucco, A., and Zomer, R. (2013). A high-resolution bioclimate map of the world: a unifying framework for global biodiversity research and monitoring. Global Ecology and Biogeography 22, 630-638. https://doi.org/10.1111/geb.12022

- Olofsson, P., Foody, G. M., Herold, M., Stehman, S. V., Woodcock, C. E., and Wulder, M. A. (2014). Good practices for estimating area and assessing accuracy of land change. Remote Sensing of Environment, 148, 42-57. https://doi.org/10.1016/j.rse.2014.02.015

- Olofsson, P., Foody, G. M., Stehman, S. V., and Woodcock, C. E. (2013). Making better use of accuracy data in land change studies: Estimating accuracy and area and quantifying uncertainty using stratified estimation. Remote Sensing of Environment, 129, 122-131. https://doi.org/10.1016/j.rse.2012.10.031

- Otsu, N. (1979). A threshold selection method from gray-level histograms. IEEE transactions on systems, man, and cybernetics, 9(1), 62-66. https://doi.org/10.1109/TSMC.1979.4310076

- Pekel, J.-F., Cottam, A., Gorelick, N., and Belward, A. (2016). High-resolution mapping of global surface water and its long-term changes. Nature, 540, 418-422. https://dx.doi.org/10.1038/nature20584

- Rennó, C. D., Nobre, A. D., Cuartas, L. A., Soares, J. V., Hodnett, M. G., Tomasella, J., and Waterloo, M. J. (2008). HAND, a new terrain descriptor using SRTM-DEM: Mapping terra-firme rainforest environments in Amazonia. Remote Sensing of Environment, 112(9), 3469-3481. https://doi.org/10.1016/j.rse.2008.03.018

- Roberts, D., Mueller, N., and Mcintyre, A. (2017). High-Dimensional Pixel Composites From Earth Observation Time Series. IEEE Transactions on Geoscience and Remote Sensing, 55(11). https://doi.org/10.1109/TGRS.2017.2723896

- Salamon, P., McCormick, N., Reimer, C., Clarke, T., Bauer-Marschallinger, B., Wagner, W., . . . Walli, A. (2021). The new, systematic global flood monitoring product of the Copernicus Emergency Management Service. IGARRS 2021, Paper WE4.O-6.4. https://doi.org/10.1109/IGARSS47720.2021.9554214

- Seewald, M., Riffler, M., Ralser, S., Innerbichler, F., Dulleck, B., Gruber, C., . . . Salamon, P. (2023). Global Flood Monitoring - Annual Product and Service Quality Assessment Report 2022. Luxembourg: Publications Office of the European Union. https://doi.org/10.2760/666238

- Seewald, M., Riffler, M., Ralser, S., Innerbichler, F., Dulleck, B., Leitner, A., . . . Salamon, P. (2023). Global Flood Monitoring (GFM) - Pre-operational Product and Service Quality Assessment Report. Luxembourg: Publications Office of the European Union. https://doi.org/10.2760/362585

- Tottrup, C., Druce, D., Meyer, R. P., Christensen, M., Riffler, M., Dulleck, B., . . . et al. (2022). Surface Water Dynamics from Space: A Round Robin Intercomparison of Using Optical and SAR High-Resolution Satellite Observations for Regional Surface Water Detection. Remote Sens., 14(2410). https://doi.org/10.3390/rs14102410

- Twele, A., Cao, W., Plank, S., and Martinis, S. (2016). Sentinel-1-based flood mapping: a fully automated processing chain. International Journal of Remote Sensing, 37(13), 2990-3004. https://doi.org/10.1080/01431161.2016.1192304

- Wagner, W., Freeman, V., Cao, S., Matgen, P., Chini, M., Salamon, P., . . . Briese, C. (2020). Data processing architectures for monitoring floods using Sentinel-1. ISPRS Annals of the Photogrammetry, Remote Sensing and Spatial Information Sciences, V-3-2020, 641-648. https://doi.org/10.5194/isprs-annals-V-3-2020-641-2020

- Wilks, D. S. (2019). Statistical methods in the atmospheric sciences. (Fourth ed.). Elsevier. https://doi.org/10.1016/B978-0-12-815823-4.09987-9

- Zhang, Y., Zhu, T., Spreen, G., Melsheimer, C., Huntemann, M., Hughes, N., . . . Li, F. (2021). Sea ice and water classification on dual-polarised Sentinel-1 imagery during melting season. The Cryosphere Discuss. [preprint]. https://doi.org/10.5194/tc-2021-85

List of abbreviations and definitions

ACRONYM	DEFINITION	ACRONYM	DEFINITION
AOI:	*Area of interest*	***IW GRDH:***	*Interferometric Wide swath - Ground Range Detected, High Resolution (Sentinel-1 product)*
API:	*Application Programming Interface*	***JRC:***	*Joint Research Centre of European Commission*
CEMS:	*Copernicus Emergency Management Service*	***KPI:***	*Key Performance Indicator*
LPV:	*Land Product Validation (subgroup of Committee on Earth Observation Satellites / CEOS)*	***LIST:***	*Luxembourg Institute for Science and Technology*
CI:	*Confidence interval*	***MSI:***	*MultiSpectral Instrument of Sentinel-2*
CIMA:	*Centro Internazionale in Monitoraggio Ambientale Research Foundation*	***NIR:***	*Near-infrared*
DEM:	*Digital Elevation Model*	***NDWI:***	*Normalized Difference Water Index*
WBM:	*Water Body Mask*	***NRT:***	*Near real-time*
CSI:	*Critical Success Index (also called Threat Score)*	***OGC:***	*Open Geospatial Consortium*
DLR:	*Deutsches Zentrum für Luft- und Raumfahrt (German Aerospace Centre)*	***PDD:***	*Product Definition Document of GFM product*
EDO / GDO:	*European and Global Drought Observatories of CEMS*	***Polarisation:***	*The orientation of the plane in which the SAR signal oscillates, in either the transmit or receive paths.*
EFAS / GloFAS:	*European and Global Flood Awareness Systems of CEMS*	***PUM:***	*Product User Manual of GFM product*
EFFIS:	*European Forest Fire Information System of CEMS*	***REST(ful) API:***	*An API conforming to Representational State Transfer architectural style*
EODC:	*Earth Observation Data Centre for Water Resources Monitoring GmbH*	***SAFE:***	*Sentinel-specific variation of Standard Archive Format for Europe specification*
ERCC:	*Emergency Response Coordination Centre of the European Commission*	***SAR:***	*Synthetic Aperture Radar*
QA4EO:	*Quality Assurance Framework for Earth Observation, of CEOS*	***SNAP:***	*Sentinel Application Platform (a common architecture for all Sentinel Toolboxes)*
GFM:	*Global Flood Monitoring product of CEMS*	***TUW:***	*Technische Universität Wien*
GHSL:	*Global Human Settlement Layer of CEMS*	***VH:***	*SAR polarisation: Vertical Transmit - Horizontal Receive (i.e. cross-polarised).*
GLS:	*Global Land Service of Copernicus*	***VHR:***	*Very High Resolution*
HAND:	*Height Above Nearest Drainage (a DEM normalized using nearest drainage)*	***VV:***	*SAR polarisation: Vertical Transmit - Vertical Receive (i.e. co-polarised).*
INSPIRE:	*Infrastructure for Spatial Information in Europe*	***WMS / WMS-T:***	*Web Map Service (OGC standard for serving map images using HTTP) / with time support*

Annexes

Annex 1: Technical specifications of the main GFM output layers, which are used in the automated file quality checks.

The technical specifications for the three main GFM output layers (i.e. Observed Flood Extent, Reference Water Mask, and Exclusion Mask) are shown in Table 12. Note that for the Reference Water Mask and the Exclusion Mask, no separate metadata files are available.

Table 12: Technical specifications of the GFM output layers Observed Flood Extent, Reference Water Mask, and Exclusion Mask, used in the automated file quality checks.

PARAMETER	*DEFINITION*		
	Observed Flood Extent	*Reference Water Mask*	*Exclusion Mask*
Product acronym:	ENSEMBLE_FLOOD	REFERENCE_WATER	EXCLUSION_LAYER
Geometric resolution:	Pixel size 20x20m	Pixel size 20x20m	Pixel size 20x20m
Coordinate Reference System (CRS):	CRS of corresponding Sentinel-1 scene	CRS of corresponding Sentinel-1 scene	CRS of corresponding Sentinel-1 scene
Coverage:	Extent of corresponding Sentinel-1 Scene	Extent of corresponding Sentinel-1 scene	Extent of corresponding Sentinel-1 scene
Data type:	8bit unsigned raster, LZW compression	8bit unsigned raster, LZW compression	8bit unsigned raster, LZW compression
Raster coding (thematic pixel values):	0: no flood; 1: flood; 255: nodata.	0: no water; 1: permanent water; 2: temporary water; 255: nodata.	0: not excluded; 1: excluded; 255: nodata.
Metadata:	JSON File (.json)	-	-
Data format:	GeoTIFF (.tif)	GeoTIFF (.tif)	GeoTIFF (.tif)
Filename:	[PRODUCT ACRONYM]_ [SENTINEL-1 SCENE ID].tif	[PRODUCT ACRONYM]_ OUT_S1_IW_GRDH_1SSV_ [START DATE]_ [END DATE]_MONTH*.tif	[PRODUCT ACRONYM]_ [SENTINEL-1 SCENE ID].tif

Annex 2: Overview of the worldwide flood events selected as Use Cases, and of the defined areas of interest, including the Exclusion Mask.

Table 13: Descriptions of the worldwide flood events selected as Use Cases, including on-line references, geographic locations, and names of the processed Sentinel-1 scenes.

#	USE CASE	DESCRIPTION OF FLOOD EVENT (AND ON-LINE REFERENCES)	GEOGRAPHIC COORDINATES AND SENTINEL-1 SCENE
1	**USA - Texas** (29.08.2017)	In August 2017, Hurricane Harvey hit Texas. It was the first category 4 hurricane since 1970 to make landfall along the mid-Texas Coast. It started as a tropical storm earlier in August, crossed the warm waters of the Gulf of Mexico and hit the Texan Coast on 25 August 2017. It brought destructive winds, torrential rainfall, and devastating flooding to South and Southeast Texas.[20]	▪ 30° 22' 19" N, 96° 21' 26" W ▪ S1A_IW_GRDH_1SDV_20170829T002645_20170829T002710_018131_01E74D_3220
2	**Morocco** (09.01.2021)	The start of 2021 was marked by heavy rainfall across Morocco. Casablanca was one of the worst affected regions, with floods causing much infrastructural damage. Public transport shut down, entire neighborhoods were flooded, and there were 4 fatalities.[21]	▪ 30° 26' 31" N, 9° 11' 46" W ▪ S1A_IW_GRDH_1SDV_20210109T184126_20210109T184155_036065_043A1A_8022
3	**Myanmar** (21.07.2021)	In July 2021, southern parts of Myanmar were hit by severe and widespread floods, after heavy rainfalls across Rakhine, Bago, Ayeyarwady, Kayin, Mon and Tanitharyi.[22]	▪ 16° 41' 3" N, 94° 44' 47" E ▪ S1B_IW_GRDH_1SDV_20210721T115336_20210721T115405_027892_035402_F0E6
4	**France** (16.10.2018)	Extremely heavy rain (244mm within 6 hours) over night from 14 to 15 October, 2018, led to severe floodings in the Aude department.[23]	▪ 43° 14' 48" N, 3° 2' 39" E ▪ S1A_IW_GRDH_1SDV_20181016T060051_20181016T060116_024157_02A459_BFCA
5	**Indonesia** (29.03.2023)	Floods in Central Kalimantan (Kalimantan Tengah) were caused by severe rain.[24]	▪ 2° 29' 4" S, 115° 3' 1" E ▪ S1A_IW_GRDH_1SDV_20230404T220000_20230404T220025_047952_05C352_9D53
6	**Italy** (16.05.2023)	While still recovering from catastrophic flooding earlier in May, Emilia-Romagna was hit by further heavy rain starting on 15 May 2023 causing flooding of 14 rivers and affecting 23 municipalities.[25]	▪ 44° 32' 18" N, 11° 54' 58" E ▪ S1A_IW_GRDH_1SDV_20230522T051946_20230522T052011_048642_05D9B6_20B9
7	**Venezuela** (29.07.2017)	Venezuela was hit by flooding after days of heavy rain affecting more than 6000 families and causing serious damages in several states of the country.[26]	▪ 7° 40' 41" N, 66° 43' 56" W ▪ S1B_IW_GRDH_1SDV_20170729T224054_20170729T224119_006709_00BCCD_B81B

[20] https://floodlist.com/america/usa/flooding-houston-south-east-texas-august-2017
[21] https://disasterscharter.org/es/web/guest/activations/-/article/flood-flash-in-morocco-activation-694-
[22] https://reliefweb.int/disaster/fl-2021-000095-mmr; https://ahacentre.org/flash-update/flash-update-no-01-monsoonal-flooding-myanmar-28-july-2021/
[23] https://floodlist.com/europe/france-floods-aude-department-october2018
[24] https://floodlist.com/asia/indonesia-floods-central-kalimantan-april-2023
[25] https://floodlist.com/europe/italy-floods-emiliaromagna-marche-may-2023
[26] https://floodlist.com/america/venezuela-floods-august-2017

8	**Bangladesh** (10.08.2023)	2.4 million people were exposed to flooding after heavy rainfall and water flowing down from the hills in the districts of Chattogram, Bandarban, Cox's Bazar, and Rangamati. Around 327.59 square kilometres of land have been inundated by surface waters.[27]	▪ 22° 14' 18" N, 91° 55' 23" E ▪ S1A_IW_GRDH_1SDV_20230810T115627_20230810T115652_049813_05FD92_A0D6
9	**Greece** (07.09.2023)	Storm Daniel caused heavy rainfalls, following a heat wave. Severe floods followed in central Greece in early September 2023 causing serious material damages.[28]	▪ 39° 26' 57" N, 22° 7' 13" E ▪ S1A_IW_GRDH_1SDV_20230907T162412_20230907T162437_050224_060B99_D80F
10	**Portugal** (23.12.2019)	Storm Elsa caused heavy winds and rain in Portugal and southern Spain causing severe damage.[29]	▪ 40° 9' 26" N, 8° 41' 56" W ▪ S1A_IW_GRDH_1SDV_20191223T064251_20191223T064316_030472_037D16_1012
11	**India** (22.05.2020)	North-eastern India was hit by floodings and landslides caused by heavy rain following Cyclone Amphan.[30]	▪ 21° 56' 56" N, 87° 51' 51" E ▪ S1A_IW_GRDH_1SDV_20200522T000444_20200522T000509_032670_03C8AC_A6E3
12	**Dominican Republic** (23.11.2023)	The Dominican Republic was hit by the highest rainfall ever in the country, due to a tropical disturbance in the Caribbean region.[31]	▪ 19° 10' 42" N, 69° 47' 55" W ▪ S1A_IW_GRDH_1SDV_20231123T103106_20231123T103136_051343_0631FA_AFFB

[27] https://reliefweb.int/report/bangladesh/bangladesh-chattogram-division-flash-flood-and-monsoon-rain-2023-situation-report-no-01-13-august-2023
[28] https://floodlist.com/europe/greece-floods-september-2023
[29] https://floodlist.com/europe/spain-portugal-storm-elsa-floods-december-2019
[30] https://floodlist.com/asia/india-floods-in-assam-sikkim-may-2020
[31] https://floodlist.com/america/floods-november-2023-jamaica-dominicanrepublic-haiti

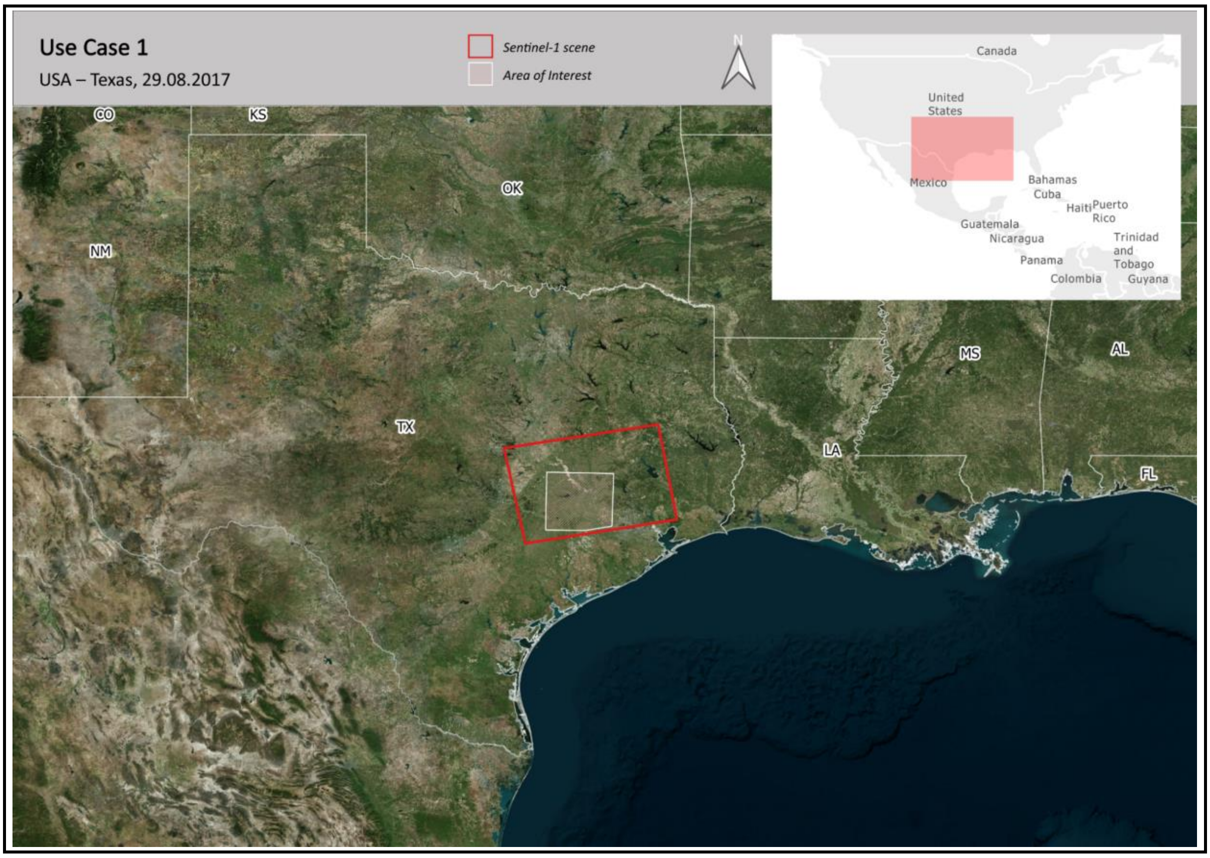

Figure 51: Use Case 1 (USA – Texas, 29.08.2017) – Defined area of interest. (Basemap: Bing – Aerial View).

Table 14: Use Case 1 (USA – Texas, 29.08.2017) - Overview of the Exclusion Mask for the area of interest. (Note that some of the Exclusion Mask sub-layers overlap).

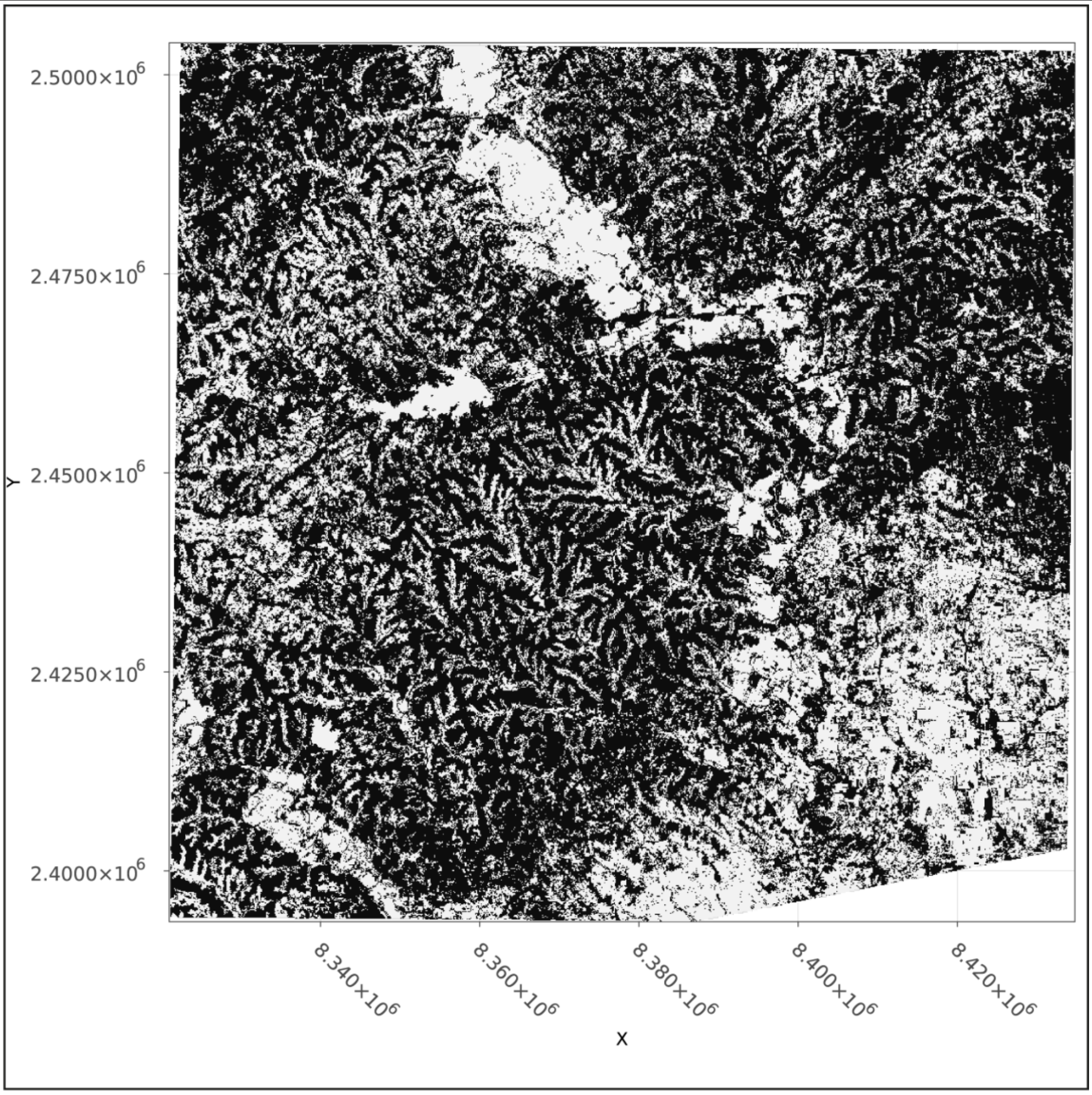

	km²	% of total
Area of interest	12,120.11	100
Excluded area	7,562.18	62.39
No sensitivity area	4,302.24	35.50
Low backscatter area	169.66	1.40
Topographic distortion area	5,346.50	44.11
Radar shadow area	1.34	0.01

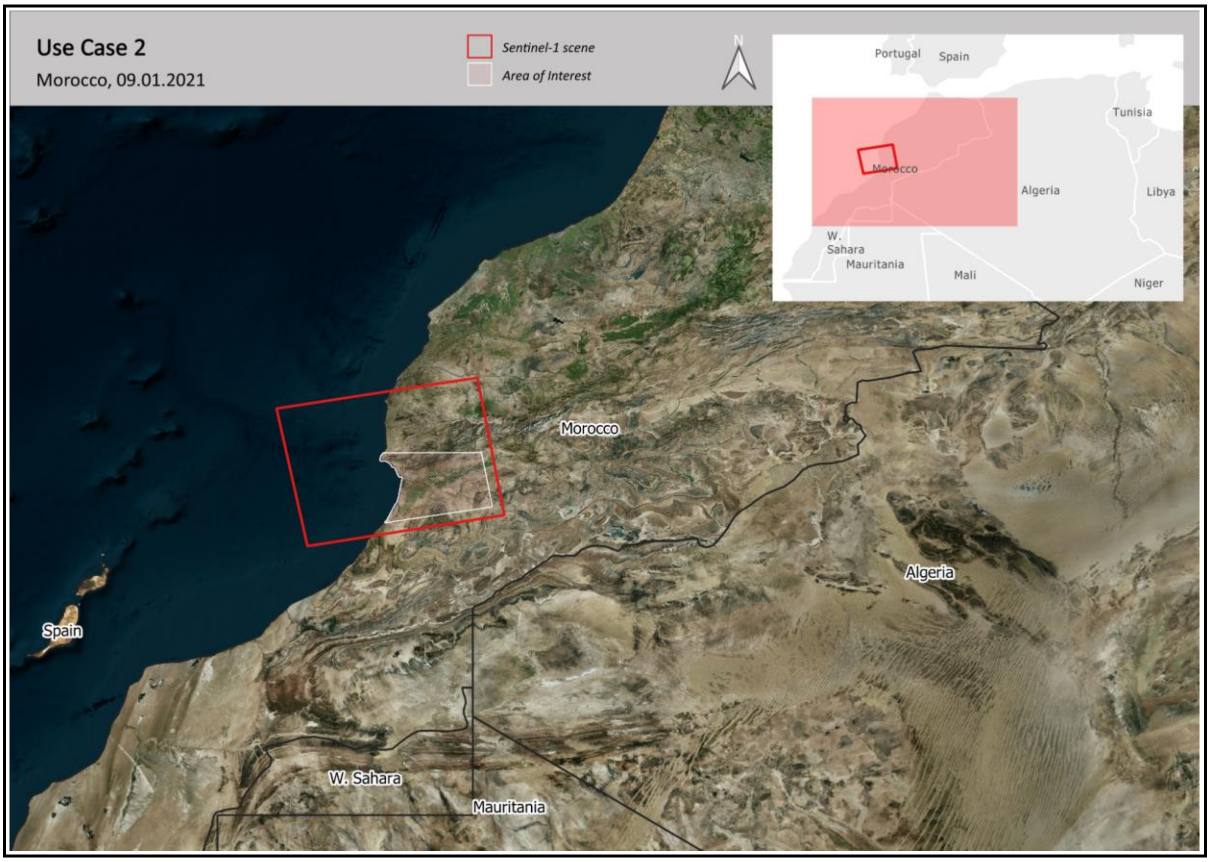

Figure 52: Use Case 2 (Morocco, 09.01.2021) – Defined area of interest. (Basemap: Bing Aerial View).

Table 15: Use Case 2 (Morocco, 09.01.2021) - Overview of the Exclusion Mask for the area of interest. (Note that some Exclusion Mask sub-layers overlap).

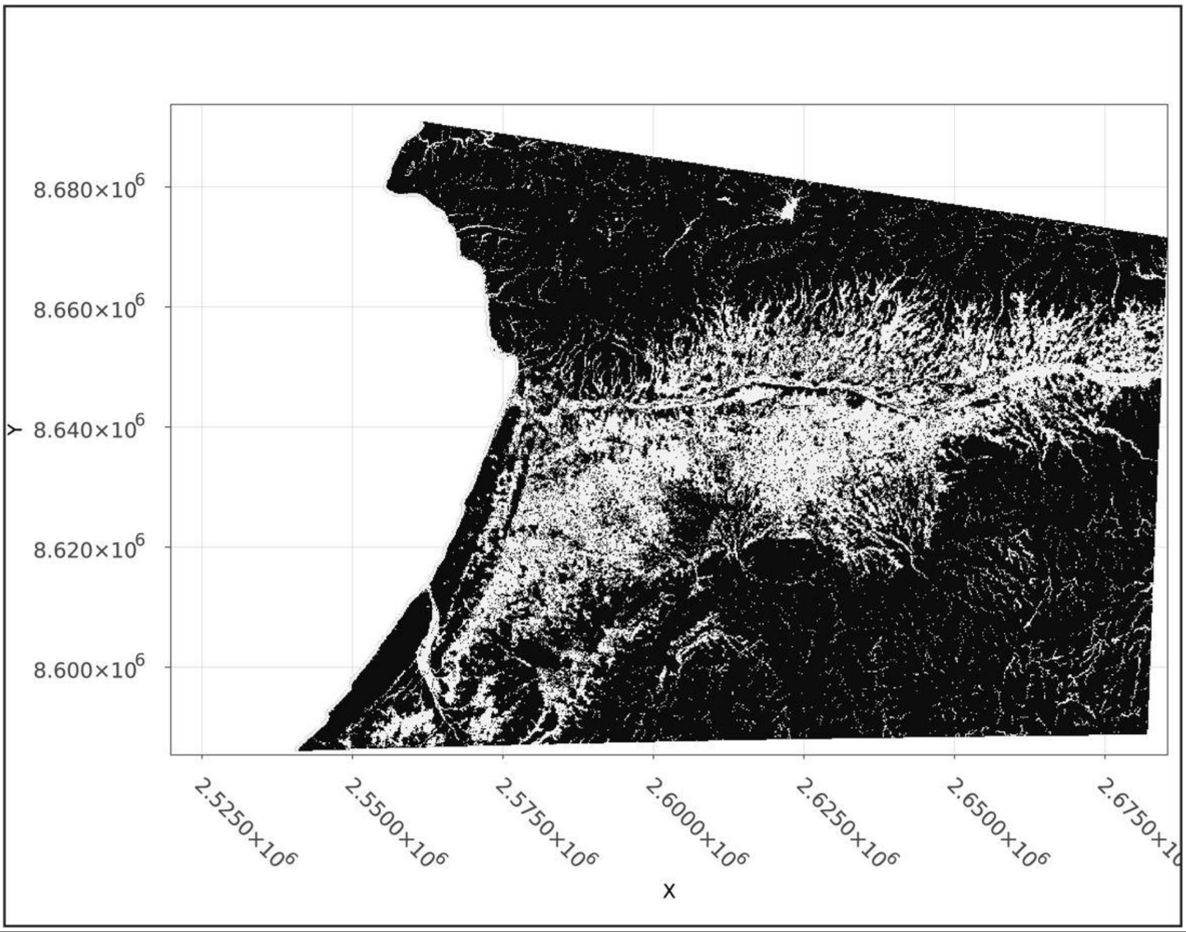

	km^2	% of total
Area of interest	11,201.92	100
Excluded area	8,424.20	75.20
No sensitivity area	3,222.33	28.77
Low backscatter area	1,044.11	9.32
Topographic distortion area	7,483.18	66.80
Radar shadow area	157.65	1.41

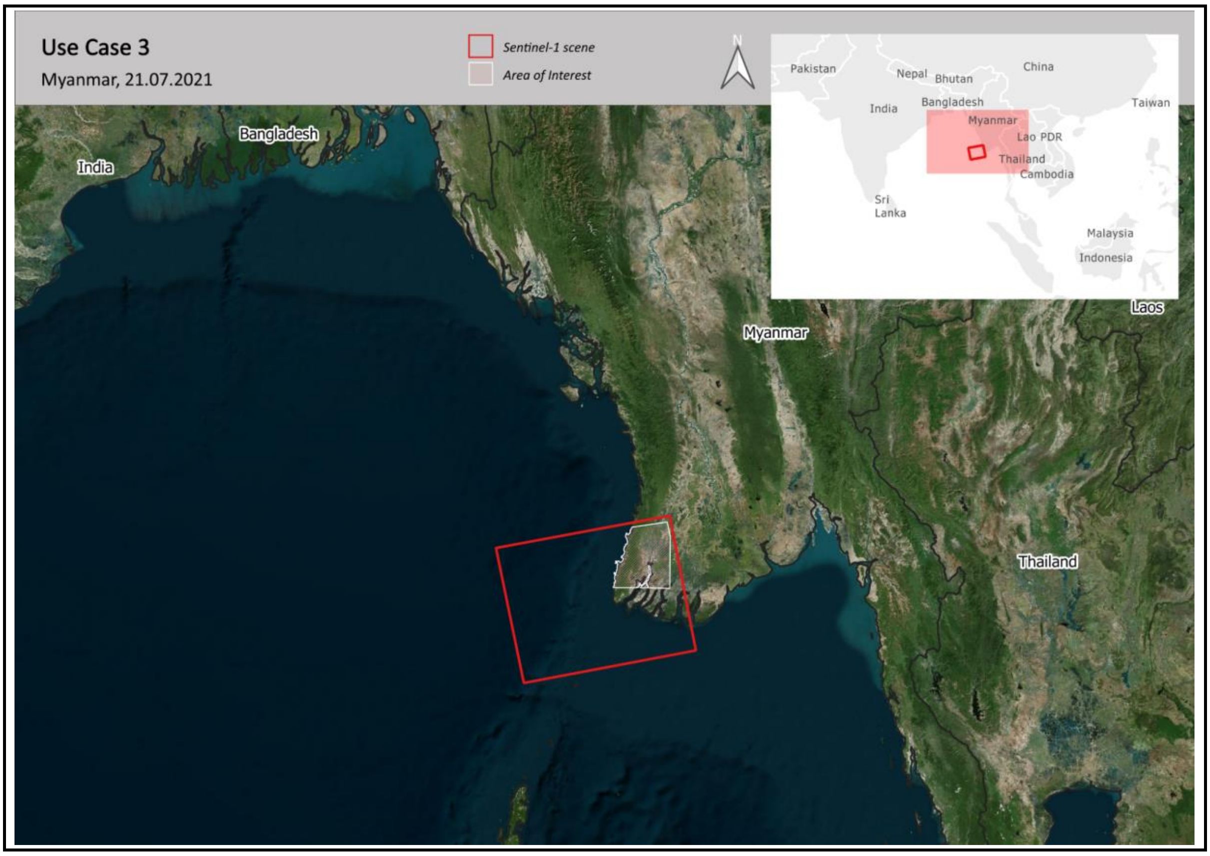

Figure 53: Use Case 3 (Myanmar, 21.07.2021) – Defined area of interest. (Basemap: Bing Aerial View).

Table 16: Use Case 3 (Myanmar, 21.07.2021) – Overview of the Exclusion Mask for the area of interest. (Note that some Exclusion Mask sub-layers overlap).

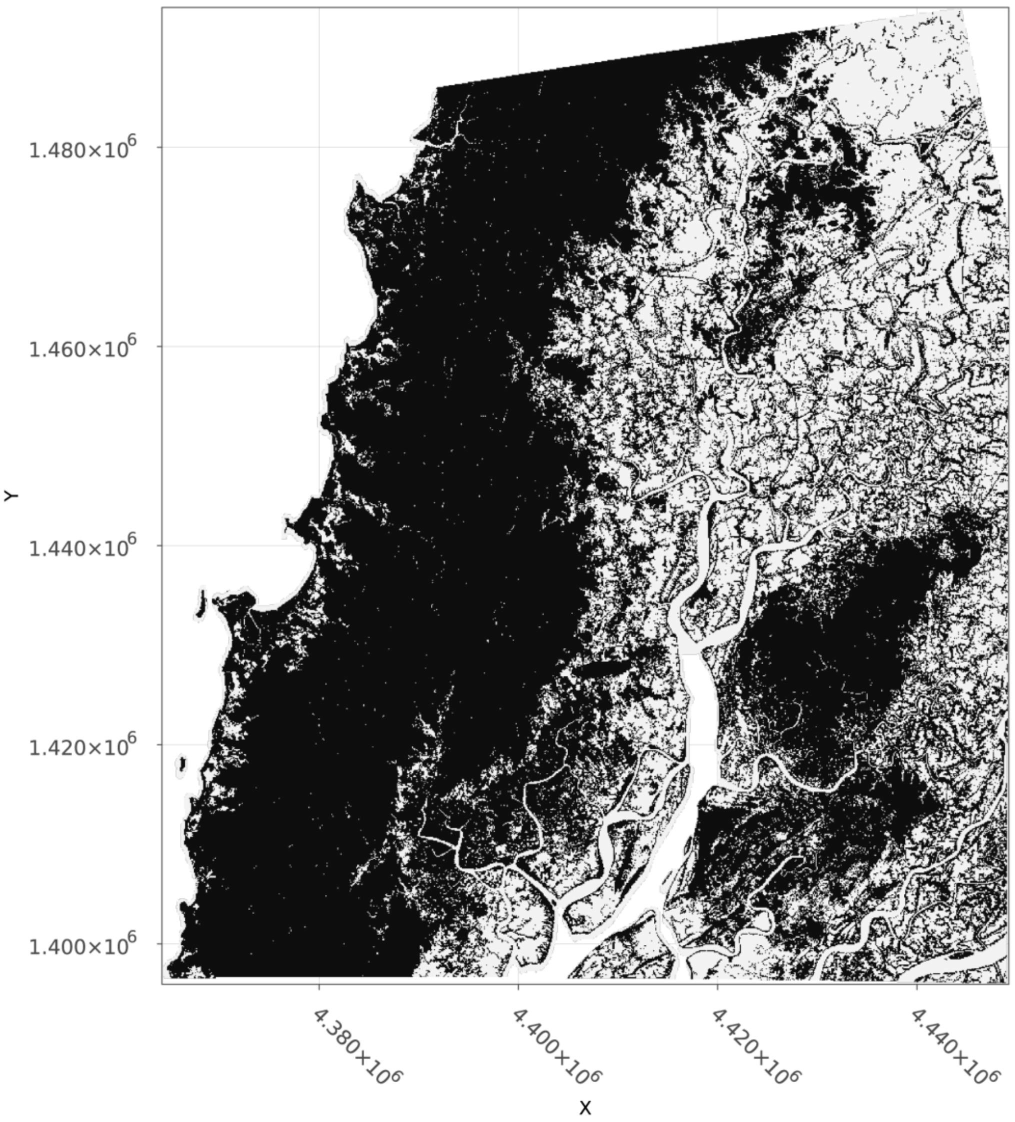

	km^2	% of total
Area of interest	6,614.72	100
Excluded area	4,281.72	64.73
No sensitivity area	4,111.24	62.15
Low backscatter area	309.58	4.68
Topographic distortion area	2,440.74	36.89
Radar shadow area	0.69	0.01

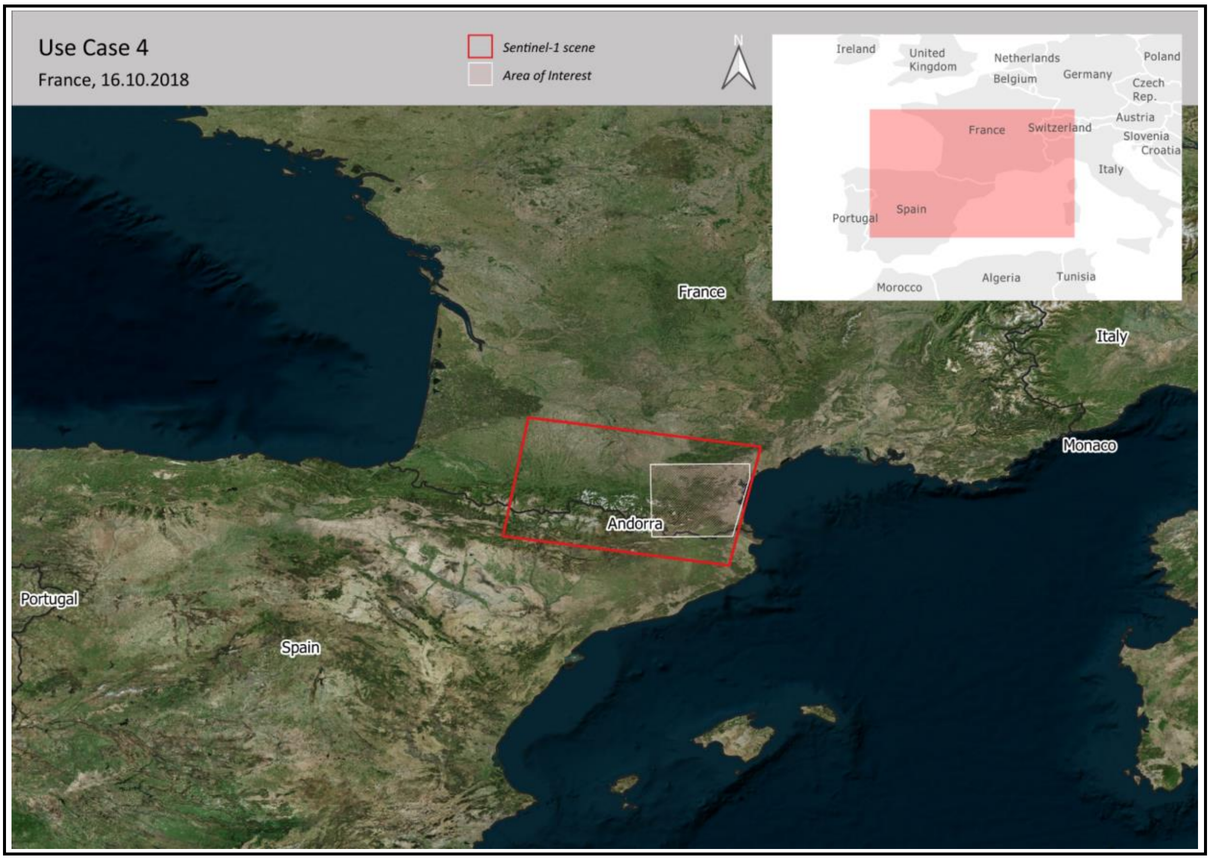

Figure 54: Use Case 4 (France, 16.10.2018) – Defined area of interest. (Basemap: Bing Aerial View).

Table 17: Use Case 4 (France, 16.10.2018) - Overview of the Exclusion Mask for the area of interest. (Note that some Exclusion Mask sub-layers overlap).

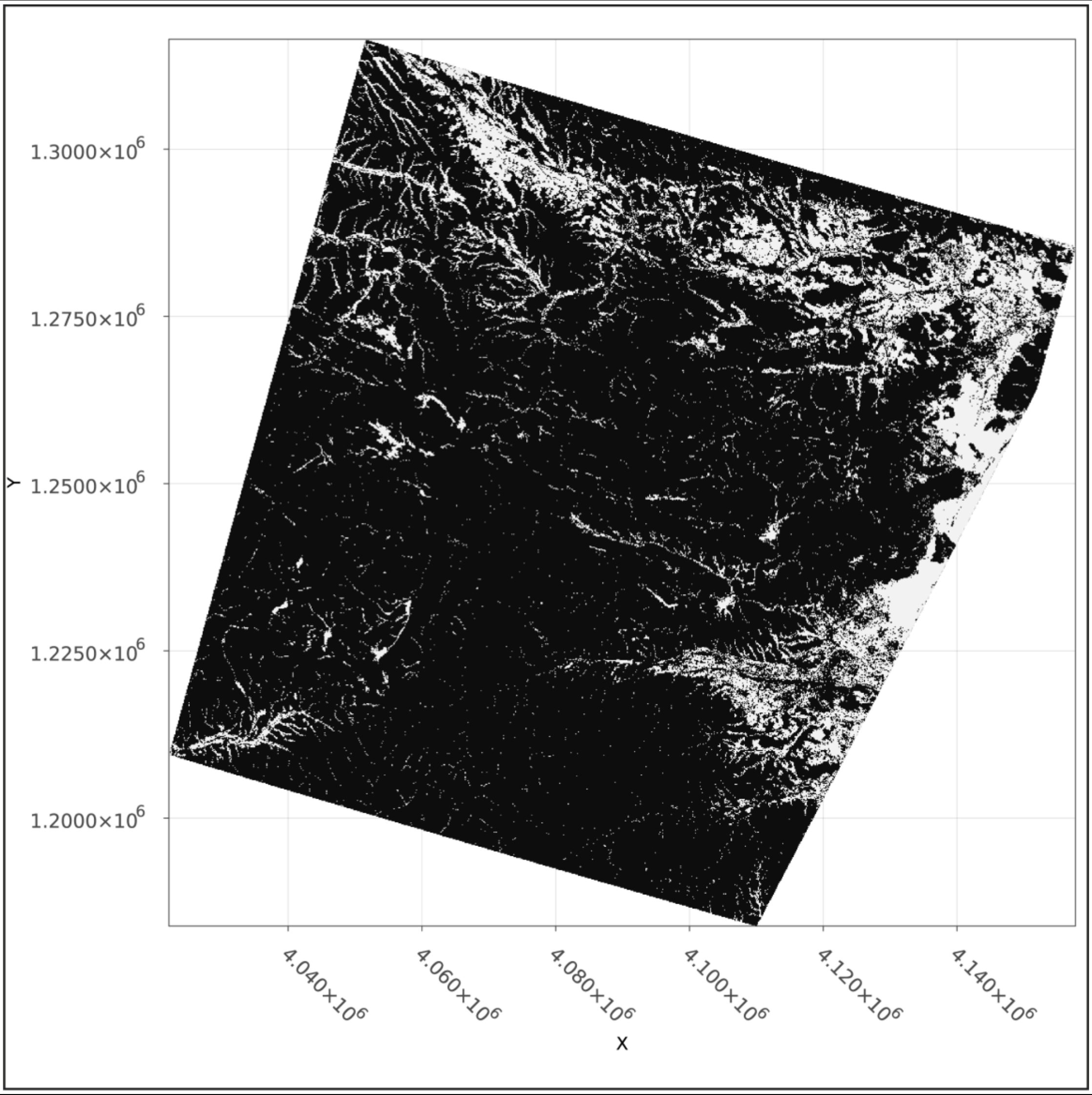

	km^2	% of total
Area of interest	11,408.98	100
Excluded area	9,744.50	85.41
No sensitivity area	6,403.83	56.13
Low backscatter area	233.01	2.04
Topographic distortion area	8,966.64	78.59
Radar shadow area	183.58	1.61

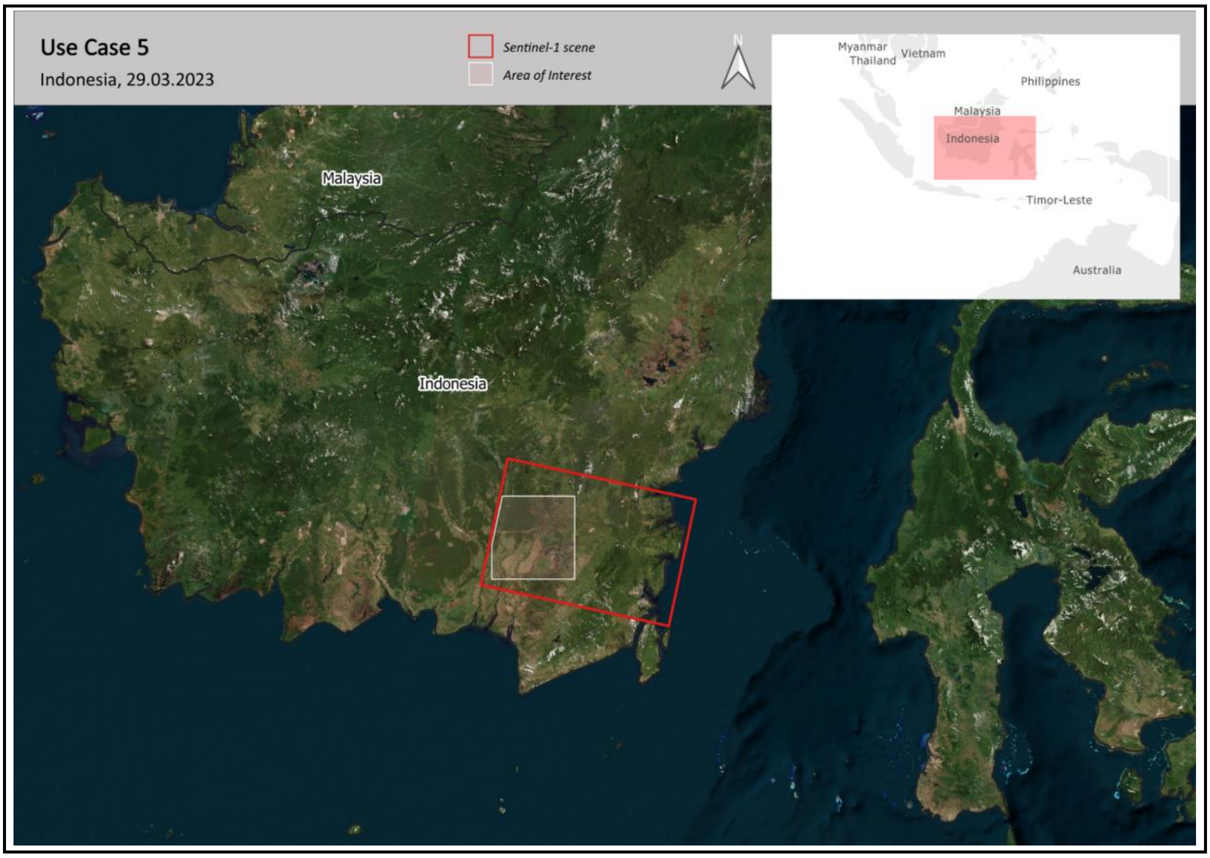

Figure 55: Use Case 5 (Indonesia, 29.03.2023) – Defined area of interest. (Basemap: Bing Aerial View).

Table 18: Use Case 5 (Indonesia, 29.03.2023) - Overview of the Exclusion Mask for the area of interest. (Note that some Exclusion Mask sub-layers overlap).

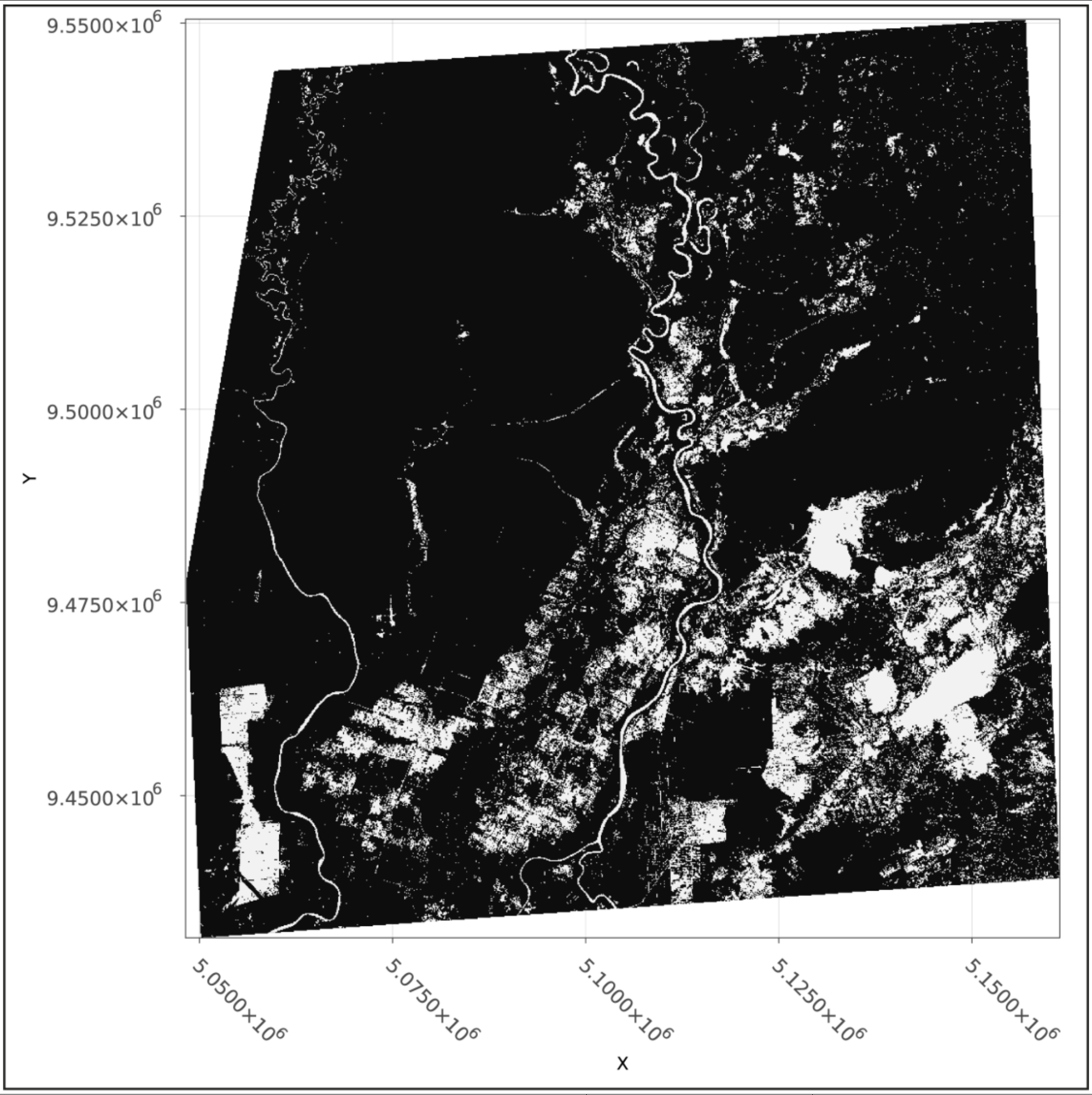

	km^2	% of total
Area of interest	11,939.03	100
Excluded area	10,370.41	86.86
No sensitivity area	10,335.08	86.57
Low backscatter area	143.49	1.20
Topographic distortion area	2,022.02	16.94
Radar shadow area	183.58	1.54

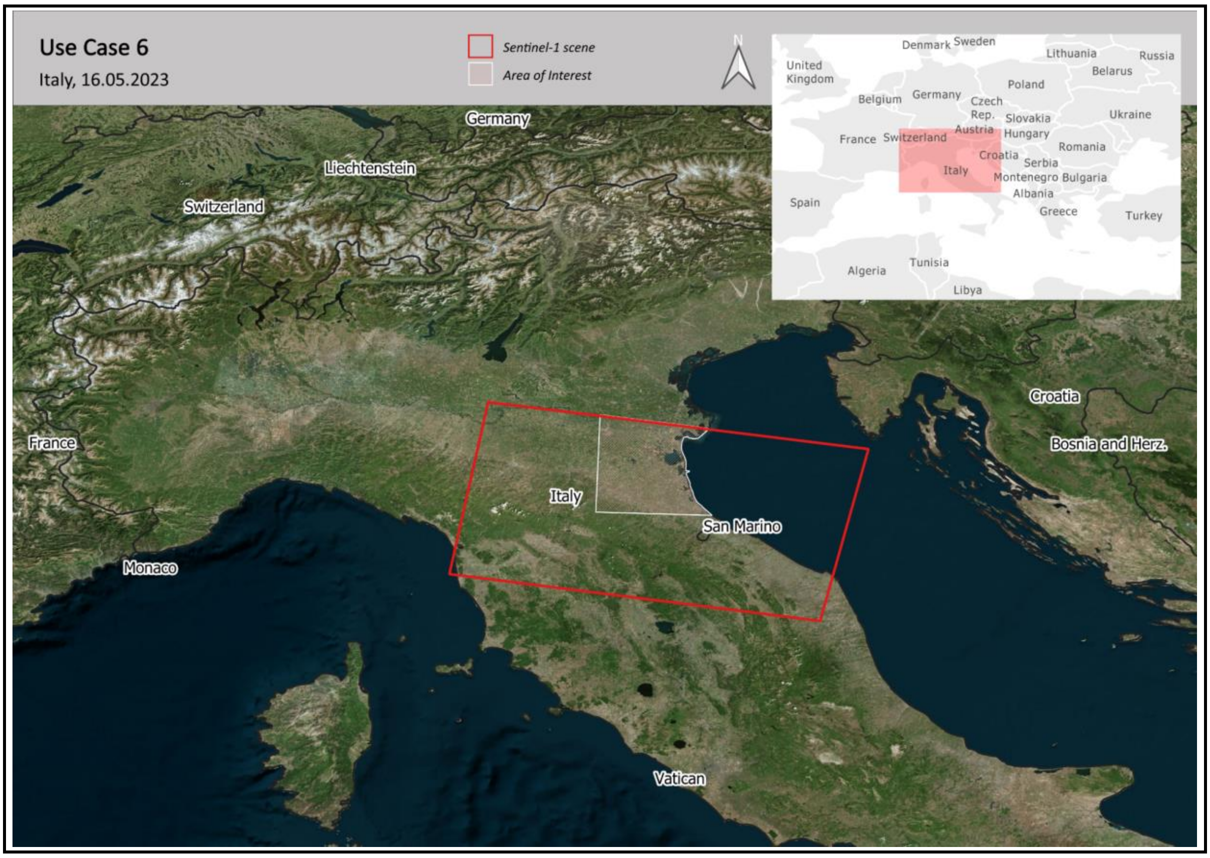

Figure 56: Use Case 6 (Italy, 16.05.2023) – Defined area of interest. (Basemap: Bing Aerial View).

Table 19: Use Case 6 (Italy, 16.05.2023) - Overview of the Exclusion Mask for the area of interest. (Note that some Exclusion Mask sub-layers overlap).

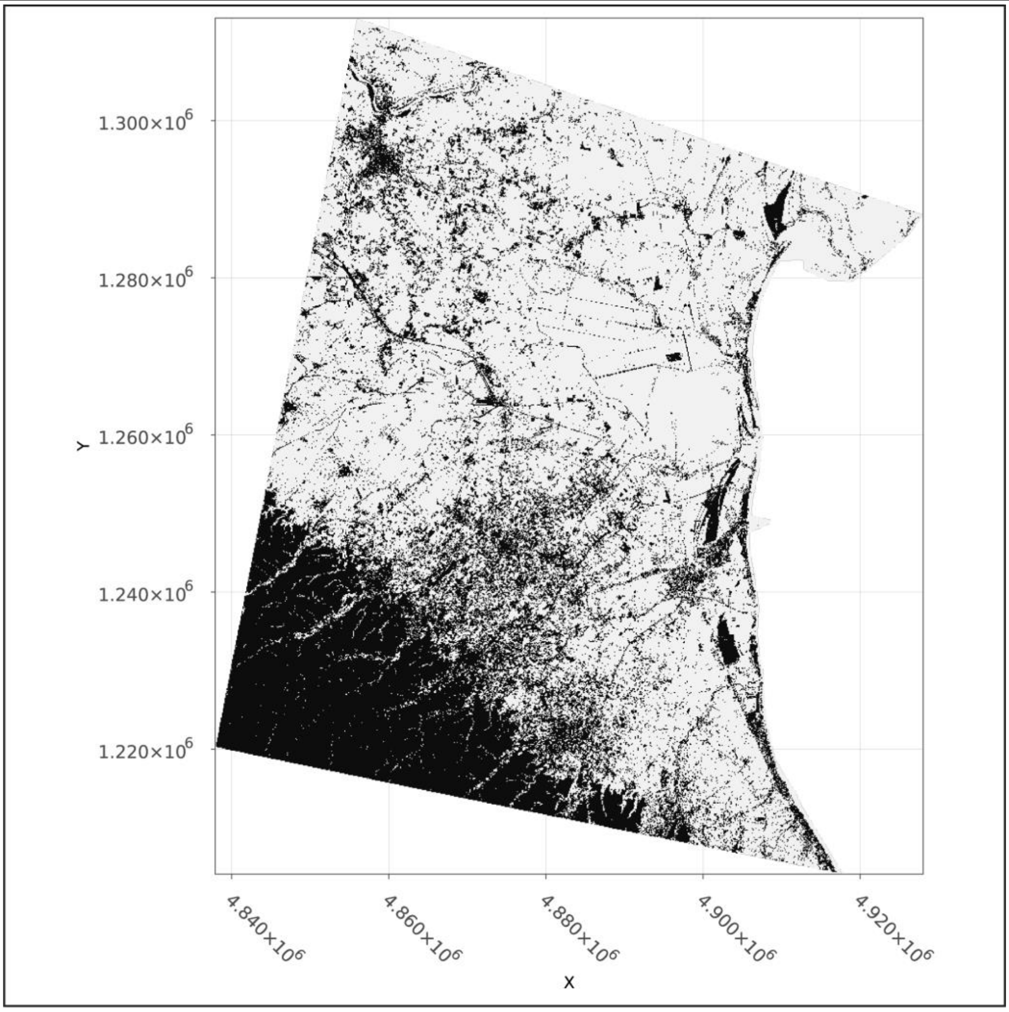

	km^2	% of total
Area of interest	5,896.58	100
Excluded area	1,894.70	32.13
No sensitivity area	1,519.65	25.77
Low backscatter area	305.41	5.18
Topographic distortion area	891.73	15.12
Radar shadow area	11.67	0.20

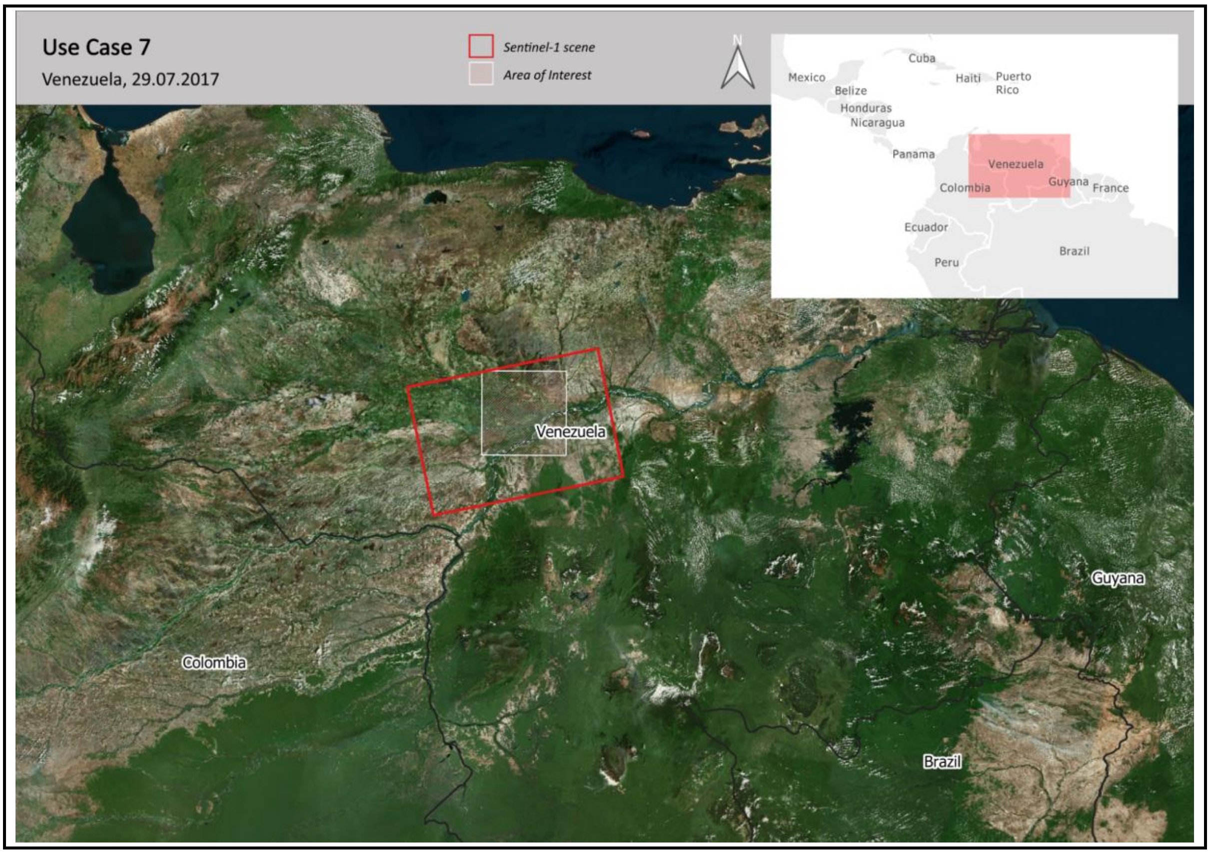

Figure 57: Use Case 7 (Venezuela, 29.07.2017) – Defined area of interest. (Basemap: Bing Aerial View).

Table 20: Use Case 7 (Venezuela, 29.07.2017) - Overview of the Exclusion Mask for the area of interest. (Note that some Exclusion Mask sub-layers overlap).

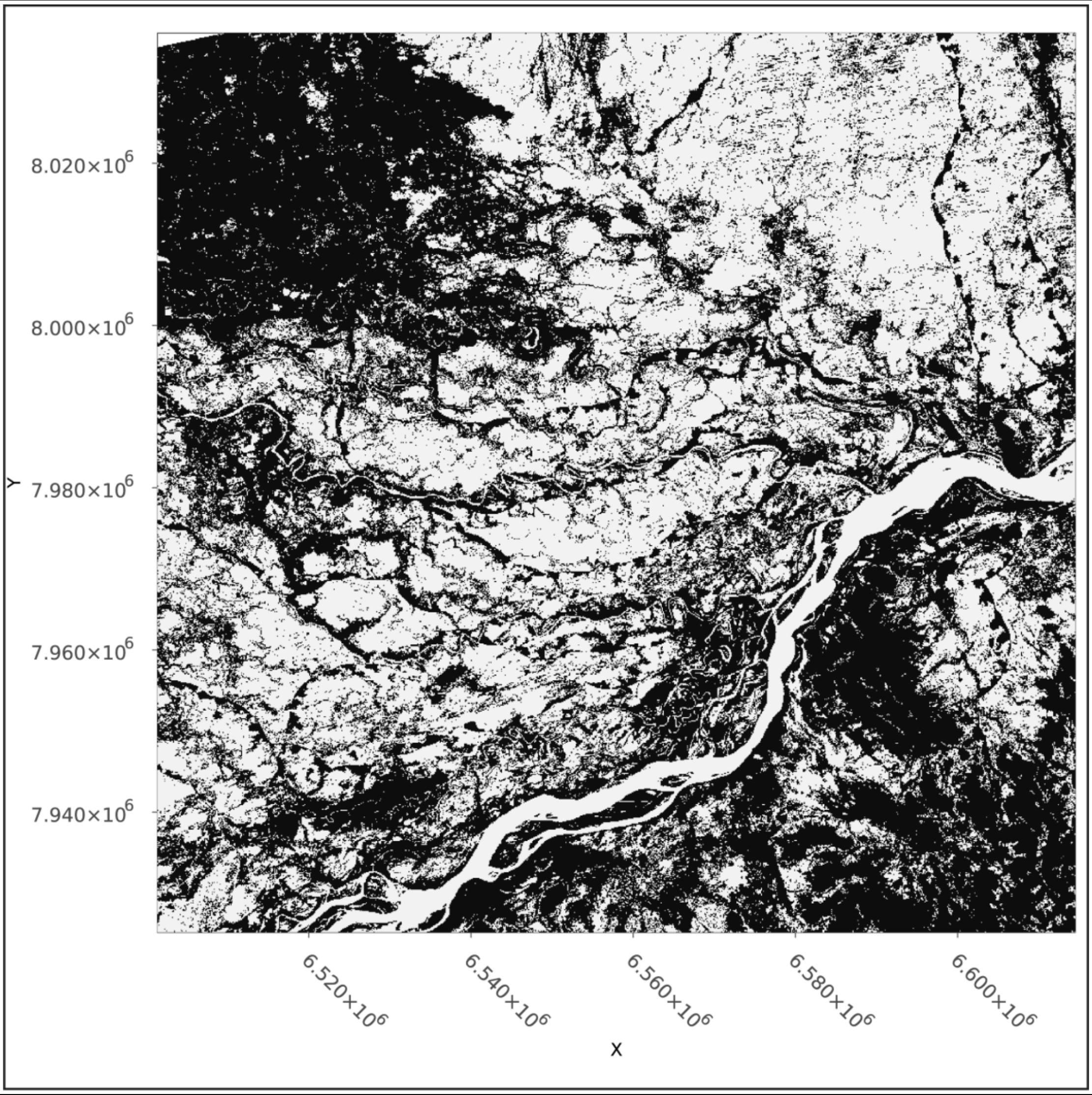

	km^2	% of total
Area of interest	12,520.21	100
Excluded area	6,225.26	49.72
No sensitivity area	5,334.19	42.60
Low backscatter area	762.30	6.09
Topographic distortion area	2,187.93	17.48
Radar shadow area	1.53	0.01

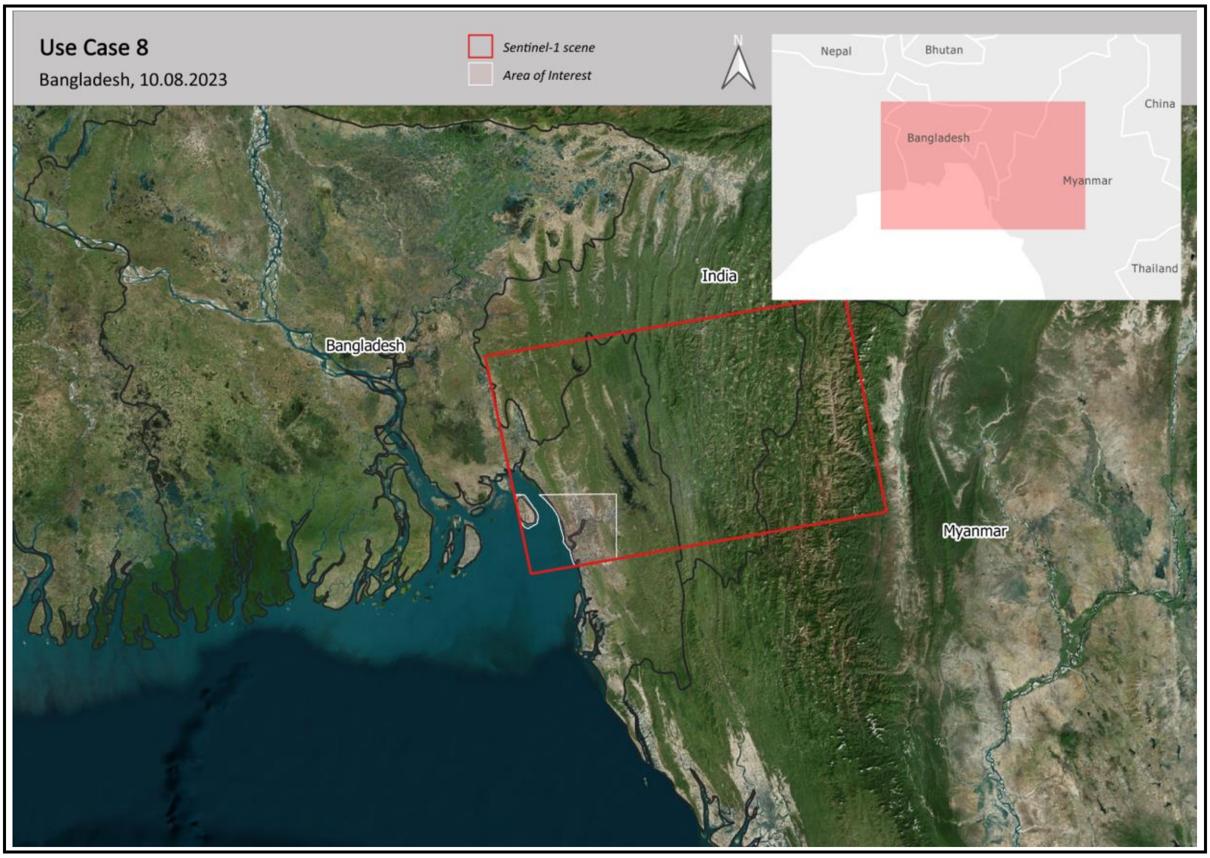

Figure 58: Use Case 8 (Bangladesh, 10.08.2023) – Defined area of interest. (Basemap: Bing Aerial View).

Table 21: Use Case 8 (Bangladesh, 10.08.2023) - Overview of the Exclusion Mask for the area of interest. (Note that some Exclusion Mask sub-layers overlap).

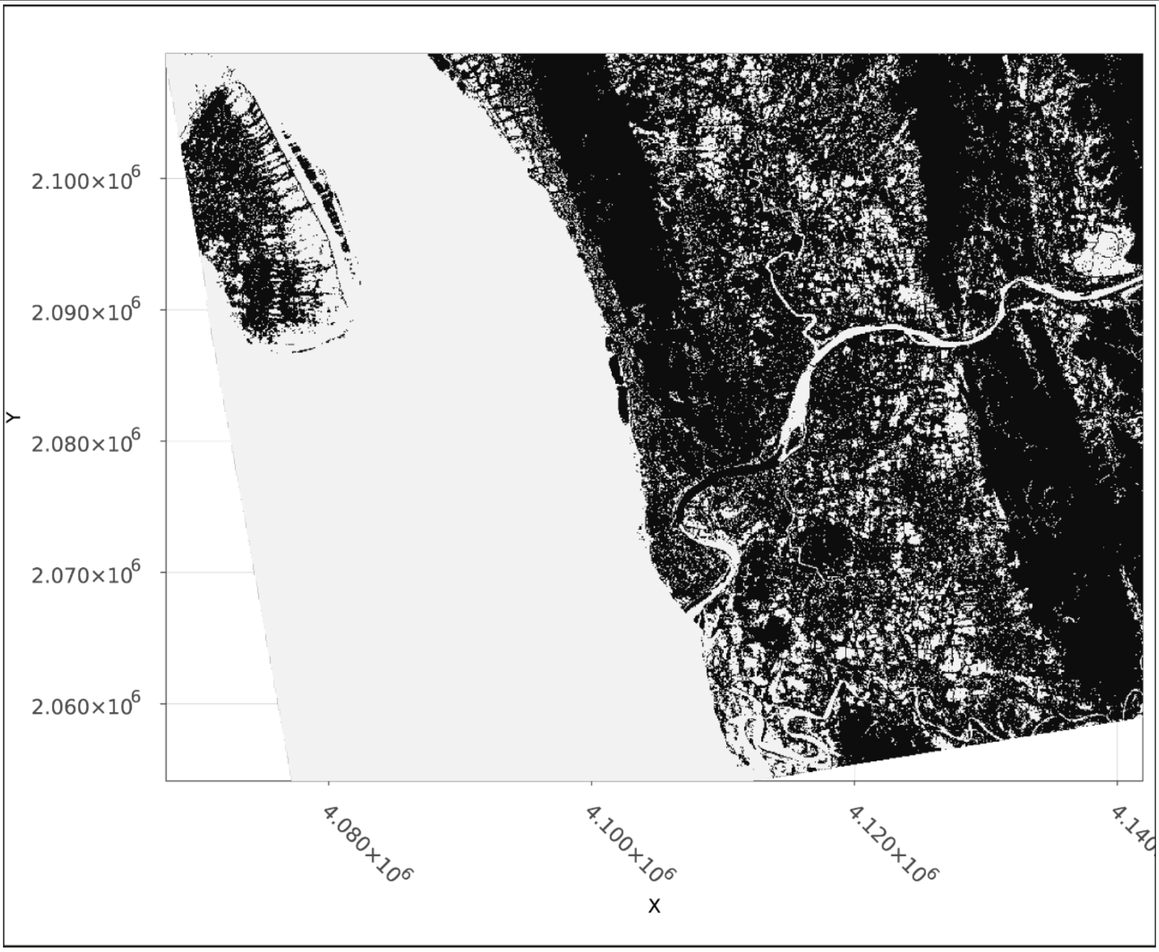

	km²	% of total
Area of interest	3,781.71	100
Excluded area	1,777.49	47
No sensitivity area	1,659.88	43.89
Low backscatter area	1,440.62	28.09
Topographic distortion area	586.81	15.52
Radar shadow area	2.94	0.08

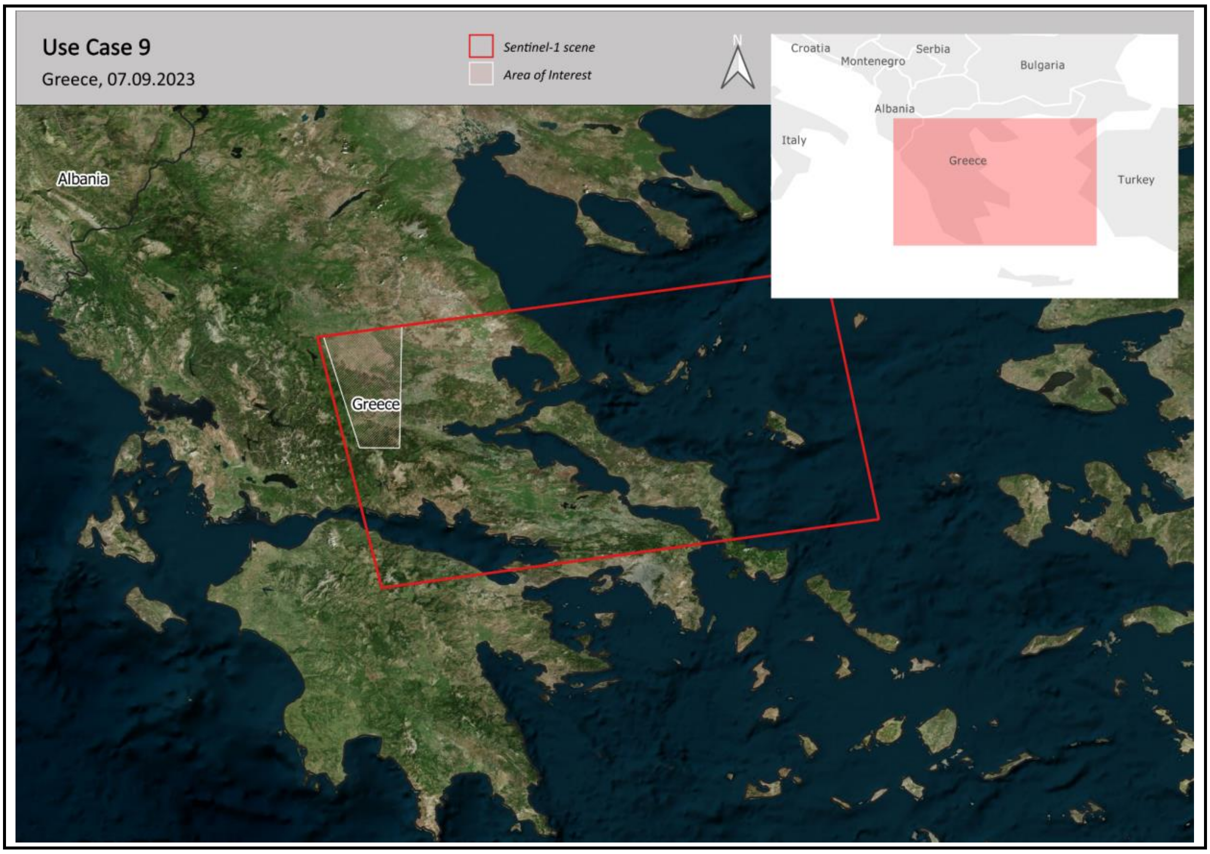

Figure 59: Use Case 9 (Greece, 07.09.2023) – Defined area of interest. (Basemap: Bing Aerial View).

Table 22: Use Case 9 (Greece, 07.09.2023) - Overview of the Exclusion Mask for the area of interest. (Note that some Exclusion Mask sub-layers overlap).

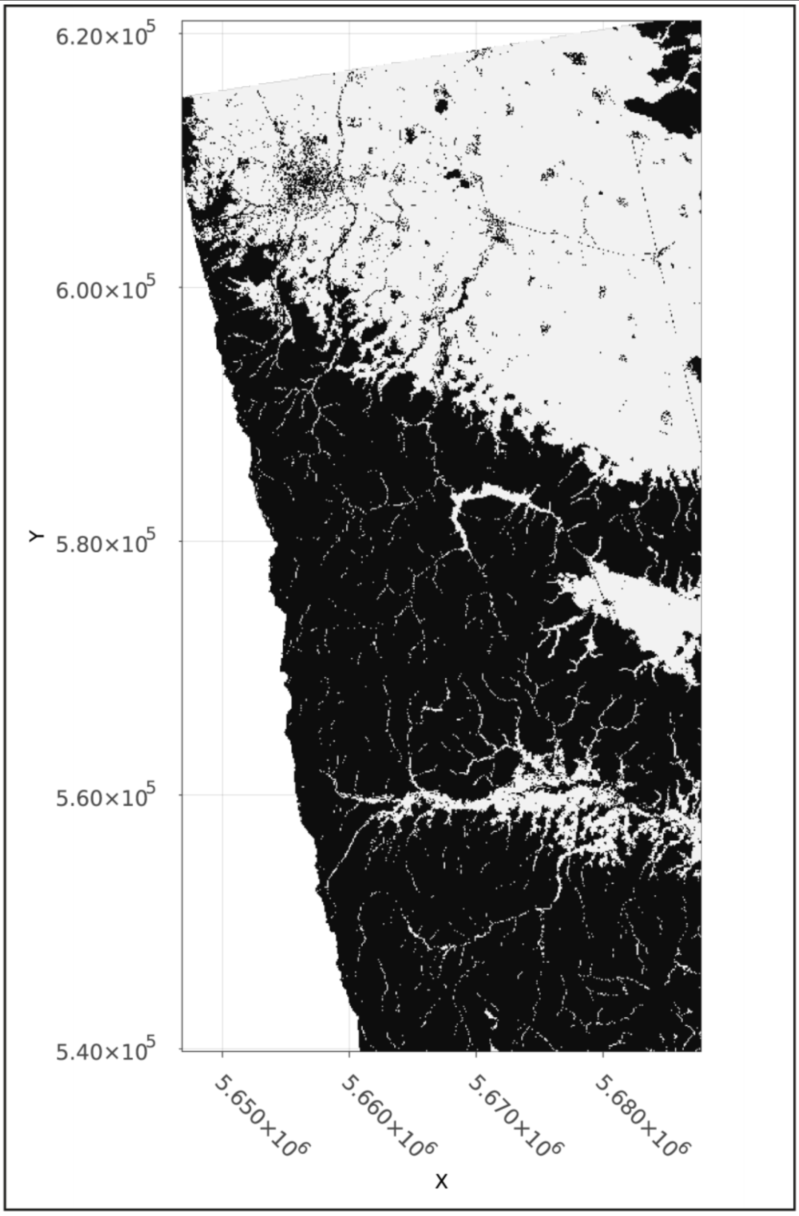

	km²	% of total
Area of interest	2,715.95	100
Excluded area	1,607.46	59.19
No sensitivity area	905.59	33.34
Low backscatter area	6.06	0.22
Topographic distortion area	1,512.74	55.70
Radar shadow area	4.91	0.18

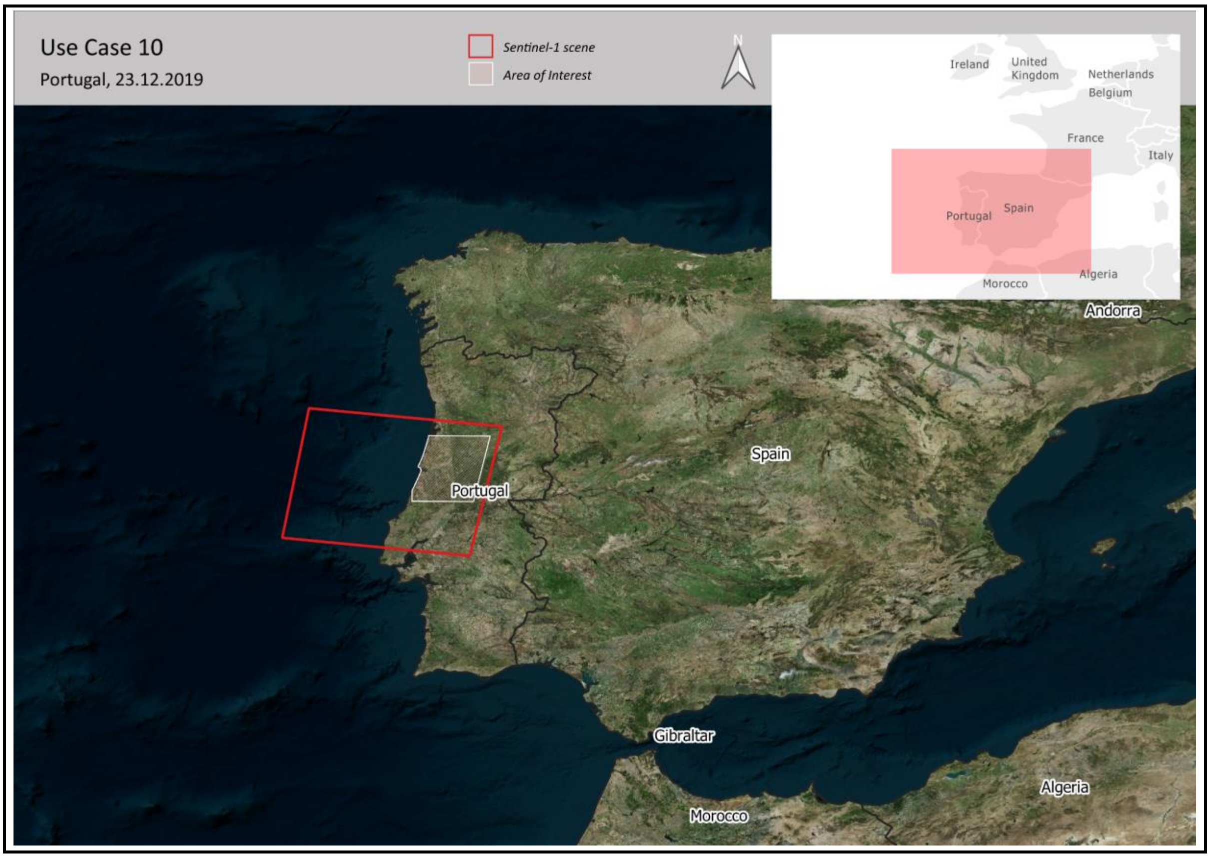

Figure 60: Use Case 10 (Portugal, 23.12.2019) – Defined area of interest. (Basemap: Bing Aerial View).

Table 23: Use Case 10 (Portugal, 23.12.2019) - Overview of the Exclusion Mask for the area of interest. (Note that some Exclusion Mask sub-layers overlap).

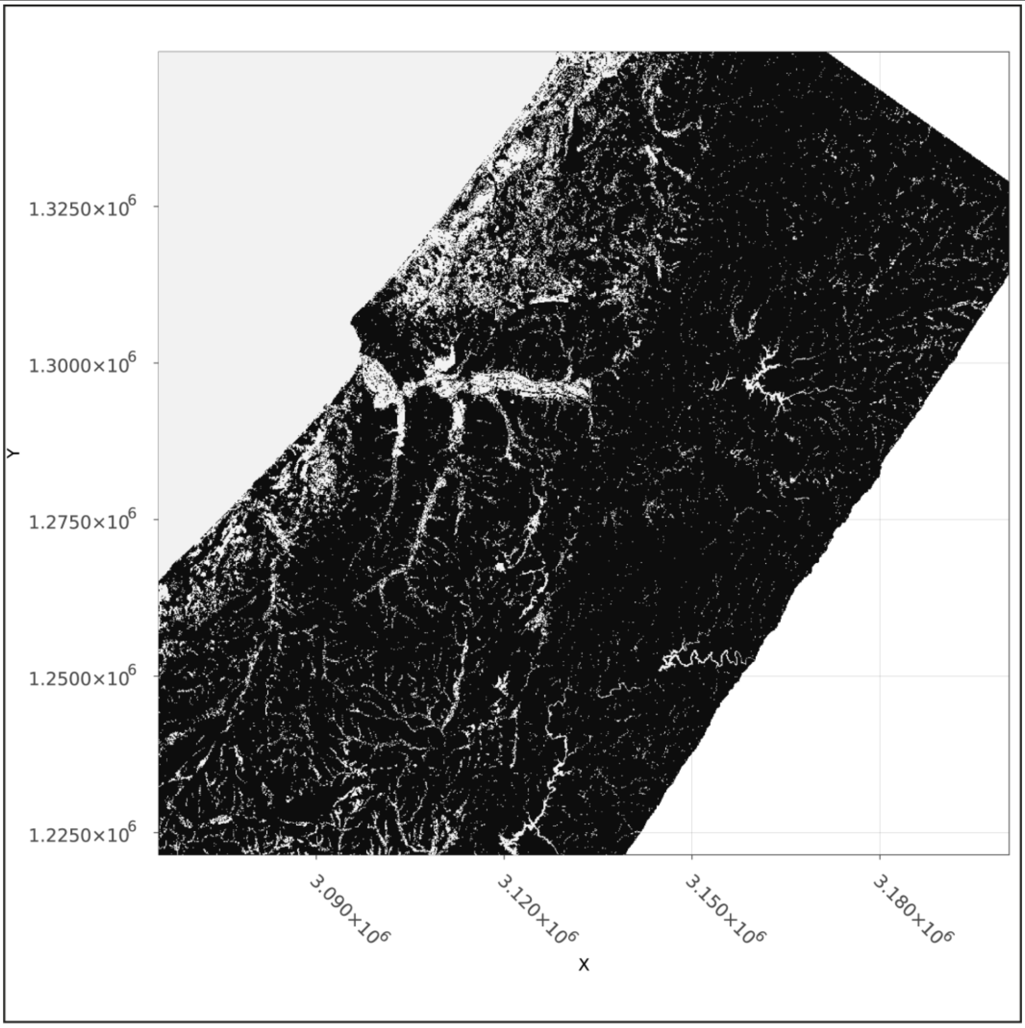

	km^2	% of total
Area of interest	14,238.45	100
Excluded area	10,193.97	71.59
No sensitivity area	8,161.82	57.32
Low backscatter area	2,953.80	20.75
Topographic distortion area	8,929.18	62.71
Radar shadow area	19.64	0.14

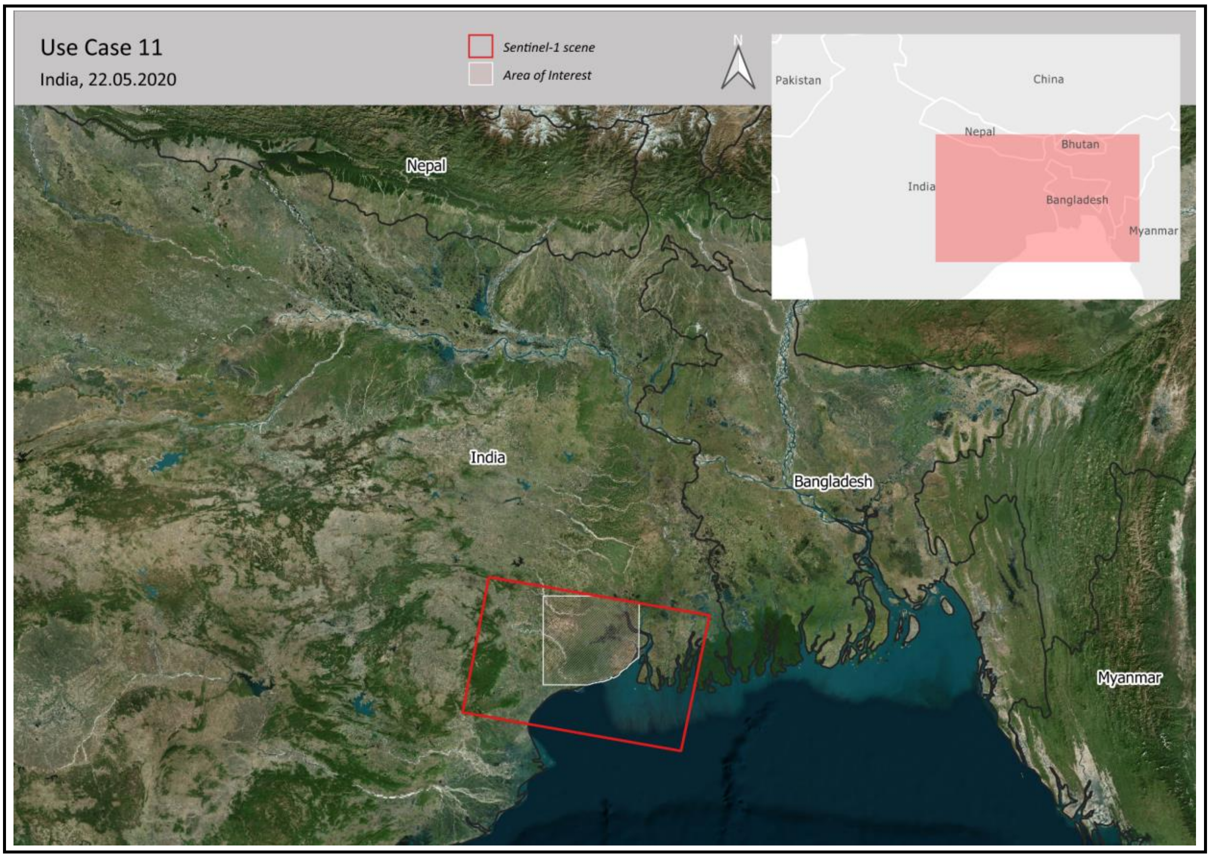

Figure 61: Use Case 11 (India, 22.05.2020) – Defined area of interest. (Basemap: Bing Aerial View).

Table 24: Use Case 11 (India, 22.05.2020) - Overview of the Exclusion Mask for the area of interest. (Note that some Exclusion Mask sub-layers overlap).

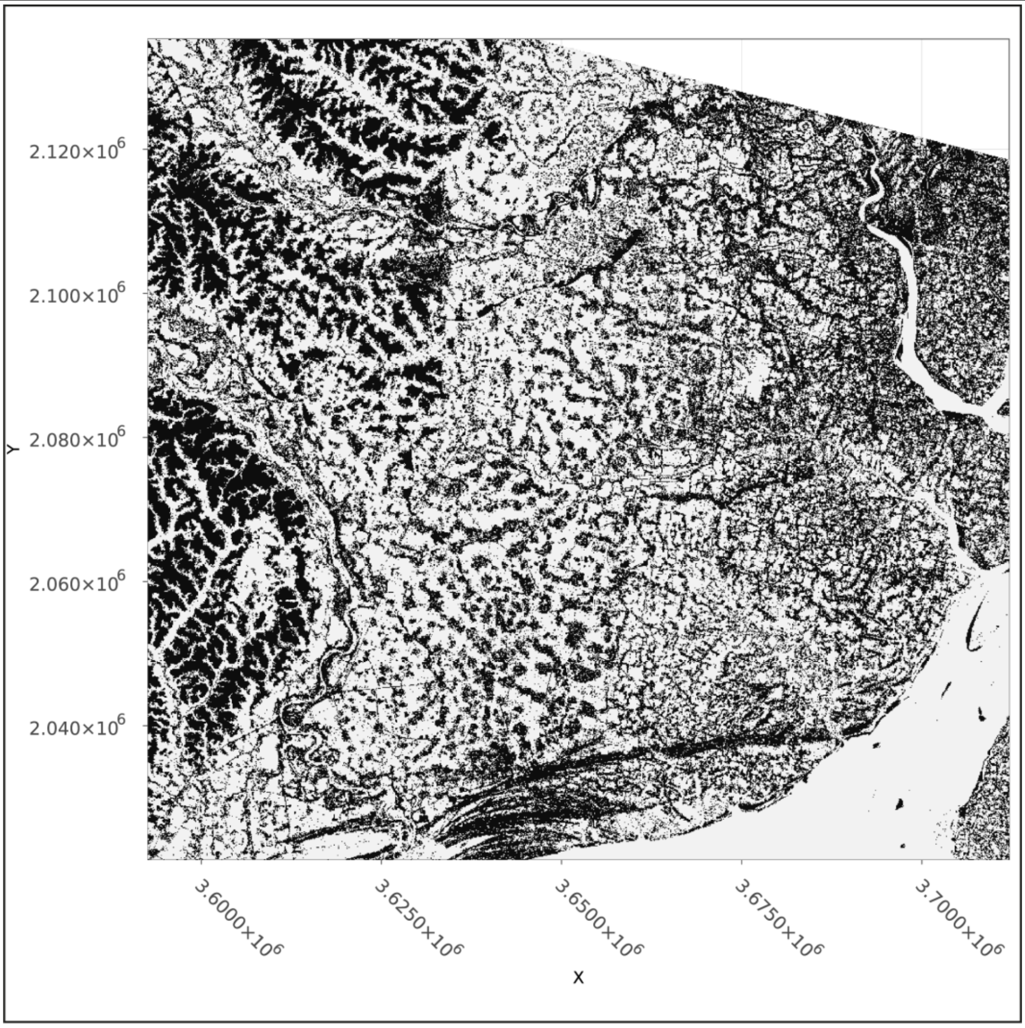

	km²	% of total
Area of interest	13,049.7	100
Excluded area	5,405.18	41.42
No sensitivity area	4,847.44	37.15
Low backscatter area	1,030.58	7.90
Topographic distortion area	1,467.80	11.25
Radar shadow area	0.60	0.005

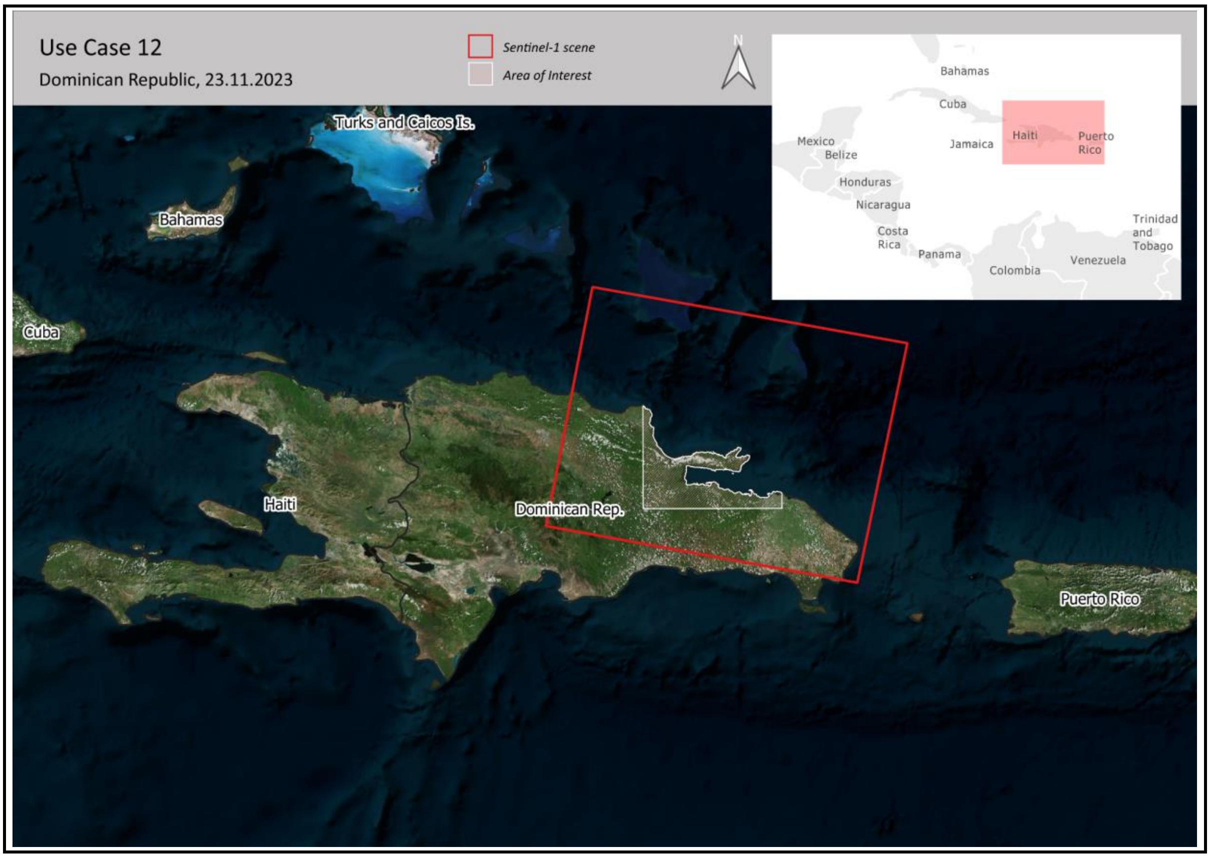

Figure 62: Use Case 12 (Dominican Republic, 23.11.2023) – Defined area of interest. (Basemap: Bing Aerial View).

Table 25: Use Case 12 (Dominican Republic, 23.11.2023) - Overview of the Exclusion Mask for the area of interest. (Note that some Exclusion Mask sub-layers overlap).

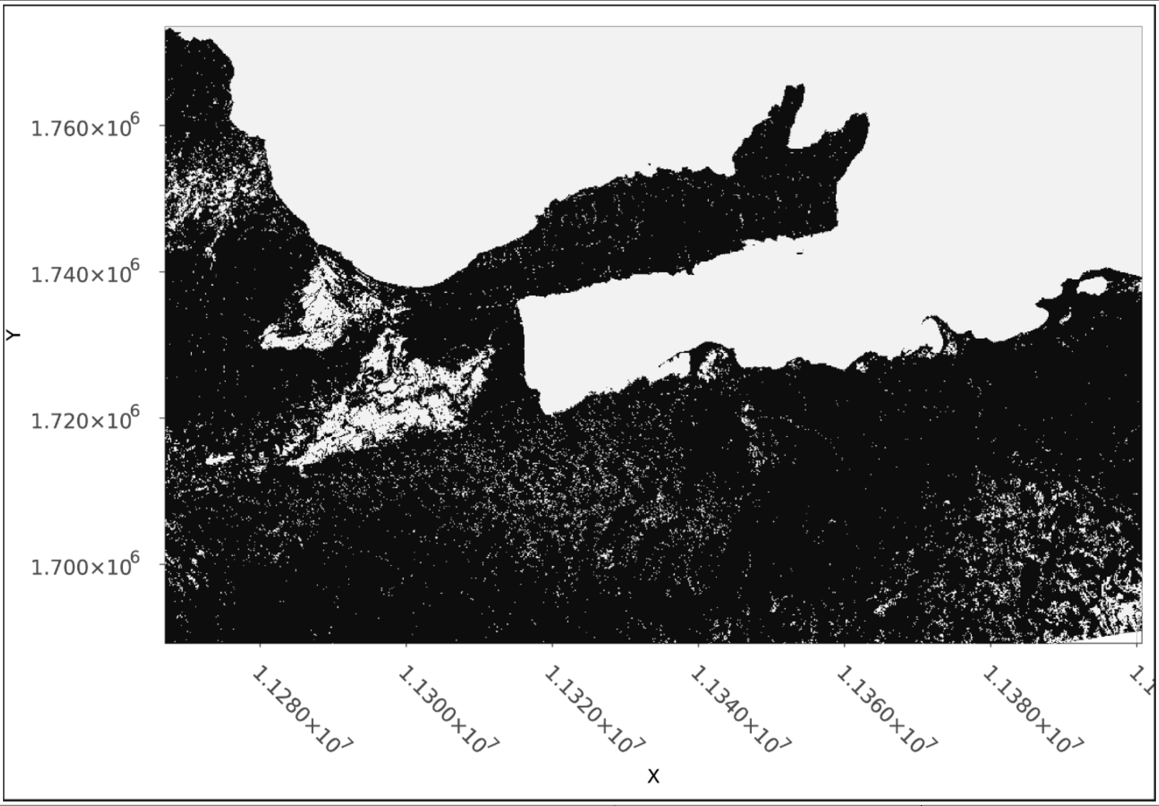

	km^2	% of total
Area of interest	11,248.18	100
Excluded area	6,392.34	56.83
No sensitivity area	5,391.05	47.93
Low backscatter area	3,165.93	28.15
Topographic distortion area	4,734.86	42.09
Radar shadow area	19.55	0.17

Table 26: Distribution of the 12 Use Cases of worldwide flood events within the 18 global environmental zones of Metzger et al. (2013).

#	GLOBAL ENVIRONMENTAL ZONES	USE CASES											
		1	***2***	***3***	***4***	***5***	***6***	***7***	***8***	***9***	***10***	***11***	***12***
A	*Arctic 1*												
B	*Arctic 2*												
C	*Extremely cold and wet 1*												
D	*Extremely cold and wet 2*												
E	*Cold and wet*												
F	*Extremely cold and mesic*												
G	*Cold and mesic*												
H	*Cool temperate and dry*												
I	*Cool temperate and xeric*												
J	*Cool temperate and moist*												
K	*Warm temperate and mesic*				X		X				X		
L	*Warm temperate and xeric*									X			
M	*Hot and mesic*												
N	*Hot and dry*	X	X										
O	*Hot and arid*												
P	*Extremely hot and arid*												
Q	*Extremely hot and xeric*							X				X	
R	*Extremely hot and moist*			X		X			X			X	X

List of Tables

List of Figures

Getting in touch with the EU

In person

All over the European Union there are hundreds of Europe Direct centres. You can find the address of the centre nearest you online (european-union.europa.eu/contact-eu/meet-us_en).

On the phone or in writing

Europe Direct is a service that answers your questions about the European Union. You can contact this service:

— by freephone: 00 800 6 7 8 9 10 11 (certain operators may charge for these calls),

— at the following standard number: +32 22999696,

— via the following form: european-union.europa.eu/contact-eu/write-us_en.

Finding information about the EU

Online

Information about the European Union in all the official languages of the EU is available on the Europa website (european-union.europa.eu).

EU publications

You can view or order EU publications at op.europa.eu/en/publications. Multiple copies of free publications can be obtained by contacting Europe Direct or your local documentation centre (european-union.europa.eu/contact-eu/meet-us_en).

EU law and related documents

For access to legal information from the EU, including all EU law since 1951 in all the official language versions, go to EUR-Lex (eur-lex.europa.eu).

EU open data

The portal data.europa.eu provides access to open datasets from the EU institutions, bodies and agencies. These can be downloaded and reused for free, for both commercial and non-commercial purposes. The portal also provides access to a wealth of datasets from European countries.

Science for policy

The Joint Research Centre (JRC) provides independent, evidence-based knowledge and science, supporting EU policies to positively impact society

EU Science Hub
Joint-research-centre.ec.europa.eu

Publications Office
of the European Union